A Review on Microchannel Fabrication Methods and Applications in Large-Scale and Prospective Industries

M. Javaid Afzal
Department of Physics, Govt. Islamia College Civil Lines Lahore

Tayyaba, S.
Department of Computer Engineering, The University of Lahore

M. Waseem Ashraf
Department of Physics (Electronics), GC University

M. I. Khan
Department of Neurosurgery, University of Pennsylvania

他

https://doi.org/10.5109/4843111

出版情報：Evergreen. 9 (3), pp.764-808, 2022-09. 九州大学グリーンテクノロジー研究教育センター
バージョン：

A Review on Microchannel Fabrication Methods and Applications in Large-Scale and Prospective Industries

M. Javaid Afzal[1], S. Tayyaba[2], M. Waseem Ashraf[3,*], M. I. Khan[4], Farah Javaid[5], M. K. Basher[6], M. Khalid Hossain[7,**]

[1]Department of Physics, Govt. Islamia College Civil Lines Lahore, Pakistan

[2]Department of Computer Engineering, The University of Lahore, Lahore 54000, Pakistan

[3]Department of Physics (Electronics), GC University, Lahore 54000, Pakistan

[4]Department of Neurosurgery, University of Pennsylvania, PA 19104, USA

[5]Government APWA College (W) Lahore 54000, Pakistan

[6]School of Science, Edith Cowan University, Perth, WA 6027, Australia

[7]Institute of Electronics, Bangladesh Atomic Energy Commission, Dhaka 1349, Bangladesh

*Author to whom correspondence should be addressed:

E-mail: *dr.waseem@gcu.edu.pk; khalid.baec@gmail.com; khalid@kyudai.jp

(Received July 10, 2022; Revised August 10, 2022; accepted August 19, 2022).

Abstract: Microchannels based on microelectromechanical systems (MEMS) have received a lot of interest in the microfluidics and biomedical fields over the past forty years. While their applications have been multifarious, a comprehensive literature review focusing on their design, type, and applications is not currently present in the literature. Researchers working on these elements of microchannels will gain targeted knowledge from the current review on microchannels. Due to its advanced properties, flexibility of mass, and small size, microdevice demand has been rising quickly, particularly in industrial applications. The classification of microchannels and their uses are the main focus of this work. These include but are not limited to molding, electroplating, lithography, lab-on-a-chip, micromolding, micromachining, micromilling, laser ablation, lithography, microcontact printing (μcp), hot embossing, electrochemical micromachining (EMM), and etching. In addition, numerous hybrid techniques for microchannel manufacturing have been reported. So, in essence, this review offers a range of advancements in microchannel manufacturing. The review also attempts to present a qualitative analysis describing the various methodologies associated with microchannels in terms of their design, shape, and flow regimes for applications such as pressure drop and transfer of heat prediction. Additionally, depending on the precise uses needed, a number of materials, including but not limited to ceramics, silicon, metals, and polymers, are utilized in the manufacture of microchannels. On metallic substrates, polymers such as silicon, glass, and polymeric materials are used. The biomedical industry uses polymeric and glass substrates instead of silicon substrates, which are used for mechanical engineering and electronic applications. In addition to outlining methods for choosing the best kind of microchannel, this paper also suggests important directions for the future.

Keywords: MEMS, microfluidics, microchannels, fabrication, flow characteristics.

1. Introduction

An emerging technology called a microelectromechanical system (MEMS) is utilized to create tiny devices using microfabrication methods [1–3]. MEMS devices can have a wide range of sizes but typically fall between 100 nm and 1000 μm (or 1 mm). Micro-Electro-Mechanical Systems (MEMS) were initially regarded as cutting-edge technology in various physical domains, such as mechanical, acoustic, and RF. Some of these include sensors, micromirrors, and switches for the RF domain. In the mechanical domain, they are used in multiple mechanical devices, such as actuators and valves. In the optical domain, they are used in multiple optical applications, such as sensors and microphones [4–8]. From such diversified spectrum of applications, it has been evident that MEMS are useful candidates in medical, chemical, and biological fields [9–11]. Recent developments in MEMS technology, in particular, have completely changed trends in a variety of industries, including sports, aerospace, biomedicine, electronics, home appliances,

and automotive [12–16]. Microscale MEMS devices can run independently or in conjunction with other hardware. MEMS devices can have a relatively straightforward construction with no movable parts or a highly sophisticated structure with numerous integrated moveable components [17–19]. Due to their cost-effective advantages over conventional devices, such as their small size, light weight, low power consumption, flexibility to create them in batches, superior performance, and more precise findings, MEMS devices have become increasingly popular. These benefits have made BioMEMS-based devices' applications in the biological and biomedical domains particularly promising [20–27]. For particular uses a variety of BioMEMS-based devices have been created [28–32]. Microfluidics is a method for manipulating fluids at submillimeter scales that have shown a significant aptitude for advancements in biological research and diagnostics. Due to its quick sample handling and precise fluidic flow control, microfluidic devices have superseded conventional experimental techniques [33–37], and hence, critical insight is required into the design, manipulation, regulation, and application of MEMS systems to further enhance the field.

As a result, a critical understanding of the design, manipulation, regulation, and application of MEMS systems is needed to advance the area. The recent widespread development of microfluidics is a result of science and technology. Little amounts of liquid can flow through microfluidic systems. In a weaker system, the flow can reach micro- and nanolitres (μL and nL). Biosensing, labeling, immobilization, purification, detection, and sample preparation are the main tasks carried out by these systems. When compared to its behavior at the micro- and nanoscales, fluid behaves very differently at bigger scales. In essence, these systems handle tiny amounts of fluids and are created at micro sizes. Microfluidic systems employ microchannels [38,39]. Fluids always flow laminarly in microchannels at such small volumes. Microfluidic devices may benefit greatly from the use of surface tension. The fluid flow may not be as predicted by traditional fluidic systems when the fluid's volume is the same as that of the microchannels via which the fluids are conveyed. Recent years have seen a lot of study in this area with biological applications focus. This decade's most significant advancement in MEMS and NEMS in microfluidics has been transdermal drug delivery (TDD) devices. The majority of this system is made up of microchannels. The microfluidic device's main component, microchannels, has a variety of inlet and output holes for fluid flow (**Fig. 1**). Applications in many disciplines, including biology, chemistry, physics, and medicine are made possible by these devices [40,41].

Different facets of microfluidic devices have been the subject of numerous review publications [42–48]. However, no review of microchannels and their classifications has yet been published focusing on their industrial relevance, i.e., fabrication techniques most suited for large-scale industry and applications in the most prospective sectors. To address this significant limitation, this review study is conducted. Essentially, this study will invoke multiple future studies to analyze their applicability at the industrial level.

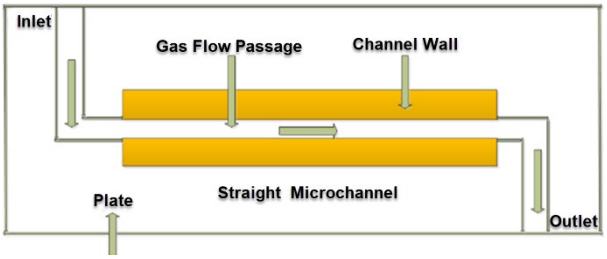

Fig. 1: Diagram of straight microchannel.

2. Classification of microchannels

Microchannels are channels with hydraulic sizes used in microtechnology. Kandlikar and Grande have offered a thorough historical perspective on the evolution of microchannels and mini-channels [49]. According to current research, microchannels can be categorized based on a number of factors, including the Knudsen number (Kn) [49–57]. All in all, the comprehensive review works along with recent insights agree that geometry is of utmost concern in the design of microchannels in terms of controlling fluid flow parameters by modifying geometry considerations [58–60]. Specifically, staggered rectangular baffles have been successfully implemented in microchannel arrays to improve gas-liquid mass transfer in terms of significantly altered volumetric mass transfer coefficient [61].

It is possible to divide microchannels into many types and subtypes. The various types of microchannels depicted in **Fig. 2** are shown in green, yellow, and purple. They can be used to resemble the letters of the English alphabet. Some of these include J, Y, T, U, and S, which can be formed to resemble any letter of the alphabet. Other types of microchannels that can be designed include square, round, triangular, double spiral, and double coil. These are also curved, curvilinear, and sinusoidal. Microchannels can thus be categorized based on their designs and applications [62–69]. **Figs. 3-5** show the schematic diagram of different types of microchannels. The parameters of various types of microchannels (dimensions, length, channel type, material, fabrication technique, fluid and fluid flow pattern, particles size, velocity, current densities, temperature, heat fluxes, flow rates, Reynolds numbers, simulation techniques, mathematical analysis, and applications) developed by various research groups are presented in a comparative manner in **Tables 1-6** [70–173]. The most frequent issues with microchannel architecture are [174–176]:

a) The inhomogeneous mixing
b) The uniform wall heat and laminar forced convection
c) The hydrodynamically growing flow

d) Independence from a grid
e) Laser scanning procedure issue to regulate the
f) Microchannel sizes
g) Boundary layer problem
h) Flow boiling in small hydraulic diameter channels
i) Flow patterns, heat transfer, and pressure drop
j) Population genetics in microchannels
k) Flows are frequently encountered in microdevices
l) Spontaneous capillary flow
m) Single-phase flow issues

2.1 Straight microchannels

Researchers have made considerable use of these channels. These microchannels exhibit laminar flow and are simple to construct. These channels' diameters can be created down to the nanometer scale. Due to their

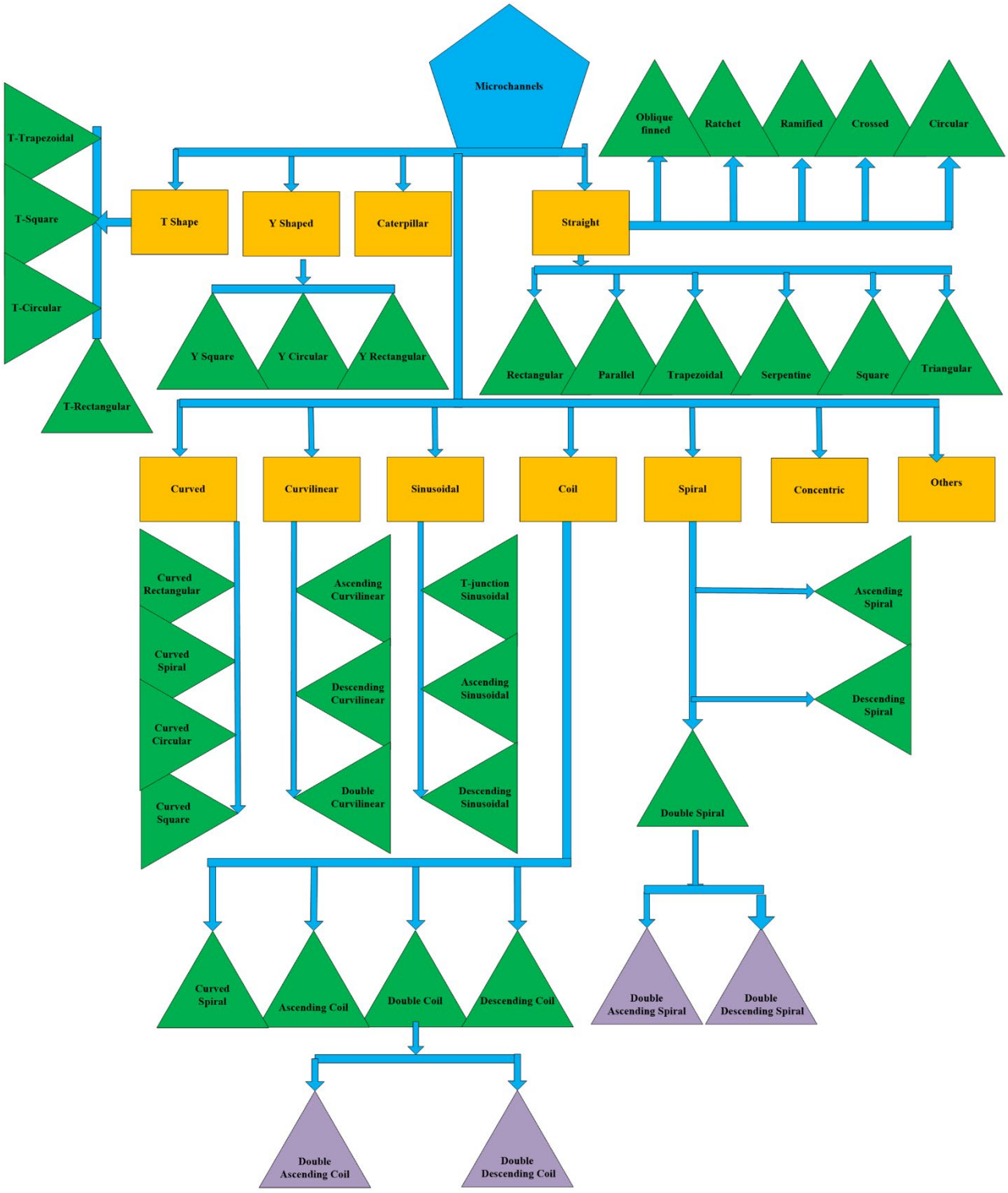

Fig. 2: Classification of microchannels.

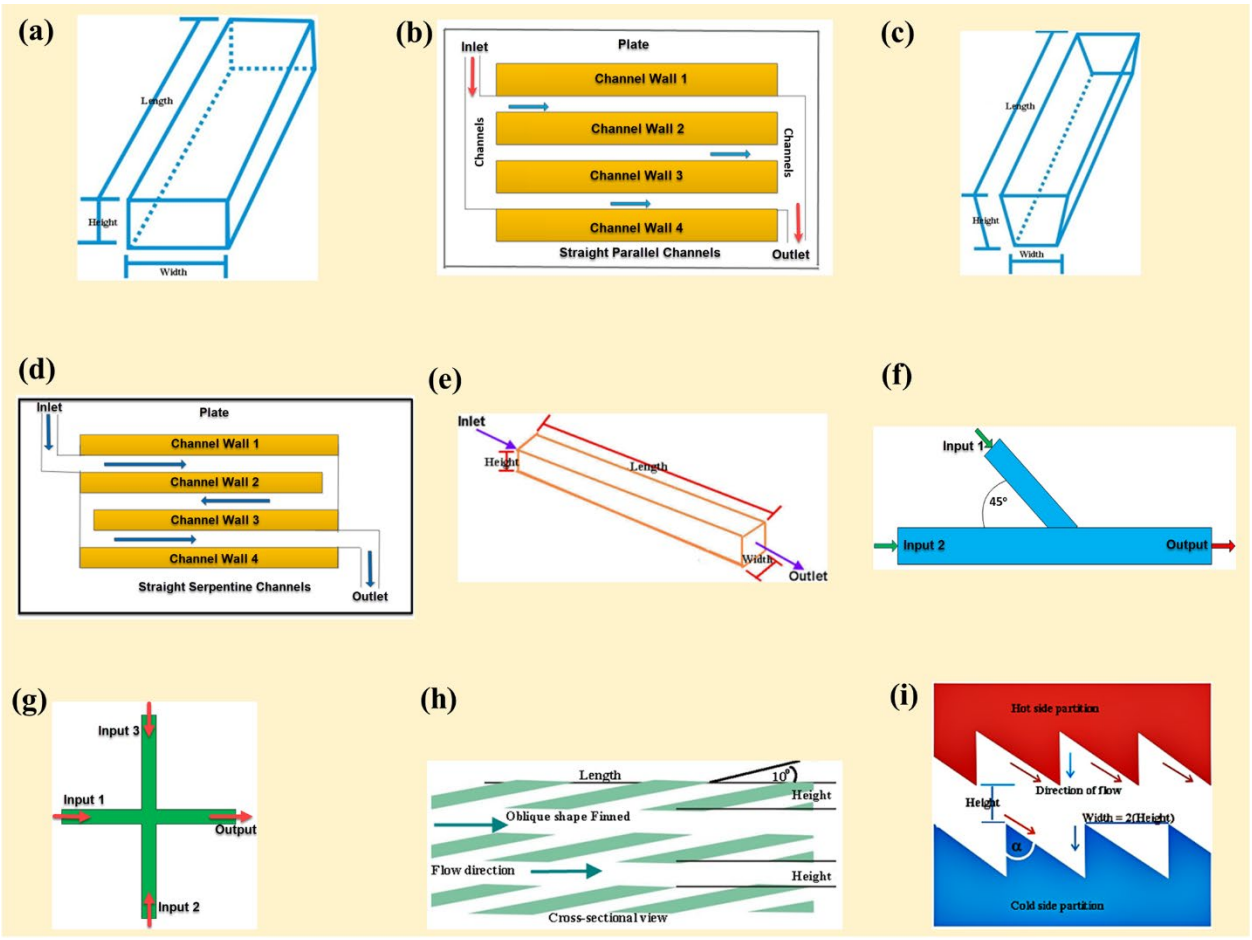

Fig. 3: Diagram of various types of straight microchannels: (a) straight rectangular, (b) straight parallel, (c) straight trapezoidal, (d) straight serpentine, (e) straight square, (f) straight ramified, (g) straight crossed, (h) straight oblique finned, and (i) straight ratchet-like microchannels.

numerous uses, these microchannels have become more significant over time. The majority of applications for straight microchannels include the emulsification of proteins, Proton-exchange membrane fuel cell, liquid and gas transfer, hemodialysis, focusing behavior, particle separation, and performance of flow boiling. **Fig. 3** depicts various types of straight microchannels.

Using a straight microchannel emulsification system, Saito et al. (2005) studied the emulsification of proteins. They effectively prepared monodispersed emulsions using proteins as an emulsifier [70]. The fabrication method wasn't discussed in this study. Three-dimensional (3D) multicomponent transport models were described by Liu et al. in 2006. This PEMFC was developed with straight gas microchannels. The PEMFC model's computational field was exceedingly extensive. The production method wasn't disclosed [71]. Masuda et al. (2008) used straight microchannels to construct a two-phase flow and 2D simulator. The transference of water at the interface of proton exchange membrane/ gas diffusion layers and gas diffusion layers /gas flow channel was carefully examined with a width of 3.2 millimeters, a length of 30 millimeters, and air and hydrogen flow rates of 58 standard cubic centimeters per minute and 22 standard cubic centimeters per minute, respectively. The relative humidity was 75% and the cell temperature was 30°Co. The rear plates and separators were made of "SUS316 standard molybdenum stainless steel," and the separators were plated in gold to reduce electrical contact resistance and shield them from corrosion. The GFC was rectangular and had dimensions of 1.6 mm in width, 1.0 mm in depth, and 30 mm in length. The fabrication process wasn't disclosed [86]. In 2010, Fazeli and Behnam employed fuel cells with zigzag and straight wall catalyst-coated microchannels. According to their analysis of mathematical modeling results, zigzag channels exhibited better discrimination for hydrogen and lower discrimination for carbon monoxide. Crisscross microchannels were, therefore, better than these microchannels. In this study, the production technique wasn't mentioned [97]. Numerical simulation was employed by Lu and Lu (2010) to resolve the issues with ultra-filtration. To solve the issues with the filtration process, they created a numerical simulation for mass transfer from a porous membrane with parallel straight microchannels that is several hundred nanometers in size. Hemodialysis could benefit from the findings. In this study, the fabrication method was not mentioned [108]. A neuro-fuzzy technique was modified by Emiroglu et al.

(2010) to forecast the ejection measurements of a side weir in these microchannels. To calculate the flow rate coefficient, they created an ANFIS model for these microchannels. In this study, the fabrication methods were not disclosed [119]. Two alternative neural network algorithms were utilized by Bilhan et al. (2010) for horizontal outflow in a straight microchannel over rectangular side weirs. The two methods that were looked at for evaluating the discharge coefficient of the rectangular side weirs were FFNN and RBNN. In this study, the fabrication methods were not disclosed [130]. To calculate the flow rate, Emiroglu et al. (2011) created another ANN technique. In this study, the fabrication methods were not discussed [141]. Straight parallel and straight serpentine microchannels with dimensions of 31.5 mm in length, 3.2 mm in width, and 6 mm in height were employed by Masuda et al. (2011). The two pieces of carbon fabric GDL and the two pieces of separator were sandwiched together to create the cell pattern of the channel. The divider was made from SUS 316 with a gold plating to signify commercial MEA. By tightening the channels' nuts and bolts, the channels were linked. The air flow rate in the straight microchannel was 58 standard cubic centimeters per minute with a current density of 0.15 Ampere per square centimeter. The air flow rate in the parallel microchannels was 116 standard cubic centimeters per minute, and the current density was 0.16 Ampere per square centimeter. The air flow rate was kept at 78 standard cubic centimeters per minute while the current density in the serpentine network was 0.16 Ampere per square centimeter. In these microchannels, they investigated the relationship between the behavior of water droplets and cell voltage. The findings showed that water accumulation and flushing of the clogged water, respectively, caused a drop and recovery of the voltage [152]. Andriy and Yaroshchuk (2011) employed a mathematical model for long-straight microchannels to analyze the transference characteristics of an electrolyte solution. In this study, the fabrication methods were not disclosed [163]. Emin et al. (2011) employed straight open channels in a different study to examine the discharge capacity of rectangular side weirs in these channels. The measurements were 12 m in length, 0.5 m in width, 0.5 m in depth, and 0.001 in slope. The sidewall was made of glass, while the channel was built with a steel bed. A channel gate was constructed at the conclusion to regulate the flow depth. Additionally, the water surface profile and surface velocity streamlines were reported in their investigation. Many hydraulic structures also utilized side weirs as an emergency assembly. To redirect flow horizontally, the side weir was typically anchored to the side of a channel. In this study, the fabrication methods were not disclosed [72]. Some researchers hypothesised in 1999, 2000, 1994, 2002, and 2003 that the surface roughness in straight microchannels was responsible for this association. These investigations [177–181] did not mention the fabrication procedures.

Many stage junctions for electronic packaging in these microchannels were first proposed by Xie et al. (2014). Utilizing computational fluid dynamics (CFD) in the ANSYS [182,183], it was possible to numerically analyze the three-dimensional streamline flow transference of heat with these junctions [78]. The complexity of the focusing behavior of sphere-shaped particles with the aspect ratio for a wide range of Re in these microchannels was investigated by Liu et al. (2014). The fabrication process was disclosed. Direct numerical simulations (DNS) in three dimensions (3D) were used to conduct the numerical analysis [184]. Liu et al. (2015) both computationally and experimentally described the viscoelastic effects based on the separation of particles and cells in these microchannels. The fabrication technique has been documented [79]. By utilizing longitudinal vortex generators, Sabaghan et al. (2016) investigated the 2-phase numerical modelling for the flow of numerous nano-fluids and heat transference in these microchannels (LVGs) [80]. The microchannel heat exchanger with five-pointed various designs in straight transverse microchannels was examined by Chai et al. (2016) using 3D numerical simulations [81]. Straight microchannels were experimentally assessed for flow boiling performance by Li et al. (2017) [185]. J. Mathew et al. (2020) compared flow patterns seen utilizing flow visualization in straight microchannels [186]. with the heat transfer, pressure drop, and stability properties of the heat sinks. In order to assess the cooling capabilities of manifold and straight microchannel heat sinks, Piotr Zajac (2021) performed a CFD simulation [187]. **Table 1** [70–72,77–81,86,97,108,119,130,141,152,163], various details about the dimension, fluid and fluid flow patterns, particles size, temperature, material, phase fluxes, heat fluxes, flow rates, simulation procedure, and field of applications of these microchannels by various researchers are offered.

2.2 Curved microchannels

Typically, curved microchannels have one curvature. **Fig. 4** depicts various types of curved microchannels. Curved microchannels have been employed by researchers in a variety of applications, such as heat transmission, flow characteristics, mass transfer, and elastic turbulence. Numerical modelling is used to study these channels as well. Wang (1996) investigated the buoyancy of force-driven modifications and the impacts of heat flow in a spinning curved microchannel. Numerical modelling was used to observe these flow configurations [188]. For the purpose of determining the transverse energy regime in curved microchannels, Fares (2000) created a quasi-two-dimensional model [134]. The flow properties might be predicted using the numerical model. By computing the friction factor "f" using the standard NS equation in this microchannel, Yang et al. (2005) evaluated the flow characteristics [135]. Shen et al. (2003) investigated the helicoidal heat transfer flow in a concave open microchannel using 3D numerical modelling. Importantly, it was established that the

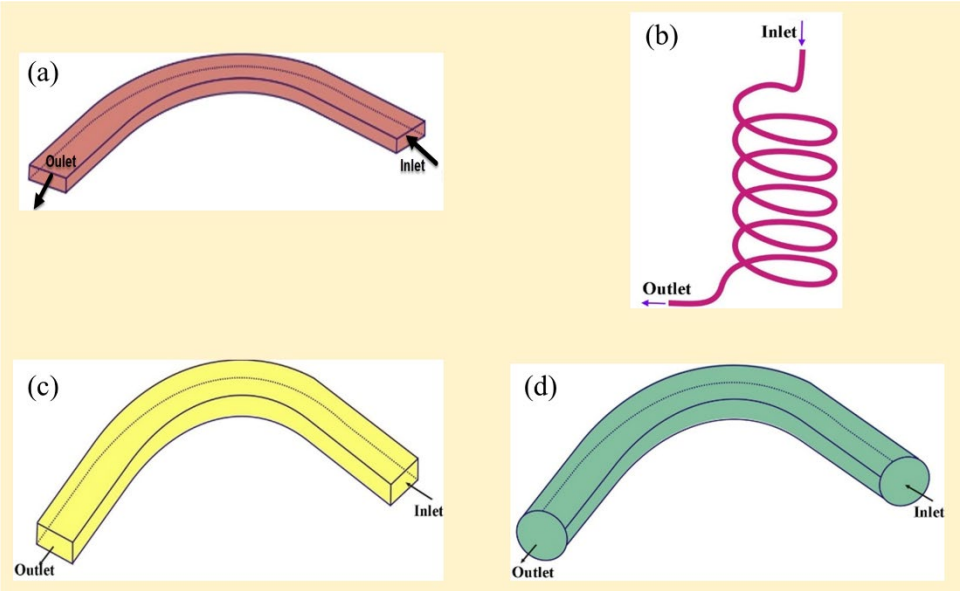

Fig. 4: Diagram of various types of curved microchannels: (a) curved rectangular, (b) curved spiral, (c) curved square, and (d) curved circular microchannel.

turbulent flow was primarily continuous and disordered, and the scientists subsequently used turbulence patterns [136,189–194]. The line placement of the 2-layer streamlined flow was reported by Yamaguchi et al. in 2004 for this channel. There have been reports of the channels' falsification [137]. With the aid of the matching eigenfunction expansion method, Khuri (2006) was able to solve the Stokes flow in curved microchannels problem [195]. For forced convection, Wang and Liu (2007) used microchannels that were slightly curved [196]. An investigational examination of the unit cell approach for the fluidic dynamics of gas and liquid combinations in this channel was carried out by Kirpalani et al. (2008) and examined the flow of curved channels from a $5x10^{-2}$ cubic meter storage container kept at 295 Kelvin temperature [138]. Seo et al. (2010) investigated secondary current velocity in these channels. The transverse velocity in this microchannel was well-defined using theoretical formulae. The performance was really co-efficient for forecasting how contaminants will mix in natural streams. Numerous researchers have looked at the profiles of transverse-type velocities [197–204]. By using numerical modelling, Ali et al. (2010) investigated the non-Newtonian fluid flow exposed to anastalsis waves in this channel. They published their analysis of the heat transfer caused by the anastalsis viscous fluid flow in this channel that same year. The authors used the RK algorithm to get a precise solution for the flow. Many fluid models have been examined by many scientists using peristaltic tools [205–215]. In order to solve the bi-harmonic equation, Che et al. (2010) published a numerical technique of plug fluid flow in these channels. For the stream functions, they created a series solution [139]. Data from Emiroglu et al. [216,217] were utilized. The numerous linear and nonlinear regression techniques, which had a root mean square error of 0.2926 and, 0.2054 correspondingly, were shown to produce a worse approximation of the discharge coefficient during the validation stage than ANN model [140]. Numerous studies have looked into discharge co-efficient estimation based on simple lateral weir analysis [218–230]. In a mathematical model, a group of researchers (2011) investigated the anastalsis transference of a thick fluid down the curved channel [231]. By using computational fluid dynamics simulation, Xuan et al. (2011) investigated mass transference of a 2-layer streamlined fluid flow in this channel [142]. In 2016, Renault et al. created a brand-new curved microchannel architecture that enables neuronal populations to generate axonal projection in a single direction. This is an important use of these axons and their rebuilding in relation to brain pathways [143]. In curved microchannels, elastic turbulences were investigated by Li et al. (2017) [232]. Below is a diagram of the curved microchannel. A U-shaped Gaussian beam microchannel is another name for it.

2.3 Curvilinear microchannel

Curved motion is the term used to describe a liquid's wave motion in a curvilinear channel. Curves like this are fixed curves. Curves can be numerous in curvilinear microchannels. These channels require the fluid to flow in both straight and curved patterns. There is not much research on these microchannels. Most often, malignant cells are separated via these microchannels. In order to separate malignant cells from blood, Wewala et al. (2012) examined the shape and simulation procedure of ascending curvilinear channel. They separated cells using the inertia-focusing method. They employed computational fluid dynamics for the simulations (CFD). The microchannel measured 150 µm, 55 µm, and 625 µm in width, height, and radius, respectively. 100×10^{-6} m was

the bare minimum inner radius. The channel had a length of 14450 x 10^{-6} m and a maximum inner radius of 1150 x 10^{-6} m. Only one input and three outlets were needed for the two ascending and descending microchannels to cooperate [153]. A unique design of ascending and descending curvilinear microchannels was reported by Wewala et al. (2013). The results of separating malignant cells from blood were simulated and compared. The malignant cells were estimated to be about 15 μm in size. The ascending microchannel, out of the two, was most effective at separating malignant cells [154].

2.4 Coil microchannel

These microchannels are shaped like coils. They may be turned several times, just like a spring. Systems for cooling use them. This kind of microchannel has just been researched by Schutte et al. (2016). Their research used a condenser with cooling coil microchannels as the basis for a cooling system. There was no mention of the fabrication [233].

2.5 Spiral microchannel

The shape of these microchannels is similar to a hair spring. Their turns have radii that are bigger. Every circular turn is centric. They are widely used in bio-MEMS applications. These microchannels are employed in a number of processes, including DNA hybridization, particle separation, particle focusing, Dean flow, and ultrafast plasma blood separation. DNA hybridization by CD was explored by Peng et al. (2007), who found advantages in the use of high sampling, multiple sampling, and the hybridization rate. Spiral microchannels were also used to complete analyses of antibody-antigen binding and enzyme-substrate reactions [155]**.** Bhagat et al. (2008) investigated the way that particles are separated in spiral channels. For the investigations, they used Dean flows and differential migration. They used CFD-ACE+ (ESI-CFD Inc., Huntsville, AL) technology to analyze the spiral microchannel they had designed. The microchannel measured 100 m, 50 m, 3 mm, and 13 cm in width, height, radius, and overall length, respectively. According to Kuntaegowdanahalli et al. (2009), dean flow applied in spiral channels allowed for the passive separation of particles. The microchannel was 130 micrometers high, and the particles that were to be separated ranged in size from 10 to 20 μm. Transient incompressible flows were the method they employed [156,173]. In 2013, Nivedita et al. looked into the growth of dean vortices in spiral microchannels. They separated the cells. The relevance of Dean flows was significantly improved by the spiral channels, which also improved particle focusing [157]. Guan et al. (2013) investigated particle separation. They made use of helical channels with trapezoidal and rectangular cross sections. Actually, this tactic was a method of size-based separation. For the concentrating of particles with improved separation resolution, they used a three-dimensional observational approach [158]. Blood components, blood samples, and their separation using spiral microchannels were studied by Rafeie et al. (2016). They developed the multiplexing of spiral channels to achieve ultra-rapid plasma blood separation. The blood flow rate measured for this study was 530 liter per minute. This rate showed that the channel could handle blood flow more quickly—one mm of blood in under a minute—than previously thought [159]. Dean vortices with secondary flows were studied by Nivedita et al. in 2017 in these channels [234].

2.6 Double spiral microchannel

In contrast to microchannels with a single spiral, these microchannels have two distinct turns. Together, the two spiral microchannels function as a single microchannel. Clockwise and anticlockwise flows are separated in the double spiral microchannel. Researchers use these microchannels for a variety of purposes, such as continuous particle separation, dielectrophoresis, particle capture, addition, and transport, as well as the impact of droplet deformation on fluid flow. In order to create double spiral shapes for application in hybridization, Chen et al. (2008) explored second generation 2D microarray [160,235]. In double spiral microchannels, Zhu et al. (2011) investigated the continual separations of particles in diverse combination. The creation of double spiral shapes DEP induced for the dis-aggregation of numerous particles was the focus of this investigation. The fundamental properties of the particles (size, charge, conductivity) varied [161]. For the 5- and 10-m particles, respectively, the amendment feature for dielectrophoretic velocity was remain fixed at 0.6 and 0.4 [147–149,236,237]. A potent technique for sorting and classifying particles according to their size and polarizability is dielectrophoresis. Their polarizability is influenced by the frequency of the ac field, permittivity, and electric conductivity. Based on electrode and insulator techniques, these effects are comprehended [238–248]. In a double spiral microchannel, Sun et al. (2012) investigated the improvement and parting of tumorous cells [162]. DuBose et al. (2014) investigated how to separate bio-particles based on their form and design in these channels. Using a constructed model known as the Arbitrary Lagrangian-Eulerian numerical model, they ran simulations to comprehend the particle separation system and the motions of the particles. A key parameter for the identification of particles and perhaps a cell cycle indicator was the form and architecture of the double spiral microchannel [75,249–254]. A double spiral microchannel was investigated by Xue et al. (2016) for the adjacent motion of two-fold droplets train at small Reynolds number. Droplet motion was employed to addition and transference the tiny particles in these channels, supply the lowest scale, release segments for the analysis, catch cells for exposure, and deliver [255–259]. They talked about the effectiveness of migration and the impact of droplet deformation on motion in these channels [165].

2.7 T-Shaped microchannel

The shape of these microchannels is a T in English. In microfluidics, microchannels joined by T-junctions are particularly prevalent and crucial. They can be used for emulsification, gas supply systems, and mixing. The majority of investigations on fluid flow in these microchannels involve numerical models and micro element image velocimetry studies [260–270]. In T-shaped microchannels, Husny et al. (2006) investigated the impact of elastic forces on drop formation. In this work, the fabrication procedure was described. They came to the conclusion that these T-shaped microchannels were created by the resulting polydispersity and quantity of secondary drops [166]. Graaf et al. (2006) modelled droplet formation in a microchannel with a T shape. Different flow rates and interfacial pressures were used to simulate droplet formation [167]. Gat et al. (2010) looked at the Hele-Shaw approach to use mathematical analysis to examine the gas flows across a system of parallel microchannels and shallow T-junctions. Parallel microchannels were created by combining three T-junction microchannels [168]. Santos and Kawaji (2010) conducted an experimental analysis and mathematical analysis of the production of two-phase flow slugs in a T-shaped microchannel. They created slugs in the channel using the CFD application FLUENT 6.2 [169]. The combined effect of mixing and heat transmission was described by Ebrahimi et al. (2014) employing electroosmotic pressure flow past in these channels. The Hele-Shaw approach was studied by Gat et al. (2010) to observe the gas T-shaped microchannels. For flow in a T-shaped microchannel, they conducted a numerical 2D quasi-steady investigation [171]. Zhuang and Zhu (2015) used electro-osmotic pressure in T-shaped microchannels to study the cumulative influence of the flow of power law-driven fluids. They used the solutions to the Poisson-Boltzmann and Laplace equations to modify the Navier-Stokes equations. The shape and optimization of bio-MEMS applications may benefit from the findings of this work [271]. By the use of the mathematical technique (Nek-5000 codes) [272], Andreussi et al. (2015) examined the fluid flow regimes present in T-shaped microchannels. In T-shaped microchannels, Cardiel et al. (2016) studied the flow behavior of micellar membranes. They provided important analysis for fluid flow behavior, membrane behavior, proteins, and thermodynamical phases of lipid membrane through numerical modelling and experimental work. They created a model that integrated the properties of the micro-micellar membrane's (MM) diffusivity, viscoelasticity, and local concentration gradient [172,273–282]. Fluid wetting properties in these channels were compared by Omer et al. (2017) [283].

2.8 Other types of microchannels

Other kinds of microchannels exist in the industry. **Fig. 5** depicts other types of curved microchannels. Some microchannels are exclusively intended to serve a single function. Different kinds of microchannels were coupled by Kashid et al. (2011) to comprehend the flow properties. They made use of Concentric, Caterpillar, T-junction, and Y-junction microchannels. According to the mixer type, flow rate, flow ratio, microchannel design, and finally fluid flow characteristics, the analytical results showed different flow regimes [284]. investigated the flow boiling properties in microchannels. Their studies were concentrated on 200 m wide and deep radial microchannels. In comparison to straight microchannels, there was less pressure decrease in these channels. The pressure loss and flux in the channel were 16.03 kPa and 267.5 W/cm2, respectively, as the flow rate gradually increased up to 400 mL/min.

Table 6 [153–162,164–172] represents the different information of the length, fluid and flow pattern, particles size, temperature, material, Reynolds numbers, heat fluxes, flow rates, simulational method, mathematical modelling method, and applications of the channels used by various researchers.

3. Fabrication of microchannels

Microfluidics and the biomedical industry are the two principal uses of microchannels [64]. As it is challenging to create microchannels using standard engineering methods, it is impossible to understand all the fabrication procedures in a clear manner. In addition, a variety of materials, including but not limited to ceramics, silicon, metals, and polymers, are employed in the manufacturing of microchannels depending on the specific uses desired. Polymers including glass, polymeric materials, and silicon are employed on metallic substrates [285]. Instead of silicon substrates, which are used for mechanical engineering and electronic applications, the biomedical sector uses polymeric and glass substrates. During fabrication of microchannels following issues were found [286–288]:

a) Bulge formation
b) Surface roughness
c) Irregular profile of the channels
d) Scanning times
e) Scanning velocity
f) Microchannels with higher aspect ratios could not be demoulded defect free,
g) Broke off during fabrication
h) Integration with other devices
i) Compatibility issues

Microchannel fabrication involves a variety of procedures, including:

a) Lab on a chip
b) Micromolding
c) Electroplating
d) Injection molding
e) Ultrasonic machining
f) Electrochemical micromachining (EMM)
g) 3D Printing

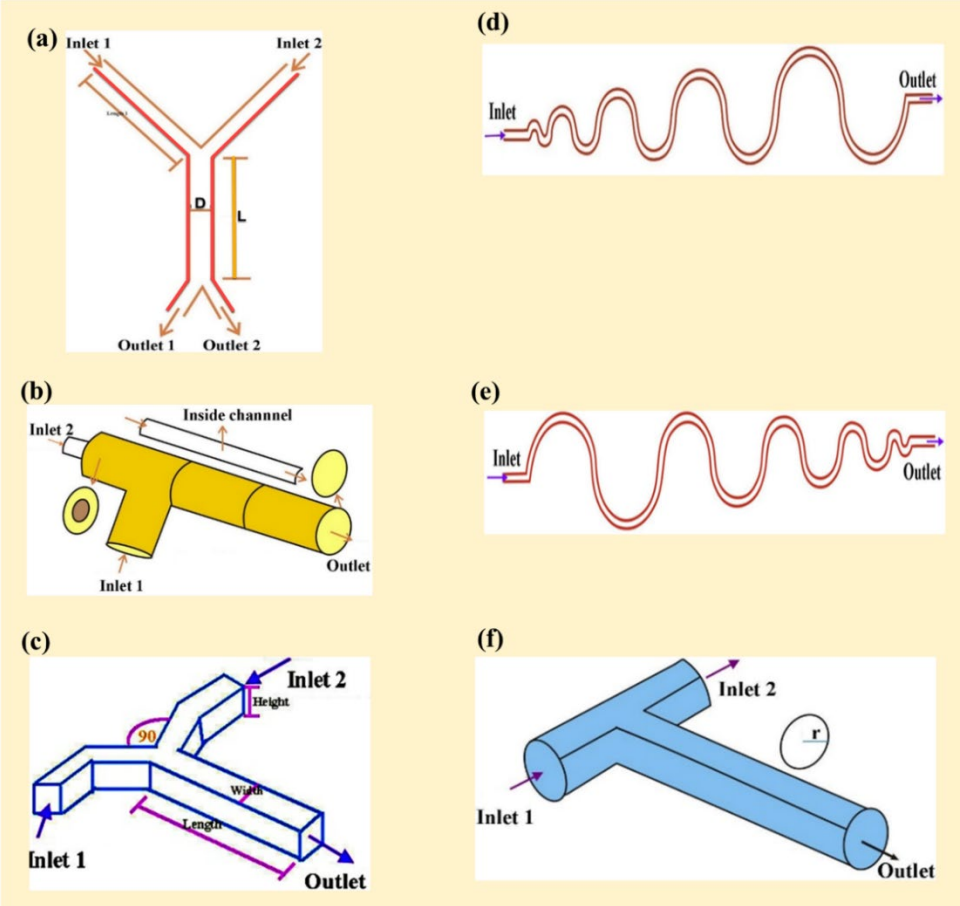

Fig. 5: Diagram of miscellaneous microchannels: (a) Y-shaped, (b) concentric, (c) caterpillar, (d) ascending sinusoidal, (e) descending sinusoidal channel, and (f) T-shape circular microchannel.

h) Laser Direct Writing
i) Laser micromachining
j) Micromachining
k) Laser ablation
l) Microcontact printing (μCP)
m) Micro Total Analysis System
n) Rapid Prototyping
o) Hot embossing
p) Etching
q) Photolithography
r) Lithography
s) Micromilling
t) Excimer laser micromachining
u) Femtosecond laser bulk micromachining
v) Lithography, electroplating, and molding (LIGA, from the German lithographie, galvanoformung, abformung)
w) Modified techniques combining the aforementioned

Microchannel construction has also been accomplished using hybrid techniques. The use of laser micromachining as a potential channel fabrication method is expanding quickly [289]. For research and industrial use, quicker and less expensive fabrication methods are required because some of these procedures take a long time.

It is important to note that, with the exception of micromilling, unconventional procedures are frequently used in the production of microchannels. With the exception of circular channels, which are essentially manufactured on the interior of the base material, the channels are produced on the exterior of the base material [285,290–297]. Other fabrication methods have been utilised in several research, however much of this literature is unavailable. The first investigation using the Mask and Fill approach on SU-8 was conducted by Guerin et al. in 1997 [298]. On the surface of silicon and glass substrates, channels were created by Papautsky et al. in 1998 [299]. The first electrospun polymeric microchannels were created by Vempati and Natarajan in 2011 [300]. Kee et al. (2011) employed the PLIS technique for the creation of microchannels [301]. The method of micromolding for creating parylene channels was first described by Noh et al. (2004) [302]. The spacer approach was initially employed for fabrication by Hakamada et al. (2007) [303]. Lee et al. (1998) employed the low-energy ion beam etching method for the first time [304]. The first study to fabricate microchannels using plasma etching was Rossier et al. (2000) [305]. A road map for considerable advancement in various facets of the thermal manufacturing of microchannels was provided by Kandlikar and Grande in 2002 [306].

Moreover, Wu and Cheng (2003) also created silicon

microchannels with straight trapezoidal shapes. The diameters used ranged from 25.9 to 291.0 µm. Wet etching was used to create the microfluidic device [91]. On a PMMA plate, Yamaguchi et al. (2004) mechanically constructed curved microchannels. By employing a Robo-drill with a flat end mill (Ø200 x µm), the area was measured as 3mm x 7mm [137]. Similar implementations of curved microchannels are also found in a recent work, where microfluidics physics is explained from a theoretical perspective to comprehend the accurate positioning of particles in the fluid [307]. T-shaped microchannels were created utilising a polycarbonate substrate by Husny et al. (2006). The stiff material polycarbonate offers excellent optical transparency. The fabrication process employed was the modified laser-LIGA procedure [166]. Particles were separated in spiral channels by Bhagat et al. (2008). The microchannel was 100 µm wide, 50 µm high, 3 mm in diameter, and 13 cm long overall. They created the channels using a common soft lithography method. Kuntaegowdanahalli et al. used a similar method in 2009. The diameters of the particles to be separated ranged from 10 to 20 µm, and the channel employed had a height of 130 µm [156]. 2008 saw the fabrication of spiral and double spiral patterns by Chen et al. In a clean room, photolithography procedures involving photomasks were carried out. The PDMS plate had a 2 mm thickness and a 92 mm diameter. The microchannels ranged in depth from 25 to 50 µm [160].

Furthermore, a curving spiral microchannel made of polydimethylsiloxane (PDMS) was also created in 2009 by Zhu and Xuan utilising the common soft lithography method [147]. Chu et al. (2010) created microchannels with curved, rectangular shapes. Using common microelectromechanical techniques, the fabrication was carried out on a silicon substrate in accordance with the physical microstructure's properties [144]. In double spiral microchannels, Sun et al. (2012) investigated the enrichment and separation of tumor cells. Standard soft lithography was used to create the channels. They employed a SU8-2050 master mold and silicon material [308]. Straight oblique-finned microchannels were experimentally created by Law et al. (2014). The copper-made MHS had a 25 mm × 25 mm surface area. Following that, 40 parallel microchannels were created using the wire cut electro-discharge machining technique. On MHS, 780 oblique fins in total were created [107]. In more recent studies, it is emphasized that geometrical considerations such as parallelization of microchannels and utilizing the effect of flow area variation are vital in terms of controlling multiphase flows and up-scaling from a design perspective [59,309,310].

Similar straight rectangular microchannels were created by Liu et al. (2015) using the traditional soft lithography technique [311]. Yan et al. (2015) created serpentine and rectangular straight microchannels. They used the soft lithography approach to create polydimethylsiloxane (PDMS) serpentine microchannels [100]. Experimentally sinusoidal microchannels with alternating secondary branches were created by Chiam et al. (2016). The fabrication procedure of micro machining was applied [131]. Zhang et al. (2016) created rectangular microchannels that are perfectly straight. Wire electric discharge machining (WEDM) was used to produce the channels [88]. Using an etching technique, Guo et al. (2016) created experimentally straight, rectangular microchannels. The microchannels' manufactured depth and breadth ranged from 50 nm to a few microns and 3 µm, respectively [89]. Curved rectangular microchannels were created by Li et al. (2016). Throughout the experiments, the radius of curvature was modified three times. The microchannel's rectangular shape was curled at a 120° angle. The microchannel measured 35 mm x 80 mm in size. Transparent plexiglass was utilised for construction in order to facilitate interactions with light. The channel was carefully built by connecting two PIV pipelines of equal size that were both straight and curved, without the use of any special techniques [146]. In 2016, Akhtar et al. created a square, straight microchannels by micromachining with an exciplex laser. They created oblique and circular channels using this method, employing square and rectangular laser dots. The waterway had a nearly 10 µm edge roughness and a maximum width of 150 µm. This process turned out to be an additional approach for directly milling MEMS components and micro-fluidic channels [312].

Additionally, the splitting of more viscous fluid threads in square, straight microchannels was studied by Cubaud et al. (2016). This groundbreaking work demonstrated a highly regulated thread route with the mechanical stability of more viscous flows in multipart microchannels. These channels were created using the etching process (typical silicon-based microfabrication), and they all had diameters of 250 µm [73]. In order to replace the outdated traditional procedures, Ling et al. (2017) developed a novel technique called the "Xurograhy Method" for fabricating microchannels [313]. The most recent development in the production of microchannels is the use of lasers. This method of manufacture is quicker, simpler, and less expensive. However, there are several drawbacks to this method. Microchannel manufacturing is an extremely challenging and intricate procedure. The level of accuracy needed for production necessitates thorough investigation [314]. Microchannels for hybrid electrolytes were printed in three dimensions by Zekoll et al. (2018) [315]. A method of 3D printed microchannels for bone restoration was developed by Daly et al. (2018) [316]. With the inclusion of a controller cover, Serex et al.'s research on 3D printing in microfluidics was conducted [317]. Burtch et al. (2018) developed a new subtractive approach for 3D manufacturing microchannels [318].

The primary methods for 3D manufacturing microchannels include 2-photon polymerization, extrusion printing, Inkjet, laser, and stereo-lithography [319]. Here, it is discussed how various strategies have limits.

The 2-photon polymerization process has taken up the most time for building complicated structures. The restrictions in extrusion printing are poor resolution, roughness, nozzle obstruction, and lower detection limits. Inkjet printing cannot be used for channels less than 100 μm or with poor precision or distortion. The constraints of the laser 3D printing technology are low resolution, optical clarity, and roughness. Stereolithography's limits are its hardware and adhesive characteristics' incompetence [320]. The constraints on the micromilling process are low stiffness and surface roughness [321]. The lithography process involves replication, pattern registry, curling, and material restrictions [322]. The photolithography procedure results in photo-resistance and limited chemical compatibility [323]. The geometrical structure of microchannels is restricted during the micromachining process [324]. The LIGA's limits are in the kinetic and transportation of response rates [325]. The limits of the micro total analysis system are time, space, and the combination of micropumps, micro-valves, and microchannels [326].]. The lengthy cooling time required by the hot embossing process is its main drawback [327]. The material that can get stuck internally and some gels that can impede this technique are the constraints of fast prototyping [328].

Table 7 summarizes the numerical modeling method, numerical modeling method, flow rate, heat flux, Reynolds number, length, temperature, material, fluid type/particle size, simulation methodology, and applications of various channels employed in various investigations [58,73,79,88–90,100,107,131,137,144,146,147,156,160,162,166,173,329–331].

4. Applications of microchannels

Microchannels can be divided into many varieties according to their specialised usage. optical properties, molecule adsorption, surface charge, machinability, thermal conductivity, and electro-osmotic flow. Aside from these primary considerations, many other properties are considered for applications of microchannels[332,333]. In this section, the most important applications of microchannels in terms of prospect and relevance to large industrial scale are reported.

4.1 Microchannels used as radiation detector

A handful of studies have justified the use of microchannels as radiation. Among the seminal studies on the detection efficiency of microchannels, Blasé *et al.* have studied the photon detection efficiency of microchannel plates in the range of 2.5-20 MeV [334]. Leskovar (1977) also used microchannels to create a powerful radiation detector. There were many microchannel plates utilised in the detector. As a result, the MCPs were used to measure the energy of ions, electrons, neutrons, and photons (up to X-rays). The MCP detector coupled high-resolution capacity with picture intensity. As a result, the MCP's increased speed and decreased noise were completely attributed to the usage of microchannels [335]. Jagutzki et al. (2002) created yet added an efficient radiation indicator to find photons and other high-tech elements. Compared to its predecessor, this detector was more adaptable and could analyze the position and time of a single particle [336].

4.2 Microchannels used in creation of bubbles and droplets

Numerous scientists produced bubbles and droplets using microchannels. The T-shaped microchannel was used by Garstecki et al. (2006) to produce bubbles and droplets. These channels had heights and widths that varied from 10 to 100 μm. There was a flow of 0.01 to 1 μL/s [74]. There are numerous more processes that utilise microchannels to produce droplets and generate bubbles [337–351]. Chu and colleagues (2010) created bent rectangular tubes. Using common microelectromechanical techniques, the fabrication procedure is carried out on a substrate made of silicon based on the physical microstructure's properties [144]. A double spiral microchannel was created by DuBose et al. (2014) using a common soft lithography technique. For fabrication, they used polydimethylsiloxane (PDMS). The microchannels have lengths of 50 μm, 100 μm, and 25 μm, correspondingly [75].

4.3 Microchannels used as heat sinks

Throughout the last few decades, significant advancements have been made in the field of microchannel implementation as heat sinks [352,353]. Recent review studies and original studies strengthen the view that thermodynamic parameters such as air-side friction factors and heat transfer correlations can be manipulated based on the fin geometry [354–356]. Additionally, using silicon microchannels, Petralia et al. (2015) created a novel method for surface wettability for molecular analytical applications. They made a connection between the wettability and the microchannels' use in biomedicine [357]. A coil microchannel was successfully implemented in a condenser by Schutte et al. (2016). Gao et al. (2016) looked at the price of making microchannels. The industry's utilisation of microchannels is constrained by their expensive fabrication costs. Because of their highly compact design, MCHSs are used in the industry to handle heat transfer acceleration more effectively. They applied methods that have already been discussed, such as those that Leith et al. (2010) [358] and Lajevardi et al. (2011) [359] have documented. For the industry to advance, manufacturing costs must be sufficiently low [360]. The first use of microchannels in the creation of microreactors to comprehend the impacts of deactivation in the PROX reaction was made by Laguna et al. (2016). The results were exceptional and really helpful, and they can help with the design of a future new prototype microreactor [361]. In this regard, optimization of the design to maximize the

efficiency of microchannel heat sinks has been rampant, such as by implementation Harris Hawks algorithm [362]. All in all, specific aspects of the microchannel are getting attention in recent years, such as manipulating catalyst activation-related mechanisms [363]. Some recent works have also highlighted the implementation of microchannels from the heat exchange perspective [364], which is not discussed in detail in the current review.

4.4 Microchannels used in space shuttles

Many scientists employed these channels in space ships, space crafts, and shuttles. Lee and Mudawar observed the applied applications of these channels in 2016. To lower the pressure in the crew H/inlet, X's the MCHS collaborated with throttling valves and crew H/X. For thermal management in space shuttles, this method has been applied. It is believed that this use will reduce the size and weight of space travel vehicles. Replace this single-phase temperature control system with a two-phase one [76].

4.5 Integration with other devices

Microchannels are passive devices. Microchannels can be integrated with other kinds of stuff. A method was developed by Babcock et al. (2017) to examine bacterial contamination and antimicrobial resistance in these channels [365]. Afzal et al. (2016-2020) simulated and developed silver ascending and descending (ASMC, DSMC) sinusoidal microchannels and polydimethylsiloxane (PDMS) microchannels for the implantation of varicose veins 366–370). Micropumps or being a component of microfluidic and capillary circuits are key applications of microchannels in microfluidics [371]. Only the use of microchannels makes it possible to pump micropumps. Micropumps come in a variety of varieties. Micropumps for liquid and gas were researched by Richter et al. in 1998. They discovered that microchannels are necessary for the operation of micropumps. Gas or liquid must entirely fill the microchannels. If there was no leak in the system, the micropumps functioned properly [372]. The cooling system of the microchannels employed in micropump technology was researched by Singhal et al. in 2004 [373].

Mechanical and non-mechanical micropumps for drug delivery via microchannels were researched, according to Ashraf et al. (2011). To achieve minimum flow rates, drug delivery requires microchannels. They talked about how to combine series or parallel microchannels for pressure and medication administration, as well as all different types of micropumps, their structure, pressure characteristics, and more [42]. The pressure-generating liquid or gas is forced through the microchannels. The flow properties of micropumps with microchannels have received extensive attention. Micropumps have used almost all forms of microchannels, although the most common types are spiral, curved, and straight. Piezoelectric [374], phase change [375], thermopneumatic [376], electromagnetic [377], bimetallic [378], ion-conductive polymer film (ICPF) [376], electrostatic [379], and shape memory alloy (SMA) [380] are some of the several types of mechanical micropumps. Magnetohydrodynamic (MHD) [381], electrochemical [382], flexural planar wave (FPW) [383], evaporation [159], bubble [384], electrohydrodynamic (EHD) [385]electroosmotic (EO) [386] (straight rectangular microchannel), and electrowetting (EW [387], micropumps are examples of non-mechanical micropumps. For flawless operation, microchannels have been utilised with each of these micropumps. Material, construction method, Reynolds number, dimensions, dean number, flow rate, temperature, fluid type/particle size, and applications for which these channels were employed, among other information, are all discussed in detail by different researchers are presented in **Table 8** [74–76,144,388].

5. Discussion

The key findings of this review are critically discussed in this section. The sub-topics are the feasibility of fabrication of microchannels in terms of materials and with the relevancy of flow characteristics, channel design in terms of relevant mechanical, structural, thermodynamical, and fluid mechanics parameters, and prospective grounds to develop microchannel research to obtain a bigger impact in a large industry, and experimental parameters relevant for designing and implementing microchannels.

The flow characteristics in microchannels depend on a number of factors, such as laminar flow, non-viscous fluid, static pressure, the interaction of the fluid with the channel walls, energy dissipation, incompressible fluid, and microchannel design [389].

In microfluidics, there are adaptable techniques for creating microchannels [44]. Material choice is the most crucial factor in manufacture. The materials that are typically employed for the production of these channels are glass, silicon, and polymers [46]. Glass' high price is the main barrier [47].

Due to their lower cost, greater durability, and ability to facilitate quicker fabrication processes, polymers have been suggested as an appealing replacement for glass and silicon. A variety of polymers, such as polydimethylsiloxane, polycarbonate (PC), polyvinyl chloride (PVC), cyclic olefin copolymer (COC), polymethyl methacrylate (PMMA), and polystyrene (PS), can be utilised to create microfluidic chips (PDMS). Microfluidic device prototyping is carried out quickly using PDMS. Due to their low cost and ease of manufacture, PDMS chips are frequently used in laboratories and are especially popular in the academic sector. Despite having excessively high oxygen and gas permeability, they have the best optical transparency. They have excellent robustness, non-toxicity, and biocompatibility. The usage of PDMS chips has been encouraged by these qualities [46,48].

Table 1. Straight microchannels

References	Dimensions	Fluid type/ particle size	Current density	Temperature	Material	Flow rate	Simulation technique	Numerical modelling	Applications
Saito et al. [70]	41 to 44.1 µm	Oil in water/ Protein 40 and 10 µm	NR	25ºC	Silicon	NR	NR	NR	Protein as Emulsifier
Liu et al. [71]	L= 71.12x103 µm, W = 7.62×102 µm, H = 7.62×102 µm	Ideal gas	0.5 to 1.2 Acm^{-2}	353K	NR	NR	NR	3D multi-component Transport model	PEM fuel cell
Masuda et al. [86]	30 x 3.2 $x10^3$µm	Water	0.6 Acm^{-2}	30º C	Glass	0.0009 L/s	PEFC	Multiphase mixture model	Mass transport in PEM/GDL and GDL/GFC
Fazeli et al. [97]	30.4$x10^3$µ m	Hydrogen	NR	540 k	Stainless-steel	NR	NR	TOX and SR	PEM fuel cell
Lu et al. [108]	1$x10^6$µm	NR/0.3nm	NR	NR	NR	NR	NR	Half Channel model	Filtration process Haemodialysis
Emiroglu et al. [119]	0.25$x10^6$µ m, 0.50$x10^6$µ m, and 0.75$x10^6$µ m	Water	NR	NR	NR	NR	Neuro fuzzy technique	ANFIS model	Discharge coefficient
Bilhan et al. [130]	L= 0.15 - 1.50 x 10^6µm, H= 0.12 - 0.20 $x10^6$µm	Water	NR	NR	NR	10 –150 L/s	Neural network technique	FFNN and RBNN model	Discharge co-efficient
Emiroglu et al. [141]	L= 0.25 - 0.75$x10^6$µm, H= 0.12 - 0.20$x10^6$µm	Water	NR	NR	NR	NR	Levenberg Marquardt Technique	ANN model	The ANN model is better than the regression model.
Masuda et al. [152]	L=31.5$x10^6$µ m, W= 3.2$x10^6$µ m	Water	0.15 Acm^{-2}	30ºC	Carbon and SUS 316 gold	0.0009 L/s	NR	NR	PEFC water management
Yaroshchuk et al. [163]	NR	Electrolyte solution	NR	NR	NR	NR	NR	Local Thermo-Dynamic equilibrium	Diffusion potential field
Emiroglu et al. [72]	L= 12$x10^6$µm, W= 0.5x 10^6µm, D= 0.5x 10^6µm	Water	NR	NR	Steel and glass Side wall	0.010 –0.150 L/s	NR	NR	Hydraulic structure
Om et al. [77]	NR	Water	NR	293 K	NR	NR	NR	Finite Volume method	Heat transfer performance
Xie et al. [78]	L= 35$x10^6$µ m, W= 35$x10^6$µ m	Water	NR	311 K	Silicon	8.3 $x10^{-5}$–2.0$x10^{-5}$ L/s	CFD ANSYS software	3D model	Heat transfer performance

Xie et al. [78]	L= 35x10^{6}µm, W= 35x10^{6}µm	Water	NR	311 K	Silicon	0.0083 –0.02 L/s	CFD ANSYS software	3D model	Heat transfer performance
Liu et al. [79]	L= 60x10^{6}µm, H=50 µm, W=50, 100, 200 and 300 µm	Glycerine-water/15 µm	NR	70ºC	PDMS	4.16x10-7 L/s and 8.3x10-7 L/s	NR	3D DNS model	Inertial microfluidic devices
Sabaghan et al. [80]	NR	Water/15 µm	NR	298 K	Silicon	NR	CFD ANSYS software	SIMPLEC model	Longitudinal Vortex Generators
Chai et al. [81]	L= 10 x10^{6}µm, W= 0.25x10^{6}µm, H= 0.35x10^{6}µm	Water	NR	NR	Silicon	NR	CFD ANSYS software	3D simulation	Heat transfer performance

Table 2. Straight rectangular microchannels.

References	**Dimensions (µm)**	**Fluid type /Particle size (nm)**	**Temperature (ºC)**	**Material**	**Heat flux (Kw/m^2)**	**Flow rate (L/s)**	**Simulation Technique**	**Numerical Modelling**	**Applications**
Wörner [82]	NR	NR	NR	NR	NR	NR	CFD ANSYS	Finite difference method	Laminar flow
Yadav et al. [83]	L=231, W=713	water/170	NR	Copper	100 and 200	NR	3D CFD ANSYS	Univariate search method	Heat transfer performance
Muller et al. [84]	L=35, W=377, H=157	water/0.5	25	NR	NR	NR	NR	Time-averaged second-order perturbation model	Acoustophoretic
Ma et al., [85]	W=200, D=150	Oil	25	PDMS	NR	NR	NR	3D topology	Flow topology
Liu et al. [87]	L=30x10^6, H=30x10^6	RBCs/ 1000 - 3000	NR	NR	NR	1.1x10^{-9}	NR	NR	Separation of particles
Zhang et al. [88]	45 x 20 x 2x10^6 µm^3	Water	10	Copper	585, 780 and 875	8x10^{-5}	NR	NR	Heat transfer performance
Guo et al. [89]	L=5.5, W=5, D=1.6	Water	27	Glass	NR	NR	NR	Director over relaxation algorithm	Liquid crystals

Table 3. Different straight microchannels.

Reference	**Dimensions**	**Fluid type/Particle size**	**Temperature**	**Material**	**Reynolds number**	**Flow Rate**	**Current Density**	**Heat flux**	**Simulation Technique**	**Numerical Modelling**	**Applications**
Straight Trapezoidal Microchannels											
Wu [90]	Dia=25.9 -291 µm	Water	NR	Si	Re = 1500 - 2000	NR	NR	NR	NR	Navier Stokes equation for analysis	Friction factor theory for laminar flow
Wu [91]	NR	Water	NR	NR	Re<100 and	NR	NR	NR	NR	NR	Heat transfer

					>100						performance
Liao [92]	NR	Water	NR	NR	NR	NR	NR	NR	NR	Depth integral form of RANS	Jacobian elliptical functions
Kuppusamy [93]	NR	Water/ CuO 25 nm	300 K	Si	NR	NR	NR	10^6 w/m^2	CFD analysis	Navier Stokes equation with modelling using the Finite Volume method.	TGMCHS
Fani et al. [94]	NR	Water/CuO	293 K	Si	500	NR	NR	430 Kw/m^2	NR	Eulerian-Eulerian method	Heat transfer performance
Abed et al. [95]	L= 95x10^{3}µm, H=12.5x10^{3}µm	Water/CuO 25nm	300 K	NR	12000	NR	NR	6 Kw/m^2	NR	SIMPLEC algorithm	Heat transfer Performance
Straight Serpentine Microchannels											
Xiong et al. [96]	L=30x10^{3}µm, W=12x10^{3}µm, H=2x10^{3}µm	Water	27ºC	Si	Re =100 - 200	1x10^6 L/s	NR	NR	CFD simulation	NR	Laminar flow characteristics
Afzal et al. [98]	L = 2.8x10^{3}µm	Water	NR	NR	0.05 ≤ Re ≤ 200	2.2x10^{-4} L/s	NR	NR	CFD simulation	Viscosity modelled using Carreau-Yasuda and Casson [96,99]	Flow and mixing performance
Yan et al. [100]	D= 20.5 µm, W=100 µm	Water	65ºC	PDMS	Re < 1	NR	NR	NR	NR	3D numeric simulation of solute dispersion	Design of micro gas chromatic column and other devices
Ashrafi et al. [101]	L=4x10^{3}µm	Water	298.3 K	Plexiglass and teflonated carbon paper	Re < 650	7.5 x 10^{-10} L/s	0.8 A/cm^2	NR	NR	Finite Volume technique to solve equation	PEMFC
Straight Square Microchannels											
Roudet et al. [102]	L= 0.24x10^{6}µm	Water	NR	PMMA	NR	8.3x10^{-4} L/s	NR	NR	NR	Numerical simulation of bubble formation to understand its dynamics and mechanism in the microchannel	Heat exchanger reactors
Dietrich et al. [103]	L= 5x10^{3}µm	Water	NR	Resazurin dye	Re = 200 - 1500	8.3x10^{-4} L/s	NR	NR	CFD simulation	Colourimetric technique	Local characterization of gas-liquid mass transfer
Yao et al. [104]	2h x 2h x 8πh	NR	NR	NR	Re =4410 - 250000	NR	NR	NR	NR	RNAS equation with closure model for the Reynolds stress	Heat exchanger reactors and chemical

											reactor
Kaya [105]	L = 10.15 µm	Water	289 K	NR	NR	NR	NR	670,1000, 1500 kw/m^2	FLUENT CFD Code	3D simulation and equations for incompressible, steady state and laminar flow in the microchannel solved numerically	Heat transfer characteristics
Straight Oblique Finned Microchannel											
Fan et al. [106]	L= 65 µm	Water	297 K	Silicon	Re = 50 - 500	0.006 L/s	NR	7.9 MW/m^2	NR	Numerical 3D conjugate heat transfer simulation	Heat transfer characteristics
Law et al. [107]	L= 10 µm	Water	29.5ºC	Stainless steel	NR	0.0016 L/s	NR	6-120W/cm^2	NR	NR	Heat transfer characteristics
Law et al. [109]	25x10^{3}µm × 25x 10^{3}µm	FC-72 dielectric fluid	29.5ºC	Copper	NR	0.0016 L/s	NR	14-42 W/cm^2	NR	NR	Thermal management techniques
Law et al. [110]	L=23x10^{3}µm, W=32x10^{3}µm, D=1.2x10^{3}µm	FC-72 dielectric fluid	29.5ºC		NR	0.00006 L/s	NR	14.9-70 W/cm^2	ANSYS	Reynolds averaged continuity and navier–Stokes equations solved using the RNG k–ε turbulence	Heat transfer characteristics
Straight Ratchet-like Microchannels											
Chen et al. [111]	L=1.0 to 6.0 µm	NR	375 K	NR	NR	NR	NR	NR	CFD simulations	Direct Simulation Monte Carlo method	Thermal transpiration effects

Table 4. Sinusoidal and sinusoidal T-junction microchannels.

References	**Length**	**Fluid type**	**Temperature**	**Material**	**Reynolds number**	**Flow Rate**	**Simulation Technique**	**Numerical Modelling**	**Applications**
Sinusoidal Microchannels									
Goldstein and Sparrow [112]	19 mm.	Air	20°C	Naphthalene plates	500 to 3100.	NR	NR	NR	Heat transfer characteristics
Nishimura and Kojima [113]	L=14 mm, W=80 mm, D=3.5 mm	Water	25°C	NR	30 < Re < 300	NR	NR	NR	Flow patterns and mass transfer characteristics
Nishimura and Matsune [114]	L=14mm, W=80mm,	Water	25ºC.	NR	Re = ˆ 50	2.5 m^3/s	NR	Governing equations represented in terms of dimensionless vorticity and	Heat transfer characteristics

	D=3.5mm							stream function	
Rush et al. [115]	L=30cm, Dia=6.9mm	Water	0.1°C	Copper	Re = 200, 800	NR	NR	NR	Heat transfer characteristics
Niceno and Nobile [116]	NR	NR	NR	NR	Re = 175-200	NR	NR	Constant thermophysical properties were used to solve equations	Heat transfer characteristics
Metwally and Manglik [117]	NR	Water	NR	NR	10 < Re < 1000	NR	NR	control volume finite difference method	Heat transfer characteristics
Zniber et. al. [118]	NR	NR	NR	NR	NR	NR	NR	Numerical simulation of analytical solutions for various values of the Hartmann number	Heat transfer characteristics
Nilpueng and Wongwises [120]	L= 1m	Air and water	NR	NR	Re < 3500 and Re > 3500	NR	NR	NR	Engineering
Rosaguti et al. [121]	NR	Water	NR	NR	5 ≤Re≤200	NR	CFD code ANSYS	Solution of the Navier Stokes and energy equations on an unstructured mesh using the vertex-based finite volume method	Heat transfer characteristics
Xie et al. [122]	L=5 mm	NR	NR	NR	Re=100 - 1100	NR	NR	Finite volume method with SIMPLER algorithm	Heat transfer characteristics
Yang and Liu [123]	L= 100µm, Dia=10 µm	Water	298 K	NR	Re < 1	NR	2Dcode, COMSOL Multiphysics 3.3 based on FEM	Electric double layer (EDL) theory relating the electrostatic potential and the distribution of counterions and co-ions in the bulk solution by the Poisson equation	Electroosmotic flow (EOF)
Tolentino et. al. [124]	L=1.5 m, H=0.508m, W=0.381m	Water	300° C	Plexiglass and aluminium	Re = 200 - 1200	NR	NR	Feasibility and advantages of the chaotic mixing promotion technique	Flow visualization Study
Chang et al. [125]	L=194 mm, W=54 mm, Th=0.1mm	Water	65–120°C	Fiberglass	Re= 1500, 2000, 5000, 10,000, 15000,.20,000, 25,000 and 30,000	NR	NR	NR	Heat transfer characteristics
Tolentino et al. [126]	L=1.5 m, W=0.381 m, H=0.508 m	Water	NR	Tempered glass	Re < 250	NR	NR	Experimental model	Flow visualization study
Heidary and Kermani [127]	NR	Copper-Water Nanofluid	NR	NR	Re 5 ≤ Re ≤ 1500	NR	NR	Maxwell-Garnett's (MG model)	Heat exchanger
Lu et al. [128]	L=183 mm, W=0.7	Water-air	293 K	NR	NR	$3.3x10^{-8}$ m^3/s for	NR	Experimental model	PEM fuel cells

	mm, D=0.4 mm					water $6.6x10^{-5}$ m^3/s for air			
Chang et al. [129]	NR	Water	NR	NR	NR	NR	NR	NR	Electroosmotic flow (EOF)
Chiam et al. [131]	L=450 µm, D=600 µm, W=300 µm	Water	10°C	Copper	Re = 50–200	NR	ANSYS Mesh	3-dimensional conjugate domain used in the simulations	Heat flow and fluid flow characteristics
Sinusoidal T-junction Microchannels									
Solehati et al. [132]	L=10000µm, W=500 µm, H=500 µm	Water	NR	NR	Re = 5–10	NR	Auto-CAD 2010	Solution of the mathematical model by using finite-volume based CFD software.	Mixing performance of a micromixer
Ozkan and Erdem [133]	L=100 µm W=100 µm	NR	NR	NR	NR	$1.11m^3/s$	NR	Iterative level set method for tracking interface and shapes	Hydrodynamic mixing performance

Table 5. Curved microchannels.

References	**Length**	**Fluid type**	**Temperature**	**Material**	**Reynolds number**	**Flow Rate**	**Simulation Technique**	**Numerical Modelling**	**Applications**
Curved microchannels									
Fares [134]	NR	Water	NR	NR	NR	NR	NR	Quasi two-dimensional model for simulation	River applications
Yang et al. [135]	33 < R < 53 mm, 0.5 < W < 1 mm	Water	NR	NR	Re ≤ 2300	NR	NR	The non-staggered grid technique was used to calculate the Navier Stokes equation, and the algebraic equation was solved by the SIP method	flow characteristics
Shen et al. [136]	L = 4.0 m, W = 0.40 m, H = 0.6 m	Water	NR	NR	NR	NR	NR	The basic foundation for modelling turbulent flow is the Navier–Stokes equations, and therefore a statistical approach was taken here.	Engineering
Yamaguchi et al. [137]	L= 20 mm, W= 200 µm, D= 200 µm	Water	NR	PMMA	Re = 5	NR	Fluent 6.0 ANSYS	Experimental method	Flow characteristics
Kirpalani et. al. [138]	D=1 and 3 mm	Water Air	295 K	Glass	NR	Water 0–$1.6 x10^6$ and $1.6 x10^6$ - $3.3x10^6 m^3/s$, Air	NR	Experimental method	flow characteristics

						0 – .3x10 ^{6}, 1.6 x10^{6}-6.7x10^{6} m^3/s			
Che et. al. [139]	NR	Air	NR	NR	NR	NR	NR	2D analytical model (Finite Fourier Transform method) to investigate the flow pattern	Droplet-based microfluidics
Bilhan et al. [140]	NR	Water	NR	NR	NR	NR	NR	ANN model with root mean square errors (RMSE)	Artificial neural networks
Xuan et al. [142]	W=400 µm, H=800 µm, R=200 and 600µm	Water	NR	NR	NR	NR	CFD model ANSYS	The classical continuum model with non-slip boundary	Mass transfer characteristics
Renault et. al. [143]	W=10 µm, H=5 µm, R=30 µm	NR	NR	PDMS	NR	NR	NR	A new axon diode design	Directional axon guides
Curved Rectangular Microchannels									
Chu et al. [144]	L= ±20 µm, W= ±2 µm, H=±2 µm	Water	297K	Silicon	Re= 80 - 876	1.8 x 10^{-7} m^3/s	CFD model ANSYS	Experimental method and numerical simulation according to the Field synergy principle	Hydrodynamic characteristics
Guo et al. [145]	D= 3 nm	Water	NR	NR	Re= 100 - 900	NR	CFD software ANSYS CFX 12.0	NR	Heat exchanger
Li et al. [146]	35 mm x 80 mm	Water	NR	Plexiglass	Re = 2.4 x 10^{4}	NR	NR	numerical simulations	Flow development
Curved Spiral Microchannels									
Zhu et al. [147]	L=2.5 cm, W=50 µm, D=100 µm	Water	NR	PDMS	NR	NR	NR	Simplified version of the model developed by Kang et al. [148,149]	Continuous bioparticle separation and flow cytometry
Curved Square Microchannels									
Guo et al. [150]	NR	Water	NR	NR	Re= 80 - 876	NR	NR	Field synergy principle	Heat transfer Characteristics
Curved Circular Microchannels									
Kalteh et al. [151]	NR	Water and copper nano	NR	NR	Re = 100	NR	NR	Two-dimensional Eulerian–Eulerian two-phase model	Heat transfer characteristics

		particles							

Table 6. Different-shaped microchannels.

References	Dimension	Fluid type /Particle size	Temperature	Material	Reynolds number	Flow Rate	Velocity	Simulation Technique	Numerical Modelling	Applications
Curvilinear Microchannels										
Wewala et al. [153]	W=150 µm, H= 55 µm, R=625 µm	Water /15 µm	NR	NR	Re = 8.5, 9.25 and 10.06	NR	0.105m/s	CFD ANSYS	NR	Cell separation
Wewala et al. [154]	W=150 µm, H= 55 µm, R=625 µm	Water and Air/ 4, 10 and 15 µm	NR	NR	Re = 8.5	NR	0.105 m/s	CFD ACE$^+$ ANSYS	NR	Cell separation
Spiral Microchannels										
Peng et al. [155]	W= 60 µm, D=92 mm	Water	70° C	PDMS	NR	NR	NR	NR	NR	DNA hybridizations
Bhagat et al. [156]	L=13 cm, W=100 µm, H=50 µm, R=3 mm	Water/1.9 mm and 7.32 mm	NR	PDMS	Re = 10	5, 10, and 20 mL/min	NR	CFD-ACE+ (ESI-CFD Inc., Huntsville, AL)	NR	Separation of particles
Nivedita et al. [157]	250µm×100µm	Water/polystyrene10µm	NR	NR	NR	3mL/min	NR	ESI CFD-ACE+	NR	Separation of particles
Guan et al. [158]	R=8 mm to 24 mm	Water	NR	PDMS	NR	1.0 mL/min to 8.0 mL/min	NR	Computational fluid dynamics (CFD) software COMSOL 4.2a	NR	Separation of particles
Rafeie et al. [159]	W=500 µm, Hi= 70 µm and Ho=40 µm	Water	70°C	PDMS	NR	1.5 and 24 mL/min blood flow rate 530 µL/min	NR	COMSOL Multiphysics® software	NR	Blood plasma separation
Double Spiral Microchannels										
Chen et al. [160]	D=25 µm, W=50 µm, L=100 mm	Red-dyed solutions	27°C	PDMS	NR	NR	NR	NR	NR	Formation of Nucleic acid microarrays
Zhu et al. [161]	W=50 µm, L=13 mm	Water/ polystyrene10 µm	20°C	PDMS	NR	NR	NR	COMSOL® with the MATLAB® interface	NR	Separation of particles
Sun et al. [162]	W=300 µm, H=50 µm	Water/5 and 15 µm	NR	PDMS	24, 36, 48, 60	0.41 mL/min	NR	CFD software Fluent ANSYS	NR	Separation of particles

DuBose et al. [164]	W_1=50 µm, W_2=100 µm, L=39 mm	NR/polystyrene 3.5 - 6µm	NR	PDMS	NR	NR	NR	C-iDEP	Arbitrary Lagrangian Eulerian (ALE) method-based numerical model	Separation of particles
Xue et al. [165]	R=400, 1600, 2800 and 4000 µm, W=400 µm, H=100 µm	Water	27ºC	PDMS	Re = 0.13 - 0.38	NR	NR	NR	Direct numerical simulations (DNS) of the two-phase interfacial flow	Chemical and biological applications
T-shaped Microchannels										
Husny et al. [166]	27.5 x 275 µm	Water	NR	Polycarbonate	Re << 1	0.75 ml/min	NR	NR	Simple analytical drop size prediction method	Elasticity on drop creation
Graaf et al. [167]	NR	Oil and water	NR	NR	NR	0.3 mL/min	NR	CFD software package (CFD-ACE+)	Lattice Boltzmann Simulations of Droplets	Droplet Formation
Gat et al. [168]	NR	NR	NR	NR	Re << 1	NR	NR	COMSOL 3.4	Hele-Shaw scheme to analyse steady compressible viscous flows	Viscous flow analysis
Santos and Kawaji [169]	D_h=113 µm, L=60 mm, D=119 µm	Water and gas	NR	NR	NR	NR	0.5 m/s	CFD software FLUENT 6.2	3D VOF model	Slug formation
Xu et al. [170]	L=2 cm, Area, 1000 x 500µm	Water	25ºC	PMMA	Re < 1	NR	NR	SIMPLER algorithm	Analytical 2D model first built to describe the heat transfer processes	Thermal mixing
Ebrahimi et al. [171]	NR	Water	NR	NR	Re = 10	NR	NR	FLUENT software ANSYS	Pseudo (artificial) compressibility method	Mixing and heat transfer characteristics
Cardiel et al. [172]	H=80 µm, W=300 µm, L=2 cm, L=2 cm	CTAB, NaSal and water	60ºC	Silicon	Re = 0.07–1.4 Re = 0.58–2.9	0.016 mL/min	NR	NR	NR	Formation and flow characteristics

Table 7. Microchannels fabrication with various-shape.

References	Channel type	Dimensions	Fluid type /particle size	Material	Temperature	Flow rate	Dean number	Reynolds number	Fabrication technique	Application
Wu and Cheng [90]	straight trapezoidal	R=25.9 – 291.0 µm	Water	Silicon	NR	NR	NR	Re = 16	Wet etching	Laminar flow characteristics
Yamaguchi et al. [137]	Curved	L=20 mm, W=200 µm, D=200 µm	Purified water and fluorescein	PMMA	NR	NR	De < 20	Re ~ 5 and Re ~ 25	Mechanically by a Robodrill with a flat end mill	Laminar flow characteristics
Husny et al. [166]	T-shaped	27.5 x 275 µm	Glycerol–water	Polycarbonate	NR	0.003 ml/min	NR	Re ≥ 1	Laser-LIGA	Drop formation
Bhagat et al. [173]	Spiral	W=100 µm, H=50 µm, R = 3 mm, L=13 cm	Water	PDMS	NR	5,10 and 20 ml/min	De = 0.47	NR	Standard soft Lithography technique	Separation of particles
Kuntaegow danahalli et al. [156]	Spiral	H=130 µm, W=500 µm	Water/polystyrene 10 µm, 15 µm, and 20 µm	PDMS	80ºC	3 ml/min	NR	NR	Standard soft Lithography technique	Separation of particles
Chen et al.[160]	Double spiral	D=25 - 50 µm, W=50 µm, L=100 mm	Red-dyed solutions	PDMS	NR	NR	NR	NR	Photomasks in photolithography	Formation of Nucleic acid microarrays
Zhu and Xuan [147]	Curved spiral	L=2.5 cm, W=50 µm, D=100 µm	Water	PDMS	NR	NR	NR	NR	Standard soft Lithography technique	Continuous bio-particle separation and flow cytometry
Chu et al. [144]	Curved rectan-gular	D= 3 nm, L= ±20 µm, W= ±2 µm, H=±2 µm	Water	Silicon	297 k	11.3 ml/min	0 < De ≤ 450	Re = 80 - 876	Standard microelectromechanical	Hydrodynamic characteristics
Sun et al. [162]	Double spiral	W=300 µm, H=50 µm	Water/5-15 µm polystyrene	Silicon	NR	0.41 ml/min	2, 3, 4, 5	24, 36, 48, 60	Standard soft lithography	Separation of particles
Law et al. [107]	Straight oblique finned	L= 0.001 cm	Water	Stainless steel	29.5ºC	100 - 200 mL/min			Electro discharge machining	Heat transfer characteristics
Liu et al. [79]	Straight rectangular	L= 60mm, H=50 µm, W=50, 100, 200 and 300 µm	Glycerin-water/15 µm	PDMS	70ºC	0.05 mL/min	NR	Re= 0.3 and Re = 4.2	Standard soft lithography	Inertial microfluidicdevices
Yan et al. [100]	Straight rectangular and serpentine	D= 20.5 µm, W=100 µm, L= 10 mm, Dia= 100mm	Water	PDMS	65ºC	NR	NR	Re < 1	Standard soft lithography	chromatic column and other devices

Chiam et al. [131]	Sinusoidal	L=450 µm, W=300 µm, D=600 µm	Water	Copper	10ºC.	NR	NR	Re = 50–200	Micro machining	Flow characteristics
Zhang et al. [88]	Straight rectangular	45 x 20 x 2 mm^3	Water	Copper	40ºC	4.8 ml/min	NR	124, 225 and 313	WEDM	Heat transfer performance
Guo et al. [89]	straight rectangular	L=5.5 µm, W=5 µm, D=1.6 µm	Water	Glass	27ºC	NR	NR	NR	Etching	Liquid crystals
Li et al. [146]	Curved rectangular	35 mm x 80 mm	Water	Plexiglass	NR	NR	De = 6.2 $x10^4$	Re = 2.4 x 10^4 –1.4 x 10^5	Systematically joining two PIV pipes	Flow development characteristics
Cubaud et al. [73]	Straight square	H = 250 µm	NR	Silicon	NR	NR	NR	Re ≤ 21	Etching	Separation of fluid threads

Table 8. Applications of microchannels.

References	**Channel type**	**Dimensions**	**Fluid type/Particle size**	**Material**	**Temperature**	**Flow Rate**	**Reynolds number**	**Fabrication Technique**	**Application**
Garstecki et al. [74]	T-shaped	10 – 100 µm	Water	PDMS	100°C	$10x10^{-3}$ L/s	<< 1	Photolithography	Bubble formation
Chu et al. [144]	Curved rectangular	L= 2 µm, W= 2 µm, H= 20 µm	Water	Silicon	297 K	$1.6x10^{-3}$ L/s	80 -876	Etching	Engineering
Dubose et al. [75]	Double spiral	L= 50, 100 µm, D=25 µm	Phosphate and TWEEN 20 /5 µm polystyrene	PDMS	NR	NR	NR	Soft lithography	Electrical sorting mechanism
Lee and Mudawar [76]	Straight rectangular	L=1 mm, W=1 mm	Water	Copper	19.41°C	NR	57	NR	Refrigeration

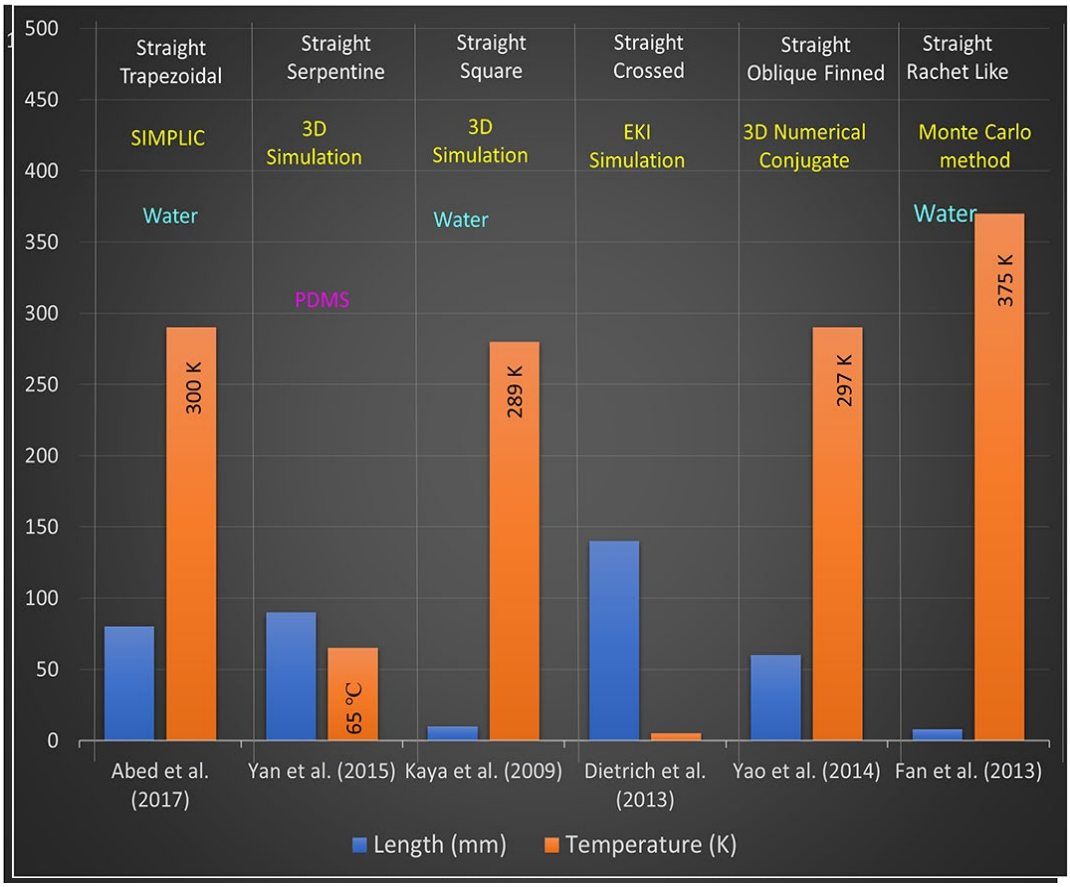

Fig. 7: Length and temperature illustration for different shaped but straight microchannels with applications.

Additionally, polymeric materials can also be used in place of silicon. Polymeric components are commonly employed because they are biocompatible, affordable, and simple to manufacture. Many researchers employ photolithography and conventional soft lithography techniques. The main variables in the examination of flow characteristics include the Dean number, flow rate, fluid velocity, temperature, fluid type, heat flux, phase flux, Reynolds number, and the material. For numerical studies, simulation techniques are the most important significant factor. Microchannels were utilized by Steinke and Kandlikar to investigate the frictional effects of a single phase in liquids. This microchannel work was significant because it improved understanding of the flow properties [390]. With regards to the enhancement of single-phase fluid flow through microchannels, Liang *et al.* have recently substantiated that such flow can be manipulated location-wise, i.e., enhancement in the entrance region and subsidization downstream [391]. Additionally, experimental studies on single-phase flow and difference from the theoretical prediction in terms of Nusselt number have been investigated in a recent review [392]. A study on the fluidic characteristics of water in straight and serpentine microchannels with miter bends has been conducted by Xiong et al. The results were extremely obvious; the bend loss co-efficient was calculated and no eddies were seen at low pressure for Reynolds numbers below 100. At tiny scales in microfluidic systems, the study of flow properties is extremely important [96]. To achieve a precise relation, however, multiple experiments must be carried out, and simulation and related theoretical work are also required.

Particularly, straight microchannels are simpler to construct because the fluid flows smoothly through them and because of their straightforward flow properties. In order for liquid to flow through the microchannels, external micropumps are needed. Pressure, flow rate, and temperature are just a few of the fluid flow parameters that are meticulously measured for study. The link between the Re number and frictional factor is the key aspect of fluid flow in straight microchannels. According to the Poiseuille theory of flow, straight microchannels experience laminar flow at low Reynolds numbers, and the pressure remains constant throughout the flow [180]. **Fig. 7** provides a graphic representation of different parameters of straight microchannels. The specific application in which the channel was used is also shown in this graphical representation. The applications shown by this illustration are PEMFC, PEFC, heat transfer, and inertial microfluidics, which have gained attention in recent years due to simpler control mechanisms and economic design [393]. The models used for numerical investigation are a multiphase mixture, Semi-Implicit Method for Pressure

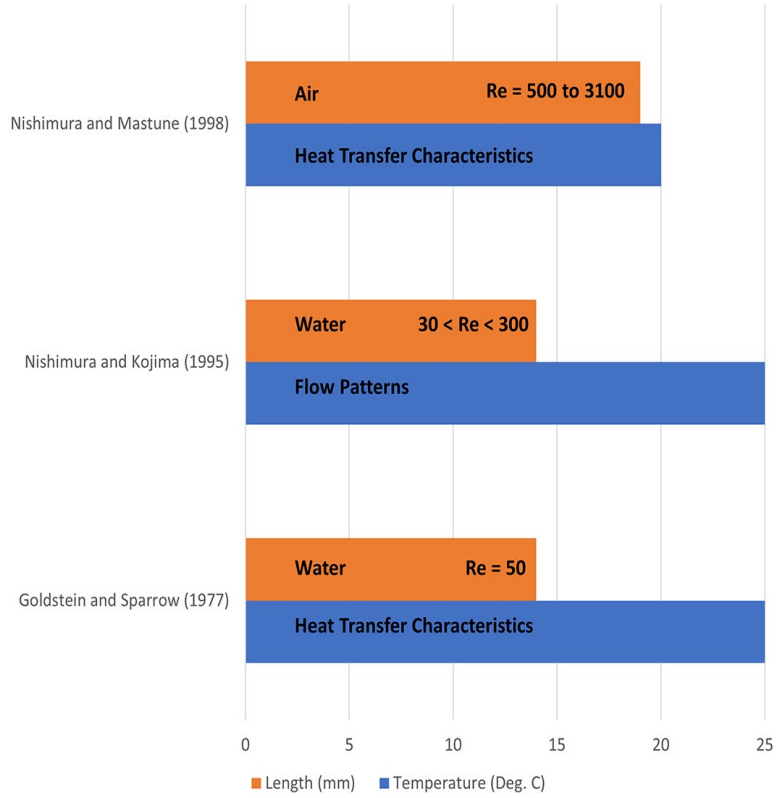

Fig. 8: Length and temperature illustration for Sinusoidal Microchannels with applications.

Linked Equations-Consistent (SIMPLEC), and a three-dimensional direct numerical simulation (3D DNS) model for these microchannels.

Another important aspect of the investigation may be the channel design. A popular design for straight microchannels is a straight rectangular microchannel. Straight microchannels like rectangular, parallel, serpentine, trapezoidal, square, triangular, circular, crossing, ramified, ratchet, and oblique finned microchannels are only a few of the many configurations available. The latter three of them are the most challenging to manufacture, yet it is still useful to analyze how they flow.

The liquid and gas flow for each of these systems is influenced by the geometry, operating circumstances, and design. Another important element for flow analysis is temperature. Close to the tips, large temperature differences in ratchet-like channels occur, and they get smaller as you get further away. **Fig. 7** displays a graphic representation of the length and temperature of various straight microchannels. The channel type and numerical modelling technique are also displayed in the graph The models and simulation methods used for numerical investigation are SIMPLEC, 3D numerical conjugate model and EKI simulation and 3D simulation, Monte Carlo method respectively.

At relatively low pressure, sinusoidal microchannels dramatically enhance heat transfer. Studies' numerical results have been verified by comparison with those of experiments. The analysis of the flow properties and heat transmission in this kind of microchannel has been done using simulations. A low-pressure drop considerably enhances heat transmission in sinusoidal microchannels [125].

It is challenging to create sinusoidal microchannels and connect them to the external circuit. Systems for cooling are also employed sinusoidal microchannels in addition to coil microchannels [394]. **Fig. 8** provides a graphic representation of the length and temperature of sinusoidal microchannels employed by various researchers. The application in which each channel was used is also displayed on the graph.

In a system, the curved microchannels and others are typically regarded as heat-exchanger parts [395]. Therefore, rather than component optimization, these channels are built based on system optimization and other important criteria. Data-based analyses have shown that the friction properties of microchannels with a plane and an uneven surface differ significantly. Similar to ramified and ratchet microchannels, the friction factor rises with roughness at the same Reynolds number [396]. As a result, current research on curved and other unique microchannel shapes is done at the component level.

This study promotes the design of these microchannels and investigations of their flow properties by providing a brief overview of their key features. A visual representation of variously shaped microchannels employed by various scientists is revealed in **Fig. 9**. The

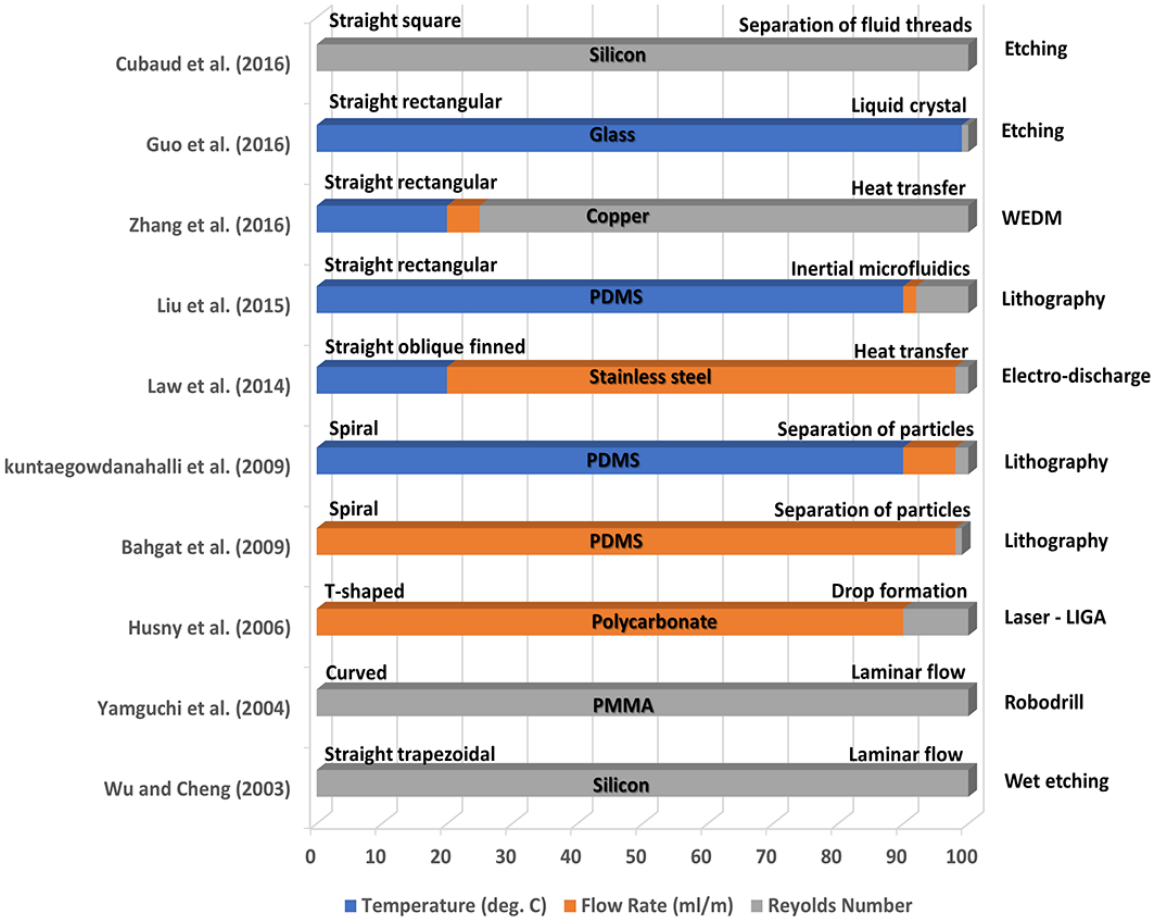

Fig. 10: Temperature, flow rate and Reynolds number illustration for fabrication of microchannels with applications.

application for which each channel was used is also displayed on the graph.

There is no method that is incredibly easy, quick, affordable, and reliable for the 3D production of microchannels. MEMS technological advancements are now addressing this significant issue. Silicon is used to create a variety of microchannels for some industrial and biological purposes, although it is not a good base material. Microfluidic, micromechanical, and micro-optics are just a few of the sectors that are advancing quickly. The flow properties are extremely important for each of these microchannels. A fluid flow may encounter resistance as a result of frictional causes. **Fig. 10** displays a graphic representation of different parameters of various microchannels created by various scientists. The material, method of production, and application of the microchannels are also shown in the graph.

In microchannel research, the experimental setup and behaviour measurement are crucial factors. A glass slide that is fastened to form a cover covers the microchannels in order to protect them. The microchannel system may be easily disassembled and cleaned thanks to this design. Because of this, any kind of analysis can be carried out during the experiment without taking the system apart. A definite indication of fluid leakage from the sample has been found in some testing of silicon microchannels. So, at such a small scale, very careful effort is required [397]. In double spiral microchannels, the continuous separation of particles in a heterogeneous mixture with charge was studied by Zhu et al. In this study, conductivity was also a factor, which led to the creation of curvature-induced DEP for the separation of many particles. Size, charge, and conductivity were the three main features that set the particles apart [161]. Many scientists, like DuBose et al., have studied how to separate bio-particles in double spiral microchannels. To separate the particles, they used a label-free synchronisation technique. Also suggested is the notion of a potential marker for C-iDEP isolation of contaminated cells [75]. A sinusoidal T-junction microchannel was examined by Solehati et al., Ozkan1, and Erdem. This kind of microchannel has received very little research [132,133]. This type of microchannel requires more research [105]. Rafeie et al. looked at the blood sample flow rate in spiral microchannels. The rate they employed was 530 L/min [159]. Kerhoas and Sollier looked at the application of active and passive devices in microfluidics for blood plasma separation [398]. Additionally, these gadgets are incompatible with the utilisation of blood samples for medical purposes [399]. In straight serpentine microchannels, Ashrafi et al. looked into the dynamics of

droplets [101]. Because straight serpentine microchannels can operate at low temperatures, they were used. The channels were simple to use and quite effective with little fluid [400]. The channels' poor performance when handling big amounts of fluid points to the necessity for more investigation. In microchannels, flow boiling characteristics were investigated by Recinella et al. Along that line, Hong et al. emphasized on the aspect ratio of parallel microchannels and their flow boiling criteria [401]. After testing multiple configurations, they have concluded that the large aspect ratio of microchannels dictates the flow instability. Therefore, several structural and thermodynamic parameters urge investigation from a designer's perspective such as aspect ratio and different modes of boiling. In comparison, the same group has established that there are several critical geometric parameters such as channel height (and resulting variation of liquid film thickness resulting change in bubble coalescence) associated with flow boiling characteristics in confined settings [402]. Moreover, Vontas *et al.* have shown that surface wettability is also an important parameter when flow boiling is considered in microchannels, where CFD modeling by using a customized volume of fluid (VOF) solver demonstrated that hydrophilic and hydrophobic surfaces can outperform single-phase models (43.9% and 17.8%, respectively) [403].

Additionally, a number of researchers have created and put to the test microchannels in theoretical [404] and numerical [331] investigations. They have established that microchannels, including radial arrays [405], straight, rectangular [406] microchannels, and pin finned microchannels [407], perform better when it comes to dispersing a significant amount of heat [408]. The outcomes of trials conducted under comparable conditions were then contrasted with those predicted by theory. The comparisons were trustworthy and showed excellent agreement [389]. Microchannels' geometric design has a number of drawbacks, including issues with backflow and sealing. Future studies should therefore examine ways to improve the geometry and design of microchannels.

6. Challenges and future aspects

The usage of microfluidic devices in the biomedical area is fraught with difficulties, including i) design, ii) manufacture, iii) material selection, and iv) assuring efficient and practical implementations.

The first consideration of the challenges of implementing microchannels comes from a fabrication and design perspective. The parameters of the microchannels are the most crucial factor in this regard [409]. To maintain the flow rate, velocity, pressure, dosing precision, material selection, ease of fabrication, fabrication technique, reliability, and durability at the lowest scale in microfluidic devices, the parameters must be precisely met. Other important factors, however, include low manufacturing costs, biocompatibility, the right channel type for a given application, the right length and diameter of the channel, flow pattern, flow boiling characteristics, and heat transfer characteristics [62,410]. Before applying a specific fabrication or design principle, experimental analysis at the prototype level or simulation with an in-house or commercial solver or analyzer is required. Among the available analyzing methodologies, CFD analysis by commercial solvers is a good choice for examining the flow characteristics. Due to the advancement of higher computational powers and the development of sophisticated numerical solvers, microchannels can be modeled with enhanced intricacy, and particular parameters can be analyzed, such as slug flow and related forces [58,411]. Furthermore, atomistic simulation can be deployed to analyze nanoparticle-level phenomena [412], as depicted by Arjmanfard et al, who implemented molecular dynamics simulation and showed that the rate of base fluid flow and temperature can be effectively manipulated by incorporating different sizes of Fe nanoparticles [413].

Micropumps are one of the more complex parts that have been documented in the literature for both medication delivery and fluid movement through channels [414]. However, due to some restrictions on commercial use in the biomedical field, the integration of these devices is extremely difficult. Therefore, the cost of manufacture must be reasonable and appropriate.

Last but not least, most of these problems have recently been addressed by research that uses polymeric materials. The primary obstacles restricting the development of microfluidic devices, according to the existing literature, are broad variables including economy, marketing, skill in the construction of microchannels, awareness, motivation, and inspiration of researchers, as well as a lack of cooperation [42]. However, in the upcoming years, the researchers can be optimistic that such factors will be managed in an organized manner if not abolished due to increased guidelines and collaboration between multicultural and diversified groups.

7. Conclusions

This review presents a brief yet focused outlook on the fabrication, applications, and prospects of microchannels to critically determine their field of implementation in large-scale and prospective industries. The major findings are as below:

a) The flow properties of straight microchannels have been extensively studied, and their fabrication is quite simple. Sinusoidal microchannels are extremely challenging to build, and it is challenging to analyze their flow characteristics. Investigations require numerical modelling and simulations. According to their uses and market demand, all other microchannels can be produced.
b) Microchannels are versatile and integrated components in a significant number of biomedical, industry-level applications. However, the most

developed fields of applications are radiation detectors, heat sink agents, integrated components in nanodevice systems, and drug delivery agents.

c) According to the requirements of industry and biomedicine, the variety of microchannel kinds may continue to grow. Heat transfer and fluid flow management are accomplished through the use of microchannels. It has been demonstrated that microchannels are useful tools for studying how cells function. Polymeric materials are employed more frequently to create microchannels because of their biocompatibility and potential for a wide range of applications.

d) From this discussion, it is substantiated that microchannels are versatile in terms of their applications. However, the most relevant and prospective ones are in radiation, heat sinking, and integration applications. With regards to the existent technology, optimized heat sinking technologies are still in high demand, and therefore, customized microchannels will be implemented at a larger scale over the next few decades. However, in terms of prospective applications, the next era will have revolutionary usage of clean energy, and therefore, nuclear reactors, fission, fusion, and related applications will be upscaled. With this regard, a significant portion of the research will be dedicated to developing microchannel applications at a larger scale in the industry in terms of radiation detection, as they have already proven their versatility in comparison with their rivals. Last but not the least, sophisticated drug delivery and nanodevices are implemented in a wide range of biomedical fields due to the increasing demand for addressing complex, chronic, and multifarious carcinogenic diseases. Therefore, microchannels will be significantly important in different aspects of such sub-fields of research.

Conflicts of interest

The authors declare that they have no competing interests.

Acknowledgments

This research did not receive any specific grant from funding agencies in the public, commercial, or not-for-profit sectors.

References

1) M.A.P. Mahmud, S.R. Bazaz, S. Dabiri, A.A. Mehrizi, M. Asadnia, M.E. Warkiani, and Z.L. Wang, "Advances in mems and microfluidics-based energy harvesting technologies," *Adv. Mater. Technol.*, 2101347 (2022). doi:10.1002/admt.202101347.

2) T. Singh, J. Arab, and P. Dixit, "A review on microholes formation in glass-based substrates by electrochemical discharge drilling for mems applications," *Mach. Sci. Technol.*, **26** (*2*) 276–337 (2022). doi:10.1080/10910344.2022.2044857.

3) G. Niu, and F. Wang, "A review of mems-based metal oxide semiconductors gas sensor in mainland china," *J. Micromechanics Microengineering*, **32** (*5*) 054003 (2022). doi:10.1088/1361-6439/ac5b98.

4) B. Malayappan, U.P. Lakshmi, B.V.V.S.N.P. Rao, K. Ramaswamy, and P.K. Pattnaik, "Sensing techniques and interrogation methods in optical mems accelerometers: a review," *IEEE Sens. J.*, **22** (*7*) 6232–6246 (2022). doi:10.1109/JSEN.2022.3149662.

5) M. Liao, "Progress in semiconductor diamond photodetectors and mems sensors," *Funct. Diam.*, **1** (*1*) 29–46 (2021). doi:10.1080/26941112.2021.1877019.

6) R.M.R. Pinto, V. Gund, R.A. Dias, K.K. Nagaraja, and K.B. Vinayakumar, "CMOS-integrated aluminum nitride mems: a review," *J. Microelectromechanical Syst.*, 1–24 (2022). doi:10.1109/JMEMS.2022.3172766.

7) M.K. Hossain, M.H. Ahmed, M.I. Khan, M.S. Miah, and S. Hossain, "Recent progress of rare earth oxides for sensor, detector, and electronic device applications: a review," *ACS Appl. Electron. Mater.*, **3** (*10*) 4255–4283 (2021). doi:10.1021/acsaelm.1c00703.

8) M.K. Hossain, S. Hossain, M.H. Ahmed, M.I. Khan, N. Haque, and G.A. Raihan, "A review on optical applications, prospects, and challenges of rare-earth oxides," *ACS Appl. Electron. Mater.*, **3** (*9*) 3715–3746 (2021). doi:10.1021/acsaelm.1c00682.

9) C. Chircov, and A.M. Grumezescu, "Microelectromechanical systems (mems) for biomedical applications," *Micromachines*, **13** (*2*) 164 (2022). doi:10.3390/mi13020164.

10) N. Alanazi, M. Almutairi, M. Muthuramamoorthy, and A. Alodhayb, "Review—measurements of ionizing radiations using micromechanical sensors," *ECS J. Solid State Sci. Technol.*, **11** (*5*) 057001 (2022). doi:10.1149/2162-8777/ac6f20.

11) vinayak pachkawade, and Z. Tse, "MEMS sensor for detection and measurement of ultra-fine particles," *Eng. Res. Express*, (2022). doi:10.1088/2631-8695/ac743a.

12) R.-J. Xu, and Y.-S. Lin, "Actively mems-based tunable metamaterials for advanced and emerging applications," *Electronics*, **11** (*2*) 243 (2022). doi:10.3390/electronics11020243.

13) H.-F. Liu, Z.-C. Luo, Z.-K. Hu, S.-Q. Yang, L.-C. Tu, Z.-B. Zhou, and M. Kraft, "A review of high-performance mems sensors for resource exploration and geophysical applications," *Pet. Sci.*, (2022).

doi:10.1016/j.petsci.2022.06.005.
14) V. Kant Bajpai, D. Kumar Mishra, and P. Dixit, "Fabrication of through-glass vias (tgv) based 3d microstructures in glass substrate by a lithography-free process for mems applications," *Appl. Surf. Sci.*, **584** 152494 (2022). doi:10.1016/j.apsusc.2022.152494.
15) T.G. Sachidananda, R.N. Chikkanagoudar, N. Pattar, and S. Nandurkar, "Investigations of the influence of geometrical parameters of carbon nanotube material for sensor and mems applications," *Mater. Today Proc.*, (2022). doi:10.1016/j.matpr.2022.05.119.
16) A. Kumar, and D. Kaur, "Magnetoelectric heterostructures for next-generation mems magnetic field sensing applications," *J. Alloys Compd.*, **897** 163091 (2022). doi:10.1016/j.jallcom.2021.163091.
17) C. Cao, Y. Ge, X. Ren, X. Peng, J. Chen, Z. Lu, and X. Zheng, "Experimental research on submarine cable monitoring method based on mems sensor," *Micro Nano Eng.*, **15** 100130 (2022). doi:10.1016/j.mne.2022.100130.
18) Y. Zhai, H. Li, Z. Tao, X. Cao, C. Yang, Z. Che, and T. Xu, "Design, fabrication and test of a bulk sic mems accelerometer," *Microelectron. Eng.*, **260** 111793 (2022). doi:10.1016/j.mee.2022.111793.
19) R.B. Mishra, F. Al-Modaf, W. Babatain, A.M. Hussain, and N. El-Atab, "Structural engineering approach for designing foil-based flexible capacitive pressure sensors," *IEEE Sens. J.*, 1–1 (2022). doi:10.1109/JSEN.2022.3174134.
20) M.I. Anik, M.K. Hossain, I. Hossain, I. Ahmed, and R.M. Doha, "Biomedical applications of magnetic nanoparticles," in: Magn. Nanoparticle-Based Hybrid Mater., Elsevier, 2021: pp. 463–497. doi:10.1016/B978-0-12-823688-8.00002-8.
21) A.M.U.. Mahfuz, M.K. Hossain, M.I. Khan, I. Hossain, and M.I. Anik, "Chapter 2: Smart drug-delivery nanostructured systems for cancer therapy," in: Gil Gonçalves (Ed.), New Trends Smart Nanostructured Biomater. Heal. Sci., Elsevier, Amsterdam, Netherlands, 2023.
22) M.I. Anik, M.K. Hossain, I. Hossain, A.M.U.B. Mahfuz, M.T. Rahman, and I. Ahmed, "Recent progress of magnetic nanoparticles in biomedical applications: a review," *Nano Sel.*, **2** (*6*) 1146–1186 (2021). doi:10.1002/nano.202000162.
23) S. Hossen, M.K. Hossain, M.K. Basher, M.N.H. Mia, M.T. Rahman, and M.J. Uddin, "Smart nanocarrier-based drug delivery systems for cancer therapy and toxicity studies: a review," *J. Adv. Res.*, **15** 1–18 (2019). doi:10.1016/j.jare.2018.06.005.
24) M.K. Hossain, M.I. Khan, and A. El-Denglawey, "A review on biomedical applications, prospects, and challenges of rare earth oxides," *Appl. Mater. Today*, **24** 101104 (2021). doi:10.1016/j.apmt.2021.101104.
25) M.I. Khan, M.I. Hossain, M.K. Hossain, M.H.K. Rubel, K.M. Hossain, A.M.U.B. Mahfuz, and M.I. Anik, "Recent progress in nanostructured smart drug delivery systems for cancer therapy: a review," *ACS Appl. Bio Mater.*, **5** (*3*) 971–1012 (2022). doi:10.1021/acsabm.2c00002.
26) N. Mahmud, M.I. Anik, M.K. Hossain, M.I. Khan, S. Uddin, M. Ashrafuzzaman, and M.M. Rahaman, "Advances in nanomaterial-based platforms to combat covid-19: diagnostics, preventions, therapeutics, and vaccine developments," *ACS Appl. Bio Mater.*, **5** (*6*) 2431–2460 (2022). doi:10.1021/acsabm.2c00123.
27) S. Manzoor, M.W. Ashraf, S. Tayyaba, M.I. Tariq, and M.K. Hossain, "Recent progress of fabrication, characterization, and applications of anodic aluminum oxide (aao) membrane: a review," *Comput. Model. Eng. Sci.*, (2022). doi:10.32604/cmes.2022.022093.
28) R. Choudhari, K. Ramesh, D. Tripathi, H. Vaidya, and K.V. Prasad, "Heat transfer and electroosmosis driven mhd peristaltic pumping in a microchannel with multiple slips and fluid properties," *Heat Transf.*, (2022). doi:10.1002/htj.22602.
29) S. Cao, N. Weerasekera, and D.R. Shingdan, "Modeling approaches for fluidic mass transport in next generation micro and nano biomedical sensors," *Eur. J. Biomed. Res.*, **1** (*3*) 1–9 (2022). doi:10.24018/ejbiomed.2022.1.3.12.
30) S. Shameem, A.P. Sindhu, V.T. Sai prabhu, K. Bhargavi, and K. Rajesh Babu, "Design of microchannel induced cantilever sensor to detect the rectal cancer," *J. Phys. Conf. Ser.*, **1804** (*1*) 012190 (2021). doi:10.1088/1742-6596/1804/1/012190.
31) A.S. Cerda-Kipper, and S. Hosseini, "Bio-microelectromechanical Systems (BioMEMS) in Bio-sensing Applications-Bioluminescence Detection Strategies," in: 2021: pp. 111–121. doi:10.1007/978-981-15-6382-9_5.
32) F. Marvi, and K. Jafari, "A measurement platform for label-free detection of biomolecules based on a novel optical biomems sensor," *IEEE Trans. Instrum. Meas.*, **70** 1–7 (2021). doi:10.1109/TIM.2021.3052001.
33) T. Habib, C. Brämer, C. Heuer, J. Ebbecke, S. Beutel, and J. Bahnemann, "3D-printed microfluidic device for protein purification in batch chromatography," *Lab Chip*, **22** (*5*) 986–993 (2022). doi:10.1039/D1LC01127H.
34) T. Limongi, F. Guzzi, E. Parrotta, P. Candeloro, S. Scalise, V. Lucchino, F. Gentile, L. Tirinato, M.L. Coluccio, B. Torre, M. Allione, M. Marini, F. Susa, E. Di Fabrizio, G. Cuda, and G. Perozziello, "Microfluidics for 3d cell and tissue cultures: microfabricative and ethical aspects updates," *Cells*, **11** (*10*) 1699 (2022). doi:10.3390/cells11101699.
35) H. Tang, J. Niu, H. Jin, S. Lin, and D. Cui, "Geometric structure design of passive label-free microfluidic systems for biological micro-object

separation," *Microsystems Nanoeng.*, **8** (*1*) 62 (2022). doi:10.1038/s41378-022-00386-y.

36) L. Sun, T. Lehnert, S. Li, and M.A.M. Gijs, "Bubble-enhanced ultrasonic microfluidic chip for rapid dna fragmentation," *Lab Chip*, **22** (*3*) 560–572 (2022). doi:10.1039/D1LC00933H.
37) A. Zizzari, E. Bloise, E. Perrone, D.R. Perinelli, M. Schmutz, V. Arima, G. Mele, and L. Carbone, "Environmentally friendly method of assembly of cardanol and cholesterol into nanostructures using a continuous flow microfluidic device," *ACS Sustain. Chem. Eng.*, (2022). doi:10.1021/acssuschemeng.2c01554.
38) M. Afzal, S. Tayyaba, M. Ashraf, M. Hossain, M. Uddin, and N. Afzulpurkar, "Simulation, fabrication and analysis of silver based ascending sinusoidal microchannel (asmc) for implant of varicose veins," *Micromachines*, **8** (*9*) 278 (2017). doi:10.3390/mi8090278.
39) M. Afzal, M. Ashraf, S. Tayyaba, M. Hossain, and N. Afzulpurkar, "Sinusoidal microchannel with descending curves for varicose veins implantation," *Micromachines*, **9** (*2*) 59 (2018). doi:10.3390/mi9020059.
40) D.J. Beebe, G.A. Mensing, and G.M. Walker, "Physics and applications of microfluidics in biology," *Annu. Rev. Biomed. Eng.*, **4** (*1*) 261–286 (2002). doi:10.1146/annurev.bioeng.4.112601.125916.
41) K.S. Lim, M. Baptista, S. Moon, T.B.F. Woodfield, and J. Rnjak-Kovacina, "Microchannels in development, survival, and vascularisation of tissue analogues for regenerative medicine," *Trends Biotechnol.*, **37** (*11*) 1189–1201 (2019). doi:10.1016/j.tibtech.2019.04.004.
42) M.W. Ashraf, S. Tayyaba, and N. Afzulpurkar, "Micro electromechanical systems (mems) based microfluidic devices for biomedical applications," *Int. J. Mol. Sci.*, **12** (*6*) 3648–3704 (2011). doi:10.3390/ijms12063648.
43) M. Asadi, G. Xie, and B. Sunden, "A review of heat transfer and pressure drop characteristics of single and two-phase microchannels," *Int. J. Heat Mass Transf.*, **79** 34–53 (2014). doi:10.1016/j.ijheatmasstransfer.2014.07.090.
44) T. Dixit, and I. Ghosh, "Review of micro- and mini-channel heat sinks and heat exchangers for single phase fluids," *Renew. Sustain. Energy Rev.*, **41** 1298–1311 (2015). doi:10.1016/j.rser.2014.09.024.
45) S.G. Kandlikar, "History, Advances, and Challenges in Liquid Flow and Flow Boiling Heat Transfer in Microchannels: A Critical Review," in: 2010 14th Int. Heat Transf. Conf. Vol. 8, ASMEDC, 2010: pp. 441–460. doi:10.1115/IHTC14-23353.
46) D. Erickson, and D. Li, "Integrated microfluidic devices," *Anal. Chim. Acta*, **507** (*1*) 11–26 (2004). doi:10.1016/j.aca.2003.09.019.
47) A.D. Ferguson, M. Bahrami, and J.R. Culham, "Review of Experimental Procedure for Determining Liquid Flow in Microchannels," in: ASME 3rd Int. Conf. Microchannels Minichannels, Parts A B, ASME, 2005: pp. 303–311. doi:10.1115/ICMM2005-75126.
48) M. Mohammadi, and K. V. Sharp, "Experimental techniques for bubble dynamics analysis in microchannels: a review," *J. Fluids Eng.*, **135** (*2*) (2013). doi:10.1115/1.4023450.
49) S.G. Kandlikar, "Microchannels and Minichannels: History, Terminology, Classification and Current Research Needs," in: 1st Int. Conf. Microchannels Minichannels, ASMEDC, 2003: pp. 1–6. doi:10.1115/ICMM2003-1000.
50) S. Meng, W. Lu, C. Zeng, R. Qin, and Z. Xu, "Construction and analyses of molecular exchange flow for gas mixtures in microchannels," *Chem. Pap.*, **76** (*5*) 3185–3199 (2022). doi:10.1007/s11696-022-02096-1.
51) H.S. Singh, S. P.M.V., and S. Dhanekar, "Experimental and numerical study of gas flow through the microchannel with 90° bends," *J. Micromechanics Microengineering*, (2022). doi:10.1088/1361-6439/ac7b0d.
52) B. Dash, J. Nanda, and S.K. Rout, "The role of microchannel geometry selection on heat transfer enhancement in heat sinks: a review," *Heat Transf.*, **51** (*2*) 1406–1424 (2022). doi:10.1002/htj.22357.
53) F.S. Alkasmoul, M. Asaker, A. Almogbel, and A. AlSuwailem, "Combined effect of thermal and hydraulic performance of different nanofluids on their cooling efficiency in microchannel heat sink," *Case Stud. Therm. Eng.*, **30** 101776 (2022). doi:10.1016/j.csite.2022.101776.
54) J. Yim, E. Verkama, J.A. Velasco, K. Arts, and R.L. Puurunen, "Conformality of atomic layer deposition in microchannels: impact of process parameters on the simulated thickness profile," *Phys. Chem. Chem. Phys.*, **24** (*15*) 8645–8660 (2022). doi:10.1039/D1CP04758B.
55) X. He, M.O. Sidi, N.A. Ahammad, M.A. Elkotb, S. Elattar, and A.M. Algelany, "Artificial neural network joined with lattice boltzmann method to study the effects of mhd on the slip velocity of fmwnt/water nanofluid flow inside a microchannel," *Eng. Anal. Bound. Elem.*, **143** 95–108 (2022). doi:10.1016/j.enganabound.2022.05.027.
56) R. Mohammadi, and N. Shahkarami, "Performance improvement of rectangular microchannel heat sinks using nanofluids and wavy channels," *Numer. Heat Transf. Part A Appl.*, 1–21 (2022). doi:10.1080/10407782.2022.2083840.
57) H.A. Kose, A. Yildizeli, and S. Cadirci, "Parametric study and optimization of microchannel heat sinks with various shapes," *Appl. Therm. Eng.*, **211** 118368 (2022).

doi:10.1016/j.applthermaleng.2022.118368.
58) A.J. Chamkha, M. Molana, A. Rahnama, and F. Ghadami, "On the nanofluids applications in microchannels: a comprehensive review," *Powder Technol.*, **332** 287–322 (2018). doi:10.1016/j.powtec.2018.03.044.
59) K.X. Cheng, Z.H. Foo, and K.T. Ooi, "Heat transfer enhancement through periodic flow area variations in microchannels," *Int. Commun. Heat Mass Transf.*, **111** 104456 (2020). doi:10.1016/j.icheatmasstransfer.2019.104456.
60) M. Sattari-Najafabadi, M. Nasr Esfahany, Z. Wu, and B. Sunden, "Mass transfer between phases in microchannels: a review," *Chem. Eng. Process. - Process Intensif.*, **127** 213–237 (2018). doi:10.1016/j.cep.2018.03.012.
61) Y. Yin, R. Guo, C. Zhu, T. Fu, and Y. Ma, "Enhancement of gas-liquid mass transfer in microchannels by rectangular baffles," *Sep. Purif. Technol.*, **236** 116306 (2020). doi:10.1016/j.seppur.2019.116306.
62) J. Qian, X. Li, Z. Wu, Z. Jin, and B. Sunden, "A comprehensive review on liquid–liquid two-phase flow in microchannel: flow pattern and mass transfer," *Microfluid. Nanofluidics*, **23** (*10*) 116 (2019). doi:10.1007/s10404-019-2280-4.
63) F. Zhang, B. Wu, and B. Du, "Heat transfer optimization based on finned microchannel heat sink," *Int. J. Therm. Sci.*, **172** 107357 (2022). doi:10.1016/j.ijthermalsci.2021.107357.
64) L. Sha, S. Tao, and J. Tu, "Application and progress of microfluidic systems based on microchannels," in: K. Chen, N. Lin, R. Meštrović, T.A. Oliveira, F. Cen, H.-M. Yin (Eds.), Int. Conf. Stat. Appl. Math. Comput. Sci. (CSAMCS 2021), SPIE, 2022: p. 207. doi:10.1117/12.2628129.
65) H. Sadique, Q. Murtaza, and Samsher, "Heat transfer augmentation in microchannel heat sink using secondary flows: a review," *Int. J. Heat Mass Transf.*, **194** 123063 (2022). doi:10.1016/j.ijheatmasstransfer.2022.123063.
66) M.T. Al-Asadi, H.A. Mohammed, and M.C.T. Wilson, "Heat transfer characteristics of conventional fluids and nanofluids in micro-channels with vortex generators: a review," *Energies*, **15** (*3*) 1245 (2022). doi:10.3390/en15031245.
67) U. Sarma, P. Chandra, and S.N. Joshi, "Advanced Microchannel Fabrication Technologies for Biomedical Devices," in: 2022: pp. 127–143. doi:10.1007/978-981-16-3645-5_6.
68) S. Zhang, F. Ahmad, A. Khan, N. Ali, and M. Badran, "Performance improvement and thermodynamic assessment of microchannel heat sink with different types of ribs and cones," *Sci. Rep.*, **12** (*1*) 10802 (2022). doi:10.1038/s41598-022-14428-y.
69) J. Wang, Y.-P. Xu, R. Qahiti, M. Jafaryar, M.A. Alazwari, N.H. Abu-Hamdeh, A. Issakhov, and M.M. Selim, "Simulation of hybrid nanofluid flow within a microchannel heat sink considering porous media analyzing cpu stability," *J. Pet. Sci. Eng.*, **208** 109734 (2022). doi:10.1016/j.petrol.2021.109734.
70) M. SAITO, L. YIN, I. KOBAYASHI, and M. NAKAJIMA, "Preparation characteristics of monodispersed oil-in-water emulsions with large particles stabilized by proteins in straight-through microchannel emulsification," *Food Hydrocoll.*, **19** (*4*) 745–751 (2005). doi:10.1016/j.foodhyd.2004.08.005.
71) X. Liu, W. Tao, Z. Li, and Y. He, "Three-dimensional transport model of pem fuel cell with straight flow channels," *J. Power Sources*, **158** (*1*) 25–35 (2006). doi:10.1016/j.jpowsour.2005.08.046.
72) M.E. Emiroglu, H. Agaccioglu, and N. Kaya, "Discharging capacity of rectangular side weirs in straight open channels," *Flow Meas. Instrum.*, **22** (*4*) 319–330 (2011). doi:10.1016/j.flowmeasinst.2011.04.003.
73) T. Cubaud, D. Henderson, and X. Hu, "Separation of highly viscous fluid threads in branching microchannels," *Microfluid. Nanofluidics*, **20** (*4*) 1–10 (2016).
74) P. Garstecki, M.J. Fuerstman, H.A. Stone, and G.M. Whitesides, "Formation of droplets and bubbles in a microfluidic t-junction—scaling and mechanism of break-up," *Lab Chip*, **6** (*3*) 437–446 (2006).
75) J. DuBose, X. Lu, S. Patel, S. Qian, S.W. Joo, and X. Xuan, "Microfluidic electrical sorting of particles based on shape in a spiral microchannel," *Biomicrofluidics*, **8** (*1*) 14101 (2014).
76) S.H. Lee, and I. Mudawar, "Investigation of flow boiling in large micro-channel heat exchangers in a refrigeration loop for space applications," *Int. J. Heat Mass Transf.*, **97** 110–129 (2016).
77) N.I. Om, P. Gunnasegaran, and S. Rajasegaran, "Influence of sinusoidal flow on the thermal and hydraulic performance of microchannel heat sink," *IOP Conf. Ser. Earth Environ. Sci.*, **16** 012075 (2013). doi:10.1088/1755-1315/16/1/012075.
78) G. Xie, F. Zhang, B. Sundén, and W. Zhang, "Constructal design and thermal analysis of microchannel heat sinks with multistage bifurcations in single-phase liquid flow," *Appl. Therm. Eng.*, **62** (*2*) 791–802 (2014). doi:10.1016/j.applthermaleng.2013.10.042.
79) C. Liu, C. Xue, X. Chen, L. Shan, Y. Tian, and G. Hu, "Size-based separation of particles and cells utilizing viscoelastic effects in straight microchannels," *Anal. Chem.*, **87** (*12*) 6041–6048 (2015). doi:10.1021/acs.analchem.5b00516.
80) A. Sabaghan, M. Edalatpour, M.C. Moghadam, E. Roohi, and H. Niazmand, "Nanofluid flow and heat transfer in a microchannel with longitudinal vortex generators: two-phase numerical simulation," *Appl. Therm. Eng.*, **100** 179–189 (2016).

doi:10.1016/j.applthermaleng.2016.02.020.
81) L. Chai, G.D. Xia, and H.S. Wang, "Laminar flow and heat transfer characteristics of interrupted microchannel heat sink with ribs in the transverse microchambers," *Int. J. Therm. Sci.*, **110** 1–11 (2016). doi:10.1016/j.ijthermalsci.2016.06.029.
82) M. Wörner, "Approximate residence time distribution of fully develop laminar flow in a straight rectangular channel," *Chem. Eng. Sci.*, **65** (*11*) 3499–3507 (2010). doi:10.1016/j.ces.2010.02.047.
83) V. Yadav, K. Baghel, R. Kumar, and S.T. Kadam, "Numerical investigation of heat transfer in extended surface microchannels," *Int. J. Heat Mass Transf.*, **93** 612–622 (2016). doi:10.1016/j.ijheatmasstransfer.2015.10.023.
84) P.B. Muller, M. Rossi, Á.G. Marín, R. Barnkob, P. Augustsson, T. Laurell, C.J. Kähler, and H. Bruus, "Ultrasound-induced acoustophoretic motion of microparticles in three dimensions," *Phys. Rev. E*, **88** (*2*) 023006 (2013). doi:10.1103/PhysRevE.88.023006.
85) S. Ma, J.M. Sherwood, W.T.S. Huck, and S. Balabani, "On the flow topology inside droplets moving in rectangular microchannels," *Lab Chip*, **14** (*18*) 3611–3620 (2014). doi:10.1039/C4LC00671B.
86) H. Masuda, K. Ito, T. Oshima, and K. Sasaki, "Comparison between numerical simulation and visualization experiment on water behavior in single straight flow channel polymer electrolyte fuel cells," *J. Power Sources*, **177** (*2*) 303–313 (2008). doi:10.1016/j.jpowsour.2007.11.069.
87) C. Liu, C. Xue, and G. Hu, "Sheathless separation of particles and cells by viscoelastic effects in straight rectangular microchannels," *Procedia Eng.*, **126** 721–724 (2015). doi:10.1016/j.proeng.2015.11.278.
88) S. Zhang, Y. Tang, W. Yuan, J. Zeng, and Y. Xie, "A comparative study of flow boiling performance in the interconnected microchannel net and rectangular microchannels," *Int. J. Heat Mass Transf.*, **98** 814–823 (2016). doi:10.1016/j.ijheatmasstransfer.2016.03.066.
89) Y. Guo, S. Afghah, J. Xiang, O.D. Lavrentovich, R.L.B. Selinger, and Q.-H. Wei, "Cholesteric liquid crystals in rectangular microchannels: skyrmions and stripes," *Soft Matter*, **12** (*29*) 6312–6320 (2016). doi:10.1039/C6SM01190J.
90) H.. Wu, and P. Cheng, "Friction factors in smooth trapezoidal silicon microchannels with different aspect ratios," *Int. J. Heat Mass Transf.*, **46** (*14*) 2519–2525 (2003). doi:10.1016/S0017-9310(03)00106-6.
91) H.. Wu, and P. Cheng, "An experimental study of convective heat transfer in silicon microchannels with different surface conditions," *Int. J. Heat Mass Transf.*, **46** (*14*) 2547–2556 (2003). doi:10.1016/S0017-9310(03)00035-8.
92) H. Liao, and D.W. Knight, "Analytic stage–discharge formulae for flow in straight trapezoidal open channels," *Adv. Water Resour.*, **30** (*11*) 2283–2295 (2007). doi:10.1016/j.advwatres.2007.05.002.
93) N.R. Kuppusamy, H.A. Mohammed, and C.W. Lim, "Numerical investigation of trapezoidal grooved microchannel heat sink using nanofluids," *Thermochim. Acta*, **573** 39–56 (2013). doi:10.1016/j.tca.2013.09.011.
94) B. Fani, M. Kalteh, and A. Abbassi, "Investigating the effect of brownian motion and viscous dissipation on the nanofluid heat transfer in a trapezoidal microchannel heat sink," *Adv. Powder Technol.*, **26** (*1*) 83–90 (2015). doi:10.1016/j.apt.2014.08.009.
95) A.M. Abed, M.A. Alghoul, K. Sopian, H.A. Mohammed, H. sh. Majdi, and A.N. Al-Shamani, "Design characteristics of corrugated trapezoidal plate heat exchangers using nanofluids," *Chem. Eng. Process. Process Intensif.*, **87** 88–103 (2015). doi:10.1016/j.cep.2014.11.005.
96) R. Xiong, and J.N. Chung, "Flow characteristics of water in straight and serpentine micro-channels with miter bends," *Exp. Therm. Fluid Sci.*, **31** (*7*) 805–812 (2007). doi:10.1016/j.expthermflusci.2006.08.006.
97) A. Fazeli, and M. Behnam, "Hydrogen production in a zigzag and straight catalytic wall coated micro channel reactor by cfd modeling," *Int. J. Hydrogen Energy*, **35** (*17*) 9496–9503 (2010). doi:10.1016/j.ijhydene.2010.05.052.
98) A. Afzal, and K.-Y. Kim, "Flow and mixing analysis of non-newtonian fluids in straight and serpentine microchannels," *Chem. Eng. Sci.*, **116** 263–274 (2014). doi:10.1016/j.ces.2014.05.021.
99) S. Huang, J. Zhao, L. Gong, and X. Duan, "Thermal performance and structure optimization for slotted microchannel heat sink," *Appl. Therm. Eng.*, **115** 1266–1276 (2017). doi:10.1016/j.applthermaleng.2016.09.131.
100) X. Yan, M. Liu, J. Zhang, H. Zhu, Y. Li, and K. Liang, "On-chip investigation of the hydrodynamic dispersion in rectangular microchannels," *Microfluid. Nanofluidics*, **19** (*2*) 435–445 (2015). doi:10.1007/s10404-015-1576-2.
101) M. Ashrafi, M. Shams, A. Bozorgnezhad, and G. Ahmadi, "Simulation and experimental validation of droplet dynamics in microchannels of pem fuel cells," *Heat Mass Transf.*, **52** (*12*) 2671–2686 (2016). doi:10.1007/s00231-016-1771-z.
102) M. Roudet, K. Loubiere, C. Gourdon, and M. Cabassud, "Hydrodynamic and mass transfer in inertial gas–liquid flow regimes through straight and meandering millimetric square channels," *Chem. Eng. Sci.*, **66** (*13*) 2974–2990 (2011). doi:10.1016/j.ces.2011.03.045.
103) N. Dietrich, K. Loubière, M. Jimenez, G. Hébrard, and C. Gourdon, "A new direct technique for

visualizing and measuring gas–liquid mass transfer around bubbles moving in a straight millimetric square channel," *Chem. Eng. Sci.*, **100** 172–182 (2013). doi:10.1016/j.ces.2013.03.041.

104) J. Yao, Y. Zhao, and M. Fairweather, "Numerical simulation of turbulent flow through a straight square duct," *Appl. Therm. Eng.*, **91** 800–811 (2015). doi:10.1016/j.applthermaleng.2015.08.065.

105) F. Kaya, "Numerical investigation of effects of ramification length and angle on pressure drop and heat transfer in a ramified microchannel," *J. Appl. Fluid Mech.*, **9** (*2*) 767–772 (2016).

106) Y. Fan, P.S. Lee, L.-W. Jin, and B.W. Chua, "A simulation and experimental study of fluid flow and heat transfer on cylindrical oblique-finned heat sink," *Int. J. Heat Mass Transf.*, **61** 62–72 (2013). doi:10.1016/j.ijheatmasstransfer.2013.01.075.

107) M. Law, P.-S. Lee, and K. Balasubramanian, "Experimental investigation of flow boiling heat transfer in novel oblique-finned microchannels," *Int. J. Heat Mass Transf.*, **76** 419–431 (2014). doi:10.1016/j.ijheatmasstransfer.2014.04.045.

108) J. Lu, and W.-Q. Lu, "A numerical simulation for mass transfer through the porous membrane of parallel straight channels," *Int. J. Heat Mass Transf.*, **53** (*11–12*) 2404–2413 (2010). doi:10.1016/j.ijheatmasstransfer.2010.01.043.

109) M. Law, and P.-S. Lee, "Comparative study of temperature and pressure instabilities during flow boiling in straight- and 10° oblique-finned microchannels," *Energy Procedia*, **75** 3105–3112 (2015). doi:10.1016/j.egypro.2015.07.642.

110) M. Law, O.B. Kanargi, and P.-S. Lee, "Effects of varying oblique angles on flow boiling heat transfer and pressure characteristics in oblique-finned microchannels," *Int. J. Heat Mass Transf.*, **100** 646–660 (2016). doi:10.1016/j.ijheatmasstransfer.2016.04.077.

111) J. Chen, S.K. Stefanov, L. Baldas, and S. Colin, "Analysis of flow induced by temperature fields in ratchet-like microchannels by direct simulation monte carlo," *Int. J. Heat Mass Transf.*, **99** 672–680 (2016). doi:10.1016/j.ijheatmasstransfer.2016.04.023.

112) L. Goldstein, and E.M. Sparrow, "Heat/mass transfer characteristics for flow in a corrugated wall channel," *J. Heat Transfer*, **99** (*2*) 187–195 (1977). doi:10.1115/1.3450667.

113) T. Nishimura, and N. Kojima, "Mass transfer enhancement in a symmetric sinusoidal wavy-walled channel for pulsatile flow," *Int. J. Heat Mass Transf.*, **38** (*9*) 1719–1731 (1995). doi:10.1016/0017-9310(94)00275-Z.

114) T. Nishimura, and S. Matsune, "Vortices and wall shear stresses in asymmetric and symmetric channels with sinusoidal wavy walls for pulsatile flow at low reynolds numbers," *Int. J. Heat Fluid Flow*, **19** (*6*) 583–593 (1998). doi:10.1016/S0142-727X(98)10005-X.

115) T. a. Rush, T. a. Newell, and A. m. Jacobi, "An experimental study of flow and heat transfer in sinusoidal wavy passages," *Int. J. Heat Mass Transf.*, **42** (*9*) 1541–1553 (1999). doi:10.1016/S0017-9310(98)00264-6.

116) B. Ničeno, and E. Nobile, "Numerical analysis of fluid flow and heat transfer in periodic wavy channels," *Int. J. Heat Fluid Flow*, **22** (*2*) 156–167 (2001). doi:10.1016/S0142-727X(01)00074-1.

117) H.M. Metwally, and R.M. Manglik, "Enhanced heat transfer due to curvature-induced lateral vortices in laminar flows in sinusoidal corrugated-plate channels," *Int. J. Heat Mass Transf.*, **47** (*10–11*) 2283–2292 (2004). doi:10.1016/j.ijheatmasstransfer.2003.11.019.

118) K. Zniber, A. Oubarra, and J. Lahjomri, "Analytical solution to the problem of heat transfer in an mhd flow inside a channel with prescribed sinusoidal wall heat flux," *Energy Convers. Manag.*, **46** (*7–8*) 1147–1163 (2005). doi:10.1016/j.enconman.2004.06.023.

119) M. Emin Emiroglu, O. Kisi, and O. Bilhan, "Predicting discharge capacity of triangular labyrinth side weir located on a straight channel by using an adaptive neuro-fuzzy technique," *Adv. Eng. Softw.*, **41** (*2*) 154–160 (2010). doi:10.1016/j.advengsoft.2009.09.006.

120) K. Nilpueng, and S. Wongwises, "Flow pattern and pressure drop of vertical upward gas–liquid flow in sinusoidal wavy channels," *Exp. Therm. Fluid Sci.*, **30** (*6*) 523–534 (2006). doi:10.1016/j.expthermflusci.2005.10.004.

121) N.R. Rosaguti, D.F. Fletcher, and B.S. Haynes, "Low-reynolds number heat transfer enhancement in sinusoidal channels," *Chem. Eng. Sci.*, **62** (*3*) 694–702 (2007). doi:10.1016/j.ces.2006.09.045.

122) G.-N. Xie, Q.-W. Wang, M. Zeng, and L.-Q. Luo, "Numerical investigation of heat transfer and fluid flow characteristics inside a wavy channel," *Heat Mass Transf.*, **43** (*7*) 603–611 (2007). doi:10.1007/s00231-006-0133-7.

123) D. Yang, and Y. Liu, "Numerical simulation of electroosmotic flow in microchannels with sinusoidal roughness," *Colloids Surfaces A Physicochem. Eng. Asp.*, **328** (*1–3*) 28–33 (2008). doi:10.1016/j.colsurfa.2008.06.029.

124) F. Oviedo-Tolentino, R. Romero-Méndez, A. Hernández-Guerrero, and B. Girón-Palomares, "Experimental study of fluid flow in the entrance of a sinusoidal channel," *Int. J. Heat Fluid Flow*, **29** (*5*) 1233–1239 (2008). doi:10.1016/j.ijheatfluidflow.2008.03.017.

125) S.W. Chang, A.W. Lees, and T.C. Chou, "Heat transfer and pressure drop in furrowed channels with transverse and skewed sinusoidal wavy walls," *Int. J. Heat Mass Transf.*, **52** (*19–20*) 4592–4603 (2009).

doi:10.1016/j.ijheatmasstransfer.2009.02.039.
126) F. Oviedo-Tolentino, R. Romero-Méndez, A. Hernández-Guerrero, and B. Girón-Palomares, "Use of diverging or converging arrangement of plates for the control of chaotic mixing in symmetric sinusoidal plate channels," *Exp. Therm. Fluid Sci.*, **33** (*2*) 208–214 (2009). doi:10.1016/j.expthermflusci.2008.08.002.
127) H. Heidary, and M.J. Kermani, "Effect of nano-particles on forced convection in sinusoidal-wall channel," *Int. Commun. Heat Mass Transf.*, **37** (*10*) 1520–1527 (2010). doi:10.1016/j.icheatmasstransfer.2010.08.018.
128) Z. Lu, C. Rath, G. Zhang, and S.G. Kandlikar, "Water management studies in pem fuel cells, part iv: effects of channel surface wettability, geometry and orientation on the two-phase flow in parallel gas channels," *Int. J. Hydrogen Energy*, **36** (*16*) 9864–9875 (2011). doi:10.1016/j.ijhydene.2011.04.226.
129) L. Chang, Y. Jian, M. Buren, Q. Liu, and Y. Sun, "Electroosmotic flow through a microtube with sinusoidal roughness," *J. Mol. Liq.*, **220** 258–264 (2016). doi:10.1016/j.molliq.2016.04.054.
130) O. Bilhan, M. Emin Emiroglu, and O. Kisi, "Application of two different neural network techniques to lateral outflow over rectangular side weirs located on a straight channel," *Adv. Eng. Softw.*, **41** (*6*) 831–837 (2010). doi:10.1016/j.advengsoft.2010.03.001.
131) Z.L. Chiam, P.S. Lee, P.K. Singh, and N. Mou, "Investigation of fluid flow and heat transfer in wavy micro-channels with alternating secondary branches," *Int. J. Heat Mass Transf.*, **101** 1316–1330 (2016). doi:10.1016/j.ijheatmasstransfer.2016.05.097.
132) N. Solehati, J. Bae, and A.P. Sasmito, "Numerical investigation of mixing performance in microchannel t-junction with wavy structure," *Comput. Fluids*, **96** 10–19 (2014). doi:10.1016/j.compfluid.2014.03.003.
133) A. Özkan, and E.Y. Erdem, "Numerical analysis of mixing performance in sinusoidal microchannels based on particle motion in droplets," *Microfluid. Nanofluidics*, **19** (*5*) 1101–1108 (2015). doi:10.1007/s10404-015-1628-7.
134) Y.. Fares, "Calculation of transverse energy regime in curved channels," *Comput. Geosci.*, **26** (*3*) 267–276 (2000). doi:10.1016/S0098-3004(99)00131-4.
135) W. Yang, J. Zhang, and H. Cheng, "The study of flow characteristics of curved microchannel," *Appl. Therm. Eng.*, **25** (*13*) 1894–1907 (2005). doi:10.1016/j.applthermaleng.2004.12.001.
136) Y.-M. Shen, C.-O. Ng, and H.-Q. Ni, "3D numerical modeling of non-isotropic turbulent buoyant helicoidal flow and heat transfer in a curved open channel," *Int. J. Heat Mass Transf.*, **46** (*11*) 2087–2093 (2003). doi:10.1016/S0017-9310(02)00501-X.
137) Y. Yamaguchi, F. Takagi, T. Watari, K. Yamashita, H. Nakamura, H. Shimizu, and H. Maeda, "Interface configuration of the two layered laminar flow in a curved microchannel," *Chem. Eng. J.*, **101** (*1*) 367–372 (2004).
138) D.M. Kirpalani, T. Patel, P. Mehrani, and A. Macchi, "Experimental analysis of the unit cell approach for two-phase flow dynamics in curved flow channels," *Int. J. Heat Mass Transf.*, **51** (*5*) 1095–1103 (2008).
139) Z. Che, T.N. Wong, and N.-T. Nguyen, "An analytical model for a liquid plug moving in curved microchannels," *Int. J. Heat Mass Transf.*, **53** (*9*) 1977–1985 (2010).
140) O. Bilhan, M.E. Emiroglu, and O. Kisi, "Use of artificial neural networks for prediction of discharge coefficient of triangular labyrinth side weir in curved channels," *Adv. Eng. Softw.*, **42** (*4*) 208–214 (2011).
141) M.E. Emiroglu, O. Bilhan, and O. Kisi, "Neural networks for estimation of discharge capacity of triangular labyrinth side-weir located on a straight channel," *Expert Syst. Appl.*, **38** (*1*) 867–874 (2011). doi:10.1016/j.eswa.2010.07.058.
142) J. Xuan, M.K.H. Leung, D.Y.C. Leung, and M. Ni, "Density-induced asymmetric pair of dean vortices and its effects on mass transfer in a curved microchannel with two-layer laminar stream," *Chem. Eng. J.*, **171** (*1*) 216–223 (2011).
143) R. Renault, J.-B. Durand, J.-L. Viovy, and C. Villard, "Asymmetric axonal edge guidance: a new paradigm for building oriented neuronal networks," *Lab Chip*, **16** (*12*) 2188–2191 (2016).
144) J.-C. Chu, J.-T. Teng, and R. Greif, "Experimental and numerical study on the flow characteristics in curved rectangular microchannels," *Appl. Therm. Eng.*, **30** (*13*) 1558–1566 (2010).
145) J. Guo, M. Xu, and L. Cheng, "Second law analysis of curved rectangular channels," *Int. J. Therm. Sci.*, **50** (*5*) 760–768 (2011).
146) Y. Li, X. Wang, S. Yuan, and S.K. Tan, "Flow development in curved rectangular ducts with continuously varying curvature," *Exp. Therm. Fluid Sci.*, **75** 1–15 (2016).
147) J. Zhu, and X. Xuan, "Particle electrophoresis and dielectrophoresis in curved microchannels," *J. Colloid Interface Sci.*, **340** (*2*) 285–290 (2009).
148) K. Hyoung Kang, X. Xuan, Y. Kang, and D. Li, "Effects of dc-dielectrophoretic force on particle trajectories in microchannels," *J. Appl. Phys.*, **99** (*6*) 064702 (2006). doi:10.1063/1.2180430.
149) K.H. Kang, Y. Kang, X. Xuan, and D. Li, "Continuous separation of microparticles by size with direct current-dielectrophoresis," *Electrophoresis*, **27** (*3*) 694–702 (2006). doi:10.1002/elps.200500558.
150) J. Guo, M. Xu, and L. Cheng, "Numerical investigations of curved square channel from the viewpoint of field synergy principle," *Int. J. Heat Mass Transf.*, **54** (*17*) 4148–4151 (2011).

151) M. Kalteh, A. Abbassi, M. Saffar-Avval, and J. Harting, "Eulerian–eulerian two-phase numerical simulation of nanofluid laminar forced convection in a microchannel," *Int. J. Heat Fluid Flow*, **32** (*1*) 107–116 (2011).
152) H. Masuda, A. Yamamoto, K. Sasaki, S. Lee, and K. Ito, "A visualization study on relationship between water-droplet behavior and cell voltage appeared in straight, parallel and serpentine channel pattern cells," *J. Power Sources*, **196** (*13*) 5377–5385 (2011). doi:10.1016/j.jpowsour.2011.02.074.
153) W. Wewala, N. Afzulpurkar, J.K. Kasi, A.K. Kasi, A. Poyai, and D.W. Bodhale, "Design and simulation of ascending curvilinear micro channel for cancer cell separation from blood," in: Adv. Mater. Res., Trans Tech Publ, 2012: pp. 2361–2366.
154) W. Wewala, J.K. Kasi, A.K. Kasi, and N. Afzulpurkar, "DESIGN, simulation and comparison of ascending and descending curvilinear microchannels for cancer cell separation from blood," *Biomed. Eng. Appl. Basis Commun.*, **25** (*03*) 1350037 (2013).
155) X.Y.L. Peng, P.C.H. Li, H.-Z. Yu, M.P. Ash, and W.L.J. Chou, "Spiral microchannels on a cd for dna hybridizations," *Sensors Actuators B Chem.*, **128** (*1*) 64–69 (2007).
156) S.S. Kuntaegowdanahalli, A.A.S. Bhagat, G. Kumar, and I. Papautsky, "Inertial microfluidics for continuous particle separation in spiral microchannels," *Lab Chip*, **9** (*20*) 2973–2980 (2009).
157) N. Nivedita, P. Ligrani, and I. Papautsky, "Evolution of secondary dean vortices in spiral microchannels for cell separations," in: 17th Int. Conf. Miniaturized Syst. Chem. Life Sci. Freiburg, Ger., 2013.
158) G. Guan, L. Wu, A.A. Bhagat, Z. Li, P.C.Y. Chen, S. Chao, C.J. Ong, and J. Han, "Spiral microchannel with rectangular and trapezoidal cross-sections for size based particle separation," *Sci. Rep.*, **3** 1475 (2013). doi:10.1038/srep01475http://www.nature.com/articles/srep01475#supplementary-information.
159) M. Rafeie, J. Zhang, M. Asadnia, W. Li, and M.E. Warkiani, "Multiplexing slanted spiral microchannels for ultra-fast blood plasma separation," *Lab Chip*, **16** (*15*) 2791–2802 (2016).
160) H. Chen, L. Wang, and P.C.H. Li, "Nucleic acid microarrays created in the double-spiral format on a circular microfluidic disk," *Lab Chip*, **8** (*5*) 826–829 (2008).
161) J. Zhu, and X. Xuan, "Curvature-induced dielectrophoresis for continuous separation of particles by charge in spiral microchannels," *Biomicrofluidics*, **5** (*2*) 24111 (2011).
162) J. Sun, M. Li, C. Liu, Y. Zhang, D. Liu, W. Liu, G. Hu, and X. Jiang, "Double spiral microchannel for label-free tumor cell separation and enrichment," *Lab Chip*, **12** (*20*) 3952–3960 (2012).
163) A.E. Yaroshchuk, "Transport properties of long straight nano-channels in electrolyte solutions: a systematic approach," *Adv. Colloid Interface Sci.*, **168** (*1–2*) 278–291 (2011). doi:10.1016/j.cis.2011.03.009.
164) A.M. Ganán-Calvo, and J.M. Gordillo, "Perfectly monodisperse microbubbling by capillary flow focusing," *Phys. Rev. Lett.*, **87** (*27*) 274501 (2001).
165) C. Xue, X. Chen, C. Liu, and G. Hu, "Lateral migration of dual droplet trains in a double spiral microchannel," *Sci. China Physics, Mech. Astron.*, **59** (*7*) 1–10 (2016).
166) J. Husny, and J.J. Cooper-White, "The effect of elasticity on drop creation in t-shaped microchannels," *J. Nonnewton. Fluid Mech.*, **137** (*1*) 121–136 (2006).
167) S. Van der Graaf, T. Nisisako, C. Schroen, R.G.M. Van Der Sman, and R.M. Boom, "Lattice boltzmann simulations of droplet formation in a t-shaped microchannel," *Langmuir*, **22** (*9*) 4144–4152 (2006).
168) A.D. Gat, I. Frankel, and D. Weihs, "Gas flows through shallow t-junctions and parallel microchannel networks," *Phys. Fluids*, **22** (*9*) 92001 (2010).
169) R.M. Santos, and M. Kawaji, "Numerical modeling and experimental investigation of gas–liquid slug formation in a microchannel t-junction," *Int. J. Multiph. Flow*, **36** (*4*) 314–323 (2010).
170) B. Xu, T.N. Wong, N.-T. Nguyen, Z. Che, and J.C.K. Chai, "Thermal mixing of two miscible fluids in a t-shaped microchannel," *Biomicrofluidics*, **4** (*4*) 44102 (2010).
171) S. Ebrahimi, A. Hasanzadeh-Barforoushi, A. Nejat, and F. Kowsary, "Numerical study of mixing and heat transfer in mixed electroosmotic/pressure driven flow through t-shaped microchannels," *Int. J. Heat Mass Transf.*, **75** 565–580 (2014).
172) J.J. Cardiel, D. Takagi, H.-F. Tsai, and A.Q. Shen, "Formation and flow behavior of micellar membranes in a t-shaped microchannel," *Soft Matter*, (2016).
173) A.A.S. Bhagat, S.S. Kuntaegowdanahalli, and I. Papautsky, "Continuous particle separation in spiral microchannels using dean flows and differential migration," *Lab Chip*, **8** (*11*) 1906–1914 (2008).
174) S.G. Kandlikar, "Fundamental issues related to flow boiling in minichannels and microchannels," *Exp. Therm. Fluid Sci.*, **26** (*2–4*) 389–407 (2002). doi:10.1016/S0894-1777(02)00150-4.
175) S.T. Poh, and E.Y.K. Ng, "Heat transfer and flow issues in manifold microchannel heat sinks: a CFD approach," in: Proc. 2nd Electron. Packag. Technol. Conf. (Cat. No.98EX235), IEEE, n.d.: pp. 246–250. doi:10.1109/EPTC.1998.756010.
176) T.G. Karayiannis, and M.M. Mahmoud, "Flow boiling in microchannels: fundamentals and applications," *Appl. Therm. Eng.*, **115** 1372–1397

(2017). doi:10.1016/j.applthermaleng.2016.08.063.
177) X.F. Peng, G.P. Peterson, and B.X. Wang, "FRICTIONAL flow characteristics of water flowing through rectangular microchannels," *Exp. Heat Transf.*, **7** (*4*) 249–264 (1994). doi:10.1080/08916159408946484.
178) K.. Toh, X.. Chen, and J.. Chai, "Numerical computation of fluid flow and heat transfer in microchannels," *Int. J. Heat Mass Transf.*, **45** (*26*) 5133–5141 (2002). doi:10.1016/S0017-9310(02)00223-5.
179) Z.-Y. Guo, and Z.-X. Li, "Size effect on microscale single-phase flow and heat transfer," *Int. J. Heat Mass Transf.*, **46** (*1*) 149–159 (2003). doi:10.1016/S0017-9310(02)00209-0.
180) G. Mohiuddin Mala, and D. Li, "Flow characteristics of water in microtubes," *Int. J. Heat Fluid Flow*, **20** (*2*) 142–148 (1999). doi:10.1016/S0142-727X(98)10043-7.
181) Q. Weilin, G. Mohiuddin Mala, and L. Dongqing, "Pressure-driven water flows in trapezoidal silicon microchannels," *Int. J. Heat Mass Transf.*, **43** (*3*) 353–364 (2000). doi:10.1016/S0017-9310(99)00148-9.
182) Muhammad Talha Khan, Muhammad Javaid Afzal, F. Javaid, S. Tayyaba, Muhammad Waseem Ashraf, and Md. Khalid Hossain, "Study of tip deflection on a copper-steel bimetallic strip by fuzzy logic and ansys static structural," *Proc. Int. Exch. Innov. Conf. Eng. Sci.*, **7** 255–260 (2021). doi:10.5109/4738596.
183) Muhammad Javaid Afzal, F. Javaid, S. Tayyaba, Muhammad Waseem Ashraf, and M. Khalid Hossain, "Study on the induced voltage in piezoelectric smart material (pzt) using ansys electric & fuzzy logic," *Proc. Int. Exch. Innov. Conf. Eng. Sci.*, **6** 313–318 (2020). doi:10.5109/4102508.
184) C. Liu, G. Hu, X. Jiang, and J. Sun, "Inertial focusing of spherical particles in rectangular microchannels over a wide range of reynolds numbers," *Lab Chip*, **15** (*4*) 1168–1177 (2015). doi:10.1039/C4LC01216J.
185) Y. Li, G. Xia, Y. Jia, Y. Cheng, and J. Wang, "Experimental investigation of flow boiling performance in microchannels with and without triangular cavities – a comparative study," *Int. J. Heat Mass Transf.*, **108** 1511–1526 (2017). doi:10.1016/j.ijheatmasstransfer.2017.01.011.
186) J. Mathew, P.-S. Lee, T. Wu, and C.R. Yap, "Comparative study of the flow boiling performance of the hybrid microchannel-microgap heat sink with conventional straight microchannel and microgap heat sinks," *Int. J. Heat Mass Transf.*, **156** 119812 (2020). doi:10.1016/j.ijheatmasstransfer.2020.119812.
187) P. Zajac, "Comparison of cooling performance of manifold and straight microchannel heat sinks using CFD simulation," in: 2021 22nd Int. Conf. Therm. Mech. Multi-Physics Simul. Exp. Microelectron. Microsystems, IEEE, 2021: pp. 1–4. doi:10.1109/EuroSimE52062.2021.9410853.
188) L. Wang, "Buoyancy-force-driven transitions in flow structures and their effects on heat transfer in a rotating curved channel," *Int. J. Heat Mass Transf.*, **40** (*2*) 223–235 (1997). doi:10.1016/0017-9310(96)00127-5.
189) W. Rodi, "Turbulence models and their applications in hydraulics-a state-of-the-art review.," *IAHR Monogr.*, (1984).
190) H. Iacovides, and B.E. Launder, "TURBULENT momentum and heat transport in square-sectioned ducts rotating in orthogonal mode," *Numer. Heat Transf.*, **12** (*4*) 475–491 (1987). doi:10.1080/10407788708913598.
191) M.D. Su, and R. Friedrich, "Numerical simulation of fully developed flow in a curved duct of rectangular cross-section," *Int. J. Heat Mass Transf.*, **37** (*8*) 1257–1268 (1994). doi:10.1016/0017-9310(94)90210-0.
192) D. Cokljat, and B.A. Younis, "Second-order closure study of open-channel flows," *J. Hydraul. Eng.*, **121** (*2*) 94–107 (1995).
193) Y. Shen, Y. Li, and A.T. Chwang, "Quasi-three-dimensional refined modelling of turbulent flow and water quality in coastal waters," *Sci. CHINA Ser. E Technol. Sci. Ed.*, **39** 342–353 (1996).
194) S. Yong—Ming, "The two-fluid model of turbulent buoyant recirculating two-phase flow," (n.d.).
195) S.A. Khuri, "Stokes flow in curved channels," *J. Comput. Appl. Math.*, **187** (*2*) 171–191 (2006).
196) L. Wang, and F. Liu, "Forced convection in slightly curved microchannels," *Int. J. Heat Mass Transf.*, **50** (*5*) 881–896 (2007).
197) I.W. Seo, and Y.J. Jung, "Velocity distribution of secondary currents in curved channels," *J. Hydrodyn. Ser. B*, **22** (*5*) 617–622 (2010).
198) I.L. Rozovskii, "Flow of water in bends of open channels. ac. sc. ukr. ssr, isr," *Progr. Sc. Transl., Jerusalem*, (1957).
199) H. Kikkawa, S. Ikeda, and A. Kitagawa, "Flow and bed topography in curved open channels," *J. Hydraul. Div.*, **102** (*ASCE# 12416*) (1976).
200) M. Falcon, "Secondary flow in curved open channels," *Annu. Rev. Fluid Mech.*, **16** (*1*) 179–193 (1984).
201) K.-O. Baek, I.-W. Seo, and K.-W. Lee, "New equation on streamwise variation of secondary flow in meandering channels," *J. Korean Soc. Civ. Eng.*, **26** (*4B*) 371–378 (2006).
202) F. Engelund, "Flow and bed topography in channel bends," *J. Hydraul. Div.*, **100** (*Proc. Paper 10963*) (1974).
203) H.J. De Vriend, "A mathematical model of steady flow in curved shallow channels," *J. Hydraul. Res.*, **15** (*1*) 37–54 (1977).
204)H.H. Chang, "Fluvial processes in river engineering,"

1992.
205) N. Ali, M. Sajid, T. Javed, and Z. Abbas, "Heat transfer analysis of peristaltic flow in a curved channel," *Int. J. Heat Mass Transf.*, **53** (*15*) 3319–3325 (2010).
206) K.S. Mekheimer, "Peristaltic flow of blood under effect of a magnetic field in a non-uniform channels," *Appl. Math. Comput.*, **153** (*3*) 763–777 (2004).
207) N. Ali, M. Sajid, Z. Abbas, and T. Javed, "Non-newtonian fluid flow induced by peristaltic waves in a curved channel," *Eur. J. Mech.*, **29** (*5*) 387–394 (2010).
208) K.S. Mekheimer, E.F. El Shehawey, and A.M. Elaw, "Peristaltic motion of a particle-fluid suspension in a planar channel," *Int. J. Theor. Phys.*, **37** (*11*) 2895–2920 (1998). doi:10.1023/A:1026657629065.
209) K.S. Mekheimer, "Peristaltic transport of a couple stress fluid in a uniform and non-uniform channels," *Biorheology*, **39** (*6*) 755–765 (2002).
210) T. Hayat, Y. Wang, A.M. Siddiqui, and K. Hutter, "Peristaltic motion of a johnson-segalman fluid in a planar channel," *Math. Probl. Eng.*, **2003** (*1*) 1–23 (2003).
211) Y. Wang, T. Hayat, and K. Hutter, "Peristaltic flow of a johnson-segalman fluid through a deformable tube," *Theor. Comput. Fluid Dyn.*, **21** (*5*) 369–380 (2007).
212) M.H. Haroun, "Effect of deborah number and phase difference on peristaltic transport of a third-order fluid in an asymmetric channel," *Commun. Nonlinear Sci. Numer. Simul.*, **12** (*8*) 1464–1480 (2007).
213) M.H. Haroun, "Non-linear peristaltic flow of a fourth grade fluid in an inclined asymmetric channel," *Comput. Mater. Sci.*, **39** (*2*) 324–333 (2007).
214) M. Kothandapani, and S. Srinivas, "Non-linear peristaltic transport of a newtonian fluid in an inclined asymmetric channel through a porous medium," *Phys. Lett. A*, **372** (*8*) 1265–1276 (2008).
215) N. Ali, and T. Hayat, "Peristaltic motion of a carreau fluid in an asymmetric channel," *Appl. Math. Comput.*, **193** (*2*) 535–552 (2007).
216) M.E. Emiroglu, N. Kaya, and M. Ozturk, "Investigation of labyrinth side weir flow and scouring at the lateral intake region in a curved channel. the scientific and technological research council of turkey (tubitak)," *Eng. Sci. Res. Grant Group, Proj.*, (*104M394*) 253 (2007).
217) M.E. Emiroglu, and N. Kaya, "Investigation of discharge coefficient of labyrinth side weir located on the straight channels," in: With Int. Particip. Second Natl. Symp. Dam Safety, Eskisehir, Turkey [in Turkish], 2009: pp. 13–15.
218) P. ACKERS, "A theoretical consideration of side weirs as stormwater overflows. hydraulics paper no 11. symposium of four papers on side spillways," *Proc. Inst. Civ. Eng.*, **6** (*2*) 250–269 (1957).
219) A. El-Khashab, and K.V.H. Smith, "Experimental investigation of flow over side weirs," *J. Hydraul. Div.*, **102** (*9*) 1255–1268 (1976). doi:10.1061/JYCEAJ.0004610.
220) M. Ghodsian, "Supercritical flow over a rectangular side weir," *Can. J. Civ. Eng.*, **30** (*3*) 596–600 (2003).
221) F. Aghayari, T. Honar, and A. Keshavarzi, "A study of spatial variation of discharge coefficient in broad-crested inclined side weirs," *Irrig. Drain.*, **58** (*2*) 246–254 (2009).
222) P.K. Swamee, S.K. Pathak, and M.S. Ali, "Side-weir analysis using elementary discharge coefficient," *J. Irrig. Drain. Eng.*, **120** (*4*) 742–755 (1994).
223) V.K. COLLINGE, "THE discharge capacity of side weirs. hydraulics paper no 13. symposium of four papers on side spillways," *Proc. Inst. Civ. Eng.*, **6** (*2*) 288–304 (1957).
224) W. Frazer, "THE behaviour of side weirs in prismatic rectangular channels. hydraulics paper no 14. symposium of four papers on side spillways," *Proc. Inst. Civ. Eng.*, **6** (*2*) 305–328 (1957).
225) K. Subramanya, and S.C. Awasthy, "Spatially varied flow over side-weirs," *J. Hydraul. Div.*, **98** (*1*) 1–10 (1972).
226) K.G. Ranga Raju, S.K. Gupta, and B. Prasad, "Side weir in rectangular channel," *J. Hydraul. Div.*, **105** (*5*) 547–554 (1979).
227) A. Uyumaz, and R.H. Smith, "Design procedure for flow over side weirs," *J. Irrig. Drain. Eng.*, **117** (*1*) 79–90 (1991).
228) H.-F. Cheong, "Discharge coefficient of lateral diversion from trapezoidal channel," *J. Irrig. Drain. Eng.*, **117** (*4*) 461–475 (1991).
229) R. Singh, D. Manivannan, and T. Satyanarayana, "Discharge coefficient of rectangular side weirs," *J. Irrig. Drain. Eng.*, **120** (*4*) 814–819 (1994).
230) S.M. Borghei, M.R. Jalili, and M. Ghodsian, "Discharge coefficient for sharp-crested side weir in subcritical flow," *J. Hydraul. Eng.*, **125** (*10*) 1051–1056 (1999).
231) T. Hayat, M. Javed, and A.A. Hendi, "Peristaltic transport of viscous fluid in a curved channel with compliant walls," *Int. J. Heat Mass Transf.*, **54** (*7*) 1615–1621 (2011).
232) D.-Y. Li, X.-B. Li, H.-N. Zhang, F.-C. Li, S. Qian, and S.W. Joo, "Efficient heat transfer enhancement by elastic turbulence with polymer solution in a curved microchannel," *Microfluid. Nanofluidics*, **21** (*1*) 10 (2017).
233) D.J. Schutte, M. Raven, B.J. Dolcich, and Z. Lin, "COOLING system having a condenser with a micro-channel cooling coil and sub-cooler having a fin-and-tube heat cooling coil," (2016).
234) N. Nivedita, P. Ligrani, and I. Papautsky, "Dean flow dynamics in low-aspect ratio spiral microchannels," *Sci. Rep.*, **7** (2017).
235) L. Wang, P.C.H. Li, H.-Z. Yu, and A.M.

Parameswaran, "Fungal pathogenic nucleic acid detection achieved with a microfluidic microarray device," *Anal. Chim. Acta*, **610** (*1*) 97–104 (2008).
236) J. Zhu, and X. Xuan, "Dielectrophoretic focusing of particles in a microchannel constriction using dc-biased ac flectric fields," *Electrophoresis*, **30** (*15*) 2668–2675 (2009).
237) J. Zhu, T.-R.J. Tzeng, G. Hu, and X. Xuan, "DC dielectrophoretic focusing of particles in a serpentine microchannel," *Microfluid. Nanofluidics*, **7** (*6*) 751–756 (2009).
238) C. Zhang, K. Khoshmanesh, A. Mitchell, and K. Kalantar-Zadeh, "Dielectrophoresis for manipulation of micro/nano particles in microfluidic systems," *Anal. Bioanal. Chem.*, **396** (*1*) 401–420 (2010).
239) O.D. Velev, and K.H. Bhatt, "On-chip micromanipulation and assembly of colloidal particles by electric fields," *Soft Matter*, **2** (*9*) 738–750 (2006).
240) Y. Ai, S. Park, J. Zhu, X. Xuan, A. Beskok, and S. Qian, "DC electrokinetic particle transport in an l-shaped microchannel," *Langmuir*, **26** (*4*) 2937–2944 (2009).
241) B.H. Lapizco-Encinas, and M. Rito-Palomares, "Dielectrophoresis for the manipulation of nanobioparticles," *Electrophoresis*, **28** (*24*) 4521–4538 (2007). doi:10.1002/elps.200700303.
242) R. Pethig, "Review article—dielectrophoresis: status of the theory, technology, and applications," *Biomicrofluidics*, **4** (*2*) 22811 (2010).
243) P.R.C. Gascoyne, and J. Vykoukal, "Particle separation by dielectrophoresis," *Electrophoresis*, **23** (*13*) 1973 (2002).
244) M.P. Hughes, "Strategies for dielectrophoretic separation in laboratory-on-a-chip systems," *Electrophoresis*, **23** (*16*) 2569–2582 (2002).
245) C.-F. Chou, and F. Zenhausern, "Electrodeless dielectrophoresis for micro total analysis systems," *IEEE Eng. Med. Biol. Mag.*, **22** (*6*) 62–67 (2003).
246)B.H. Lapizco-Encinas, R. V Davalos, B.A. Simmons, E.B. Cummings, and Y. Fintschenko, "An insulator-based (electrodeless) dielectrophoretic concentrator for microbes in water," *J. Microbiol. Methods*, **62** (*3*) 317–326 (2005).
247) S. Sridharan, J. Zhu, G. Hu, and X. Xuan, "Joule heating effects on electroosmotic flow in insulator-based dielectrophoresis," *Electrophoresis*, **32** (*17*) 2274–2281 (2011).
248) S.K. Srivastava, A. Gencoglu, and A.R. Minerick, "DC insulator dielectrophoretic applications in microdevice technology: a review," *Anal. Bioanal. Chem.*, **399** (*1*) 301–321 (2011).
249) J. Janča, V. Halabalová, and J. Růžička, "Role of the shape of various bacteria in their separation by microthermal field-flow fractionation," *J. Chromatogr. A*, **1217** (*51*) 8062–8071 (2010).
250) J.A. Champion, and S. Mitragotri, "Role of target geometry in phagocytosis," *Proc. Natl. Acad. Sci. U. S. A.*, **103** (*13*) 4930–4934 (2006).
251) S.G. Martin, "Geometric control of the cell cycle," *Cell Cycle*, **8** (*22*) 3643–3647 (2009).
252) S. Qian, and Y. Ai, "Electrokinetic Particle Transport in Micro-/Nanofluidics: Direct Numerical Simulation Analysis," CRC Press, 2012.
253) Y. Ai, S.W. Joo, Y. Jiang, X. Xuan, and S. Qian, "Transient electrophoretic motion of a charged particle through a converging–diverging microchannel: effect of direct current-dielectrophoretic force," *Electrophoresis*, **30** (*14*) 2499–2506 (2009).
254) Y. Ai, A. Beskok, D.T. Gauthier, S.W. Joo, and S. Qian, "DC electrokinetic transport of cylindrical cells in straight microchannels," *Biomicrofluidics*, **3** (*4*) 44110 (2009).
255) H. Song, D.L. Chen, and R.F. Ismagilov, "Reactions in droplets in microfluidic channels," *Angew. Chemie Int. Ed.*, **45** (*44*) 7336–7356 (2006).
256) E.W.M. Kemna, L.I. Segerink, F. Wolbers, I. Vermes, and A. van den Berg, "Label-free, high-throughput, electrical detection of cells in droplets," *Analyst*, **138** (*16*) 4585–4592 (2013).
257) M. Chabert, and J.-L. Viovy, "Microfluidic high-throughput encapsulation and hydrodynamic self-sorting of single cells," *Proc. Natl. Acad. Sci.*, **105** (*9*) 3191–3196 (2008).
258) Z. Cao, F. Chen, N. Bao, H. He, P. Xu, S. Jana, S. Jung, H. Lian, and C. Lu, "Droplet sorting based on the number of encapsulated particles using a solenoid valve," *Lab Chip*, **13** (*1*) 171–178 (2013).
259) M. Hein, M. Moskopp, and R. Seemann, "Flow field induced particle accumulation inside droplets in rectangular channels," *Lab Chip*, **15** (*13*) 2879–2886 (2015).
260) S.K. Griffiths, and R.H. Nilson, "Low-dispersion turns and junctions for microchannel systems," *Anal. Chem.*, **73** (*2*) 272–278 (2001).
261) S.H. Wong, M.C.L. Ward, and C.W. Wharton, "Micro t-mixer as a rapid mixing micromixer," *Sensors Actuators B Chem.*, **100** (*3*) 359–379 (2004).
262) N. Fujisawa, Y. Nakamura, F. Matsuura, and Y. Sato, "Pressure field evaluation in microchannel junction flows through μpiv measurement," *Microfluid. Nanofluidics*, **2** (*5*) 447–453 (2006).
263) Y. Ma, C.-P. Sun, M. Fields, Y. Li, D.A. Haake, B.M. Churchill, and C.-M. Ho, "An unsteady microfluidic t-form mixer perturbed by hydrodynamic pressure," *J. Micromechanics Microengineering*, **18** (*4*) 45015 (2008).
264) D. Qian, and A. Lawal, "Numerical study on gas and liquid slugs for taylor flow in a t-junction microchannel," *Chem. Eng. Sci.*, **61** (*23*) 7609–7625 (2006).
265) M. DE MENECH, P. GARSTECKI, F. JOUSSE, and

H.A. STONE, "Transition from squeezing to dripping in a microfluidic t-shaped junction," *J. Fluid Mech.*, **595** 141–161 (2008). doi:10.1017/S002211200700910X.

266) K.-L. Lao, J.-H. Wang, and G.-B. Lee, "A microfluidic platform for formation of double-emulsion droplets," *Microfluid. Nanofluidics*, **7** (*5*) 709–719 (2009).

267) A.S. Arico, P. Cretı, V. Baglio, E. Modica, and V. Antonucci, "Influence of flow field design on the performance of a direct methanol fuel cell," *J. Power Sources*, **91** (*2*) 202–209 (2000).

268) S. Karvonen, T. Hottinen, J. Saarinen, and O. Himanen, "Modeling of flow field in polymer electrolyte membrane fuel cell," *J. Power Sources*, **161** (*2*) 876–884 (2006).

269) Y.M. Ferng, and A. Su, "A three-dimensional full-cell cfd model used to investigate the effects of different flow channel designs on pemfc performance," *Int. J. Hydrogen Energy*, **32** (*17*) 4466–4476 (2007).

270) J.M. MacInnes, X. Du, and R.W.K. Allen, "Prediction of electrokinetic and pressure flow in a microchannel t-junction," *Phys. Fluids*, **15** (*7*) 1992–2005 (2003).

271) Y. Zhuang, and Q. Zhu, "Numerical study of mixed electroosmotic/pressure driven flow of power-law fluids in t-shaped microchannels," *Procedia Eng.*, **126** 740–744 (2015).

272) T. Andreussi, C. Galletti, R. Mauri, S. Camarri, and M.V. Salvetti, "Flow regimes in t-shaped micro-mixers," *Comput. Chem. Eng.*, **76** 150–159 (2015).

273) A. Hatch, A.E. Kamholz, K.R. Hawkins, M.S. Munson, E.A. Schilling, B.H. Weigl, and P. Yager, "A rapid diffusion immunoassay in a t-sensor," *Nat. Biotechnol.*, **19** (*5*) 461–465 (2001).

274) S.M. Fielding, and P.D. Olmsted, "Nonlinear dynamics of an interface between shear bands," *Phys. Rev. Lett.*, **96** (*10*) 104502 (2006).

275) V. Schmitt, C.M. Marques, and F. Lequeux, "Shear-induced phase separation of complex fluids: the role of flow-concentration coupling," *Phys. Rev. E*, **52** (*4*) 4009 (1995).

276) J.K.G. Dhont, and W.J. Briels, "Gradient and vorticity banding," *Rheol. Acta*, **47** (*3*) 257–281 (2008).

277) A. He, J. Lowengrub, and A. Belmonte, "Modeling an elastic fingering instability in a reactive hele-shaw flow," *SIAM J. Appl. Math.*, **72** (*3*) 842–856 (2012).

278) J. Jimenez, "The growth of a mixing layer in a laminar channel," *J. Fluid Mech.*, **535** 245–254 (2005).

279) C.-Y. Chen, and E. Meiburg, "Miscible displacements in capillary tubes: influence of korteweg stresses and divergence effects," *Phys. Fluids*, **14** (*7*) 2052–2058 (2002).

280) P. Petitjeans, and T. Maxworthy, "Miscible displacements in capillary tubes. part 1. experiments," *J. Fluid Mech.*, **326** 37–56 (1996).

281) C. Masselon, J.-B. Salmon, and A. Colin, "Nonlocal effects in flows of wormlike micellar solutions," *Phys. Rev. Lett.*, **100** (*3*) 38301 (2008).

282) R. Ganapathy, and A.K. Sood, "Intermittency route to rheochaos in wormlike micelles with flow-concentration coupling," *Phys. Rev. Lett.*, **96** (*10*) 108301 (2006). doi:10.1103/PhysRevLett.96.108301.

283) M.F.B. Pires, R.F. Nogueira, and T.P. Navarro, "Chronic Venous Disease and Varicose Veins," in: Vasc. Dis. Non-Specialist, Springer, 2017: pp. 167–181.

284) M. N. Kashid, A. Renken, and L. Kiwi-Minsker, "Influence of flow regime on mass transfer in different types of microchannels," *Ind. Eng. Chem. Res.*, **50** (*11*) 6906–6914 (2011).

285) V. Jain, V.B. Patel, B. Singh, and D. Varade, "Microfluidic device based molecular self-assembly structures," *J. Mol. Liq.*, **362** 119760 (2022). doi:10.1016/j.molliq.2022.119760.

286) M. Benton, M. Hossan, P. Konari, and S. Gamagedara, "Effect of process parameters and material properties on laser micromachining of microchannels," *Micromachines*, **10** (*2*) 123 (2019). doi:10.3390/mi10020123.

287) A.K. Sahu, and S. Jha, "Microchannel fabrication and metallurgical characterization on titanium by nanosecond fiber laser micromilling," *Mater. Manuf. Process.*, **35** (*3*) 279–290 (2020). doi:10.1080/10426914.2020.1718702.

288) B. Su, J. Meng, Z. Zhang, F. Liu, and A. Zhang, "Fabrication of alumina micromixer with two-dimensional serpentine microchannels by centrifuge-assisted micromoulding," *Micro Nano Lett.*, **10** (*12*) 703–706 (2015). doi:10.1049/mnl.2015.0091.

289) L. Fan, Q. Yan, Q. Qian, S. Zhang, L. Wu, Y. Peng, S. Jiang, L. Guo, J. Yao, and H. Wu, "Laser-induced fast assembly of wettability-finely-tunable superhydrophobic surfaces for lossless droplet transfer," *ACS Appl. Mater. Interfaces*, (2022). doi:10.1021/acsami.2c09410.

290) G. Wang, D. Lai, X. Xu, and Y. Wang, "Lightweight, stiff and heat-resistant bamboo-derived carbon scaffolds with gradient aligned microchannels for highly efficient emi shielding," *Chem. Eng. J.*, **446** 136911 (2022). doi:10.1016/j.cej.2022.136911.

291) T. Hou, Y. Ren, Y. Chan, J. Wang, and Y. Yan, "Flow-induced shear stress and deformation of a core-shell structured microcapsule in a microchannel," *Electrophoresis*, (2022). doi:10.1002/elps.202100274.

292) W.R. Ali, and M. Prasad, "Fabrication of microchannel and diaphragm for a mems acoustic

sensor using wet etching technique," *Microelectron. Eng.*, **253** 111670 (2022). doi:10.1016/j.mee.2021.111670.
293) I.H. Karampelas, and J. Gómez-Pastora, "Novel approaches concerning the numerical modeling of particle and cell separation in microchannels: a review," *Processes*, **10** (*6*) 1226 (2022). doi:10.3390/pr10061226.
294) R. Srivastava, Y.K. Prajapati, S. Pal, and S. Kumar, "Micro-channel plasmon sensor based on a dshaped photonic crystal fiber for malaria diagnosis with improved performance," *IEEE Sens. J.*, 1–1 (2022). doi:10.1109/JSEN.2022.3181198.
295) Z. Cao, Y. Ye, G. Li, R. Zhang, S. Dong, and Y. Liu, "Monolithically integrated microchannel plate functionalized with zno nanorods for fluorescence-enhanced digital polymerase chain reaction," *Biosens. Bioelectron.*, **213** 114499 (2022). doi:10.1016/j.bios.2022.114499.
296) Z. Xu, J. Xu, Z. Guo, H. Wang, Z. Sun, and X. Mei, "Design and optimization of a novel microchannel battery thermal management system based on digital twin," *Energies*, **15** (*4*) 1421 (2022). doi:10.3390/en15041421.
297) G. Stella, M. Barcellona, L. Saitta, C. Tosto, G. Cicala, A. Gulino, M. Bucolo, and M.E. Fragalà, "3D printing manufacturing of polydimethyl-siloxane/zinc oxide micro-optofluidic device for two-phase flows control," *Polymers (Basel).*, **14** (*10*) 2113 (2022). doi:10.3390/polym14102113.
298) L.J. Guerin, M. Bossel, M. Demierre, S. Calmes, and P. Renaud, "Simple and low cost fabrication of embedded micro-channels by using a new thick-film photoplastic," in: Transducers, 1997: pp. 1419–1422.
299) I. Papautsky, J. Brazzle, H. Swerdlow, and A.B. Frazier, "A low-temperature ic-compatible process for fabricating surface-micromachined metallic microchannels," *J. Microelectromechanical Syst.*, **7** (*2*) 267–273 (1998).
300) S. Vempati, and T.S. Natarajan, "Flexible polymer microtubes and microchannels via electrospinning," *Mater. Lett.*, **65** (*23*) 3493–3495 (2011).
301) R.J. Kee, B.B. Almand, J.M. Blasi, B.L. Rosen, M. Hartmann, N.P. Sullivan, H. Zhu, A.R. Manerbino, S. Menzer, and W.G. Coors, "The design, fabrication, and evaluation of a ceramic counter-flow microchannel heat exchanger," *Appl. Therm. Eng.*, **31** (*11*) 2004–2012 (2011).
302) H.-S. Noha, Y. Huangb, and P.J. Hesketha, "Parylene micromolding, a rapid and low-cost fabrication method for parylene microchannel," *Sensors Actuators B Chem.*, **102** (*1*) 78–85 (2004).
303) M. Hakamada, Y. Asao, T. Kuromura, Y. Chen, H. Kusuda, and M. Mabuchi, "Fabrication of copper microchannels by the spacer method," *Scr. Mater.*, **56** (*9*) 781–783 (2007).
304) L.P. Lee, S.A. Berger, L. Pruitt, and D. Liepmann, "Key elements of a transparent teflon® microfluidic system," in: Micro Total Anal. Syst. 98, Springer, 1998: pp. 245–248.
305) J.S. Rossier, A. Schwarz, F. Bianchi, F. Reymond, R. Ferrigno, and H.H. Girault, "Polymer micro-structures: prototyping, low-cost mass fabrication and analytical applications," in: Micro Total Anal. Syst. 2000, Springer, 2000: pp. 159–162.
306) S.G. Kandlikar, and W.J. Grande, "Evolution of microchannel flow passages--thermohydraulic performance and fabrication technology," *Heat Transf. Eng.*, **24** (*1*) 3–17 (2003).
307) M. Rafeie, S. Hosseinzadeh, R.A. Taylor, and M.E. Warkiani, "New insights into the physics of inertial microfluidics in curved microchannels. i. relaxing the fixed inflection point assumption," *Biomicrofluidics*, **13** (*3*) 034117 (2019). doi:10.1063/1.5109004.
308) W. Sun, M. Liu, and W. Liu, "Chemically stable yttrium and tin co-doped barium zirconate electrolyte for next generation high performance proton-conducting solid oxide fuel cells," *Adv. Energy Mater.*, **3** (*8*) 1041–1050 (2013). doi:10.1002/aenm.201201062.
309) Q. Shen, C. Zhang, M.F. Tahir, S. Jiang, C. Zhu, Y. Ma, and T. Fu, "Numbering-up strategies of micro-chemical process: uniformity of distribution of multiphase flow in parallel microchannels," *Chem. Eng. Process. - Process Intensif.*, **132** 148–159 (2018). doi:10.1016/j.cep.2018.09.002.
310) C. Yao, Y. Zhao, H. Ma, Y. Liu, Q. Zhao, and G. Chen, "Two-phase flow and mass transfer in microchannels: a review from local mechanism to global models," *Chem. Eng. Sci.*, **229** 116017 (2021). doi:10.1016/j.ces.2020.116017.
311) Z. Pan, J. Chen, L. Fan, J. Zhang, S. Zhang, Y. Huang, L. Liu, L. Fang, and X. Xing, "Enhanced piezoelectric properties and thermal stability in the (k 0.5 na 0.5)nbo 3 :zno lead-free piezoelectric composites," *J. Am. Ceram. Soc.*, **98** (*12*) 3935–3941 (2015). doi:10.1111/jace.13831.
312) S.N. Akhtar, S. Sharma, S.A. Ramakrishna, and J. Ramkumar, "Excimer laser micromachining of oblique microchannels on thin metal films using square laser spot," *Sādhanā*, **41** (*6*) 633–641 (2016).
313) F.W.M. Ling, W.K. Mahmood, and H.A. Abdulbari, "Rapid Prototyping of Microfluidics Devices using Xurograhy Method," in: MATEC Web Conf., EDP Sciences, 2017: p. 1009.
314) S. Prakash, and S. Kumar, "Fabrication of microchannels: a review," *Proc. Inst. Mech. Eng. Part B J. Eng. Manuf.*, **229** (*8*) 1273–1288 (2015).
315) Y.W. Zhu, H.Z. Zhang, X.C. Sun, S.Q. Feng, J. Xu, Q. Zhao, B. Xiang, R.M. Wang, and D.P. Yu, "Efficient field emission from zno nanoneedle arrays," *Appl. Phys. Lett.*, **83** (*1*) 144–146 (2003).
316) K. Izumisawa, T. Sugimoto, Y. Nakamura, K.

Miyamoto, T. Torimoto, R. Morita, and T. Omatsu, "Plasmonic Au nano-needle fabricated by optical vortex laser illumination," in: Opt. Manip. Conf., International Society for Optics and Photonics, 2017: p. 102520I.

317) C. Chiappini, "Nanoneedle-based sensing in biological systems," *ACS Sensors*, **2** (*8*) 1086–1102 (2017).

318) X. Yang, S. Wu, W. Xie, A. Cheng, L. Yang, Z. Hou, and X. Jin, "Dual-drug loaded nanoneedles with targeting property for efficient cancer therapy," *J. Nanobiotechnology*, **15** (*1*) 91 (2017).

319) F. Spina, A. Pouryazdan, J.C. Costa, L.P. Cuspinera, and N. Münzenrieder, "Directly 3d-printed monolithic soft robotic gripper with liquid metal microchannels for tactile sensing," *Flex. Print. Electron.*, **4** (*3*) 035001 (2019). doi:10.1088/2058-8585/ab3384.

320) S. Waheed, J.M. Cabot, N.P. Macdonald, T. Lewis, R.M. Guijt, B. Paull, and M.C. Breadmore, "3D printed microfluidic devices: enablers and barriers," *Lab Chip*, **16** (*11*) 1993–2013 (2016).

321) S. Wu, X. Yang, Y. Lu, Z. Fan, Y. Li, Y. Jiang, and Z. Hou, "A green approach to dual-drug nanoformulations with targeting and synergistic effects for cancer therapy," *Drug Deliv.*, **24** (*1*) 51–60 (2017).

322)Y. Su, Y. Hu, Y. Wang, X. Xu, Y. Yuan, Y. Li, Z. Wang, K. Chen, F. Zhang, and X. Ding, "A precision-guided mwnt mediated reawakening the sunk synergy in ras for anti-angiogenesis lung cancer therapy," *Biomaterials*, (2017).

323)J.W. Gooch, "Hagen-Poiseuille equation," in: Encycl. Dict. Polym., Springer, 2011: p. 355.

324) W. Martanto, J.S. Moore, O. Kashlan, R. Kamath, P.M. Wang, J.M. O'neal, and M.R. Prausnitz, "Microinfusion using hollow microneedles," *Pharm. Res.*, **23** (*1*) 104–113 (2006).

325) A. V Prinz, V.Y. Prinz, and V.A. Seleznev, "Semiconductor micro-and nanoneedles for microinjections and ink-jet printing," *Microelectron. Eng.*, **67** 782–788 (2003).

326) X. Wu, H. Bai, C. Li, G. Lu, and G. Shi, "Controlled one-step fabrication of highly oriented zno nanoneedle/nanorods arrays at near room temperature," *Chem. Commun.*, (*15*) 1655–1657 (2006).

327) K.-Y. Chien, "Predictions of channel and boundary-layer flows with a low-reynolds-number turbulence model," *AIAA J.*, **20** (*1*) 33–38 (1982).

328) S. Fan, B. Lakshminarayana, and M. Barnett, "Low-reynolds-number k-epsilon model for unsteady turbulent boundary-layer flows," *AIAA J.*, **31** (*10*) 1777–1784 (1993).

329) H. Singh, V. Kumar, and J. Kapoor, "Multi-response optimization of wedm process parameters during the fabrication of microchannels for industrial applications," *Mater. Today Proc.*, **46** 81–88 (2021). doi:10.1016/j.matpr.2020.06.134.

330) R. Ghaemi, M. Dabaghi, R. Attalla, A. Shahid, H.-H. Hsu, and P.R. Selvaganapathy, "Use of flame activation of surfaces to bond pdms to variety of substrates for fabrication of multimaterial microchannels," *J. Micromechanics Microengineering*, **28** (*8*) 087001 (2018). doi:10.1088/1361-6439/aabd29.

331) K. Keniar, B. El Fil, and S. Garimella, "A critical review of analytical and numerical models of condensation in microchannels," *Int. J. Refrig.*, **120** 314–330 (2020). doi:10.1016/j.ijrefrig.2020.08.009.

332) H. Becker, and L.E. Locascio, "Polymer microfluidic devices," *Talanta*, **56** (*2*) 267–287 (2002).

333)M.A. Roberts, J.S. Rossier, P. Bercier, and H. Girault, "UV laser machined polymer substrates for the development of microdiagnostic systems," *Anal. Chem.*, **69** (*11*) 2035–2042 (1997).

334) R.C. Blase, R.R. Benke, and K.S. Pickens, "Review of measured photon detection efficiencies of microchannel plates," *IEEE Trans. Nucl. Sci.*, **65** (*12*) 2839–2851 (2018). doi:10.1109/TNS.2018.2877356.

335) B. Leskovar, "Microchannel plates," *Phys. Today*, **30** 42–49 (1977).

336) O. Jagutzki, V. Mergel, K. Ullmann-Pfleger, L. Spielberger, U. Spillmann, R. Dörner, and H. Schmidt-Böcking, "A broad-application microchannel-plate detector system for advanced particle or photon detection tasks: large area imaging, precise multi-hit timing information and high detection rate," *Nucl. Instruments Methods Phys. Res. Sect. A Accel. Spectrometers, Detect. Assoc. Equip.*, **477** (*1*) 244–249 (2002).

337) Y. Dong, C. Zhu, Y. Ma, and T. Fu, "Distribution of liquid-liquid two-phase flow and droplet dynamics in asymmetric parallel microchannels," *Chem. Eng. J.*, **441** 136027 (2022). doi:10.1016/j.cej.2022.136027.

338) K. Fallah, and E. Fattahi, "Splitting of droplet with different sizes inside a symmetric t-junction microchannel using an electric field," *Sci. Rep.*, **12** (*1*) 3226 (2022). doi:10.1038/s41598-022-07130-6.

339) D. Ji, N. Jin, J. Yue, Q. Wang, and Y. Zhao, "Hydrodynamics and mass transfer characteristics for extractive desulfurization of diesel using highly viscous ionic liquids in microchannels: the effect of the phase ratio and temperature," *Ind. Eng. Chem. Res.*, **61** (*15*) 5351–5362 (2022). doi:10.1021/acs.iecr.2c00077.

340) J. Qian, X. Li, Z. Wu, Z. Cao, and B. Sunden, "Determination of droplet velocity in square microchannel," *Int. J. Comput. Methods Exp. Meas.*, **10** (*1*) 62–73 (2022). doi:10.2495/CMEM-V10-N1-62-73.

341) Q. Zhu, R. Su, H. Xia, J. Zeng, and J. Chen, "Numerical simulation study of thermal and hydraulic characteristics of laminar flow in microchannel heat sink with water droplet cavities and different rib columns," *Int. J. Therm. Sci.*, **172** 107319 (2022). doi:10.1016/j.ijthermalsci.2021.107319.
342) M. Błaszczyk, J. Sęk, and Ł. Przybysz, "Analysis of droplet displacement during transport of polydisperse emulsion as drug carriers in microchannels," *Microfluid. Nanofluidics*, **26** (*3*) 19 (2022). doi:10.1007/s10404-022-02526-2.
343) L. Ma, Z. Yan, C. Du, J. Deng, and G. Luo, "Effect of viscosity on liquid–liquid slug flow in a step t-junction microchannel," *Ind. Eng. Chem. Res.*, **61** (*23*) 8333–8345 (2022). doi:10.1021/acs.iecr.2c01338.
344) C. He, S. Jiang, C. Zhu, Y. Ma, and T. Fu, "Self-assembly of droplet swarms and its feedback on droplet generation in a step-emulsification microdevice with parallel microchannels," *Chem. Eng. Sci.*, **256** 117685 (2022). doi:10.1016/j.ces.2022.117685.
345) L. Lei, Y. Zhao, J. An, B. Zhang, and J. Zhang, "Breakup dynamics of droplets in symmetric y-junction microchannels," *Appl. Sci.*, **12** (*8*) 4011 (2022). doi:10.3390/app12084011.
346) M. Nazari, S.M. Varedi-Koulaei, and M. Nazari, "Flow characteristics prediction in a flow-focusing microchannel for a desired droplet size using an inverse model: experimental and numerical study," *Microfluid. Nanofluidics*, **26** (*4*) 26 (2022). doi:10.1007/s10404-022-02529-z.
347) "Numerical investigation of the influence of microchannel geometry on the droplet generation process," *J. Appl. Fluid Mech.*, **15** (*5*) (2022). doi:10.47176/jafm.15.05.1126.
348) R. Dey, C.M. Buness, B.V. Hokmabad, C. Jin, and C.C. Maass, "Oscillatory rheotaxis of artificial swimmers in microchannels," *Nat. Commun.*, **13** (*1*) 2952 (2022). doi:10.1038/s41467-022-30611-1.
349) P. Kumari, and A. Atta, "Droplet breakup in a parallel microchannel with asymmetrical geometric constraints," *Chem. Eng. Res. Des.*, **184** 13–23 (2022). doi:10.1016/j.cherd.2022.05.037.
350) P. Kumari, and A. Atta, "Insights into the dynamics of non-newtonian droplet formation in a t-junction microchannel," *Phys. Fluids*, **34** (*6*) 062001 (2022). doi:10.1063/5.0092012.
351) Z. Li, Z. Gu, R. Li, C. Wang, C. Chen, C. Yu, Y. Zhang, Q. Shu, W. Cao, and J. Su, "A geometrical criterion for the dynamic snap-off event of a non-wetting droplet in a rectangular pore–throat microchannel," *Phys. Fluids*, **34** (*4*) 042014 (2022). doi:10.1063/5.0087523.
352) G. Narendran, N. Gnanasekaran, and D.A. Perumal, "A review on recent advances in microchannel heat sink configurations," *Recent Patents Mech. Eng.*, **11** (*3*) 190–215 (2018). doi:10.2174/2212797611666180726124047.
353) W.M.A.A. Japar, N.A.C. Sidik, S.R. Aid, Y. Asako, and T.L. Ken, "A comprehensive review on numerical and experimental study of nanofluid performance in microchannel heatsink (mchs)," *J. Adv. Res. Fluid Mech. Therm. Sci.*, **45** (*1*) 165–176 (2018).
354) N.A.A. Qasem, and S.M. Zubair, "Compact and microchannel heat exchangers: a comprehensive review of air-side friction factor and heat transfer correlations," *Energy Convers. Manag.*, **173** 555–601 (2018). doi:10.1016/j.enconman.2018.06.104.
355) J.P. Sharma, A. Sharma, R.D. Jilte, R. Kumar, and M.H. Ahmadi, "A study on thermohydraulic characteristics of fluid flow through microchannels," *J. Therm. Anal. Calorim.*, **140** (*1*) 1–32 (2020). doi:10.1007/s10973-019-08741-4.
356) K.N. Ramesh, T.K. Sharma, and G.A.P. Rao, "Latest advancements in heat transfer enhancement in the micro-channel heat sinks: a review," *Arch. Comput. Methods Eng.*, **28** (*4*) 3135–3165 (2021). doi:10.1007/s11831-020-09495-1.
357) S. Petralia, G. Panvini, and G. Ventimiglia, "A novel methodology for wettability process control of buried silicon microchannels for molecular diagnostic applications," *Bionanoscience*, **5** (*3*) 150–155 (2015).
358) S.D. Leith, D.A. King, and B. Paul, "Toward Low-Cost Fabrication of Microchannel Process Technologies-Cost Modeling for Manufacturing Development," Pacific Northwest National Laboratory (PNNL), Richland, WA (US), 2010.
359) B. Lajevardi, S.D. Leith, D.A. King, and B.K. Paul, "Arrayed microchannel manufacturing costs for an auxiliary power unit heat exchanger," in: IIE Annu. Conf. Proc., Institute of Industrial Engineers-Publisher, 2011: p. 1.
360) Q. Gao, J. Lizarazo-Adarme, B.K. Paul, and K.R. Haapala, "An economic and environmental assessment model for microchannel device manufacturing: part 2–application," *J. Clean. Prod.*, **120** 146–156 (2016).
361) O.H. Laguna, M.I. Domínguez, M.A. Centeno, and J.A. Odriozola, "Forced deactivation and postmortem characterization of a metallic microchannel reactor employed for the preferential oxidation of co (prox)," *Chem. Eng. J.*, **302** 650–662 (2016).
362) A. Abbasi, B. Firouzi, and P. Sendur, "On the application of harris hawks optimization (hho) algorithm to the design of microchannel heat sinks," *Eng. Comput.*, **37** (*2*) 1409–1428 (2021). doi:10.1007/s00366-019-00892-0.
363) A.P. Steynberg, S.R. Deshmukh, and H.J. Robota, "Fischer-tropsch catalyst deactivation in commercial

microchannel reactor operation," *Catal. Today*, **299** 10–13 (2018). doi:10.1016/j.cattod.2017.05.064.

364) N. Engelbrecht, R.C. Everson, D. Bessarabov, and G. Kolb, "Microchannel reactor heat-exchangers: a review of design strategies for the effective thermal coupling of gas phase reactions," *Chem. Eng. Process. - Process Intensif.*, **157** 108164 (2020). doi:10.1016/j.cep.2020.108164.

365) K. Babcock, and S.R. Manalis, "Method for measuring bacterial growth and antibiotic resistance using suspended microchannel resonators," (2017).

366) S. Tayyaba, M.W. Ashraf, Z. Ahmad, N. Wang, M.J. Afzal, and N. Afzulpurkar, "Fabrication and analysis of polydimethylsiloxane (pdms) microchannels for biomedical application," *Processes*, **9** (*1*) 57 (2020). doi:10.3390/pr9010057.

367) M.J. Afzal, M.W. Ashraf, S. Tayyaba, A.H. Jalbani, and F. Javaid, "Computer simulation based optimization of aspect ratio for micro and nanochannels," *Mehran Univ. Res. J. Eng. Technol.*, **39** (*4*) 779–791 (2020). doi:10.22581/muet1982.2004.10.

368) M.J. Afzal, S. Tayyaba, Fazal-e-Aleem, M.W. Ashraf, M.K. Hossain, and N. Afzulpurkar, "Fluidic simulation and analysis of spiral, U-shape and curvilinear nano channels for biomedical application," in: 2017 IEEE Int. Conf. Manip. Manuf. Meas. Nanoscale, IEEE, 2017: pp. 190–194. doi:10.1109/3M-NANO.2017.8286277.

369) S. Tayyaba, M.J. Afzal, G. Sarwar, M.W. Ashraf, and N. Afzulpurkar, "Simulation of flow control in straight microchannels using fuzzy logic," in: 2016 Int. Conf. Comput. Electron. Electr. Eng. (ICE Cube), IEEE, 2016: pp. 213–216. doi:10.1109/ICECUBE.2016.7495226.

370) M.J. Afzal, S. Tayyaba, M.W. Ashraf, and G. Sarwar, "Simulation of fuzzy based flow controller in ascending sinusoidal microchannels," in: 2016 2nd Int. Conf. Robot. Artif. Intell., IEEE, 2016: pp. 141–146. doi:10.1109/ICRAI.2016.7791243.

371) A. Olanrewaju, M. Beaugrand, M. Yafia, and D. Juncker, "Capillary microfluidics in microchannels: from microfluidic networks to capillaric circuits," *Lab Chip*, **18** (*16*) 2323–2347 (2018). doi:10.1039/C8LC00458G.

372) M. Richter, R. Linnemann, and P. Woias, "Robust design of gas and liquid micropumps," *Sensors Actuators A Phys.*, **68** (*1*) 480–486 (1998).

373) V. Singhal, S. V Garimella, and A. Raman, "Microscale pumping technologies for microchannel cooling systems," *Appl. Mech. Rev.*, **57** (*3*) 191–221 (2004).

374) W. Liu, "Research on electrostatic micropump pull-in phenomena based On reduced order model," in: Intell. Comput. Technol. Autom. (ICICTA), 2010 Int. Conf., IEEE, 2010: pp. 1154–1157.

375) R. Bodén, M. Lehto, U. Simu, G. Thornell, K. Hjort, and J.-A. Schweitz, "A polymeric paraffin micropump with active valves for high-pressure microfluidics," in: 13th Int. Conf. Solid-State Sensors, Actuators Microsystems, 2005. Dig. Tech. Pap. TRANSDUCERS'05., IEEE, 2005: pp. 201–204.

376) Y. Fang, and X. Tan, "A novel diaphragm micropump actuated by conjugated polymer petals: fabrication, modeling, and experimental results," *Sensors Actuators A Phys.*, **158** (*1*) 121–131 (2010).

377) A.T. Al-Halhouli, M.I. Kilani, and S. Büttgenbach, "Development of a novel electromagnetic pump for biomedical applications," *Sensors Actuators A Phys.*, **162** (*2*) 172–176 (2010).

378) J. Pang, Q. Zou, Z. Tan, X. Qian, L. Liu, and Z. Li, "The study of single-chip integrated microfluidic system," in: Solid-State Integr. Circuit Technol. 1998. Proceedings. 1998 5th Int. Conf., IEEE, 1998: pp. 895–898.

379) S. Lee, S.Y. Yee, A. Besharatian, H. Kim, L.P. Bernal, and K. Najafi, "Adaptive gas pumping by controlled timing of active microvalves in peristaltic micropumps," in: TRANSDUCERS 2009-2009 Int. Solid-State Sensors, Actuators Microsystems Conf., IEEE, 2009: pp. 2294–2297.

380) E. Jud, Z. Zhang, W. Sigle, and L.J. Gauckler, "Microstructure of cobalt oxide doped sintered ceria solid solutions," *J. Electroceramics*, **16** (*3*) 191–197 (2006). doi:10.1007/s10832-006-6258-8.

381) H.-J. Kang, and B. Choi, "Development of the mhd micropump with mixing function," *Sensors Actuators A Phys.*, **165** (*2*) 439–445 (2011).

382) M. Arai, K. Takahashi, M. Hattori, T. Hasegawa, M. Sato, K. Unoura, and H. Nabika, "One-directional fluidic flow induced by chemical wave propagation in a microchannel," *J. Phys. Chem. B*, (2016).

383) L.-S. Jang, S.-H. Chao, M.R. Holl, and D.R. Meldrum, "Microfluidic circulatory flows induced by resonant vibration of diaphragms," *Sensors Actuators A Phys.*, **122** (*1*) 141–148 (2005).

384) S.-C. Chan, C.-R. Chen, and C.-H. Liu, "A bubble-activated micropump with high-frequency flow reversal," *Sensors Actuators A Phys.*, **163** (*2*) 501–509 (2010).

385) M.K. Russel, S.M. Hasnain, P.R. Selvaganapathy, and C.Y. Ching, "Effect of doping ferrocene in the working fluid of electrohydrodynamic (ehd) micropumps," *Microfluid. Nanofluidics*, **20** (*8*) 1–9 (2016).

386) E. Jiménez, J. Escandon, O. Bautista, and F. Méndez, "Start-up electroosmotic flow of maxwell fluids in a rectangular microchannel with high zeta potentials," *J. Nonnewton. Fluid Mech.*, **227** 17–29 (2016).

387) G.-W. Kim, G. Kang, J. Kim, G.-Y. Lee, H. Il Kim, L. Pyeon, J. Lee, and T. Park, "Dopant-free polymeric hole transport materials for highly efficient and stable perovskite solar cells," *Energy*

Environ. Sci., **9** (*7*) 2326–2333 (2016). doi:10.1039/C6EE00709K.

388) N. Liu, T. Skauge, D. Landa-Marbán, B. Hovland, B. Thorbjørnsen, F.A. Radu, B.F. Vik, T. Baumann, and G. Bødtker, "Microfluidic study of effects of flow velocity and nutrient concentration on biofilm accumulation and adhesive strength in the flowing and no-flowing microchannels," *J. Ind. Microbiol. Biotechnol.*, **46** (*6*) 855–868 (2019). doi:10.1007/s10295-019-02161-x.

389) G. Hetsroni, A. Mosyak, E. Pogrebnyak, and L.P. Yarin, "Fluid flow in micro-channels," *Int. J. Heat Mass Transf.*, **48** (*10*) 1982–1998 (2005). doi:10.1016/j.ijheatmasstransfer.2004.12.019.

390) M.E. Steinke, and S.G. Kandlikar, "Single-phase liquid friction factors in microchannels," in: ASME 3rd Int. Conf. Microchannels Minichannels, American Society of Mechanical Engineers, 2005: pp. 291–302.

391) G. Liang, and I. Mudawar, "Review of single-phase and two-phase nanofluid heat transfer in macro-channels and micro-channels," *Int. J. Heat Mass Transf.*, **136** 324–354 (2019). doi:10.1016/j.ijheatmasstransfer.2019.02.086.

392) A. Abdollahi, S.E. Norris, and R.N. Sharma, "Heat transfer measurement techniques in microchannels for single and two-phase taylor flow," *Appl. Therm. Eng.*, **162** 114280 (2019). doi:10.1016/j.applthermaleng.2019.114280.

393) D. Jiang, C. Ni, W. Tang, D. Huang, and N. Xiang, "Inertial microfluidics in contraction–expansion microchannels: a review," *Biomicrofluidics*, **15** (*4*) 041501 (2021). doi:10.1063/5.0058732.

394) M. Khoshvaght-Aliabadi, M. Sahamiyan, M. Hesampour, and O. Sartipzadeh, "Experimental study on cooling performance of sinusoidal–wavy minichannel heat sink," *Appl. Therm. Eng.*, **92** 50–61 (2016).

395) H. Wu, C. Li, and J. Li, "Heat transfer enhancement by pulsating flow of a viscoelastic fluid in a microchannel with a rib plate," *Nanoscale Microscale Thermophys. Eng.*, 1–17 (2022). doi:10.1080/15567265.2022.2093297.

396) S.G. Kandlikar, D. Schmitt, A.L. Carrano, and J.B. Taylor, "Characterization of surface roughness effects on pressure drop in single-phase flow in minichannels," *Phys. Fluids*, **17** (*10*) 100606 (2005). doi:10.1063/1.1896985.

397) C. Eason, T. Dalton, M. Davies, C. O'Mathúna, and O. Slattery, "Direct comparison between five different microchannels, part 2: experimental description and flow friction measurement," *Heat Transf. Eng.*, **26** (*3*) 89–98 (2005).

398) M. Kersaudy-Kerhoas, and E. Sollier, "Micro-scale blood plasma separation: from acoustophoresis to egg-beaters," *Lab Chip*, **13** (*17*) 3323–3346 (2013).

399) M.E. Warkiani, L. Wu, A.K.P. Tay, and J. Han, "Large-volume microfluidic cell sorting for biomedical applications," *Biomed. Eng. (NY).*, **17** (*1*) 1 (2015).

400) V. Mehta, and J.S. Cooper, "Review and analysis of pem fuel cell design and manufacturing," *J. Power Sources*, **114** (*1*) 32–53 (2003).

401) S. Hong, Y. Tang, and S. Wang, "Investigation on critical heat flux of flow boiling in parallel microchannels with large aspect ratio: experimental and theoretical analysis," *Int. J. Heat Mass Transf.*, **127** 55–66 (2018). doi:10.1016/j.ijheatmasstransfer.2018.07.110.

402) S. Hong, Y. Tang, C. Dang, and S. Wang, "Experimental research of the critical geometric parameters on subcooled flow boiling in confined microchannels," *Int. J. Heat Mass Transf.*, **116** 73–83 (2018). doi:10.1016/j.ijheatmasstransfer.2017.09.017.

403) K. Vontas, M. Andredaki, A. Georgoulas, N. Miché, and M. Marengo, "The effect of surface wettability on flow boiling characteristics within microchannels," *Int. J. Heat Mass Transf.*, **172** 121133 (2021). doi:10.1016/j.ijheatmasstransfer.2021.121133.

404) A. Sridhar, C.L. Ong, S. Paredes, B. Michel, T. Brunschwiler, P. Parida, E. Colgan, T. Chainer, C. Gorle, and K.E. Goodson, "Thermal Design of a Hierarchical Radially Expanding Cavity for Two-Phase Cooling of Integrated Circuits," in: ASME 2015 Int. Tech. Conf. Exhib. Packag. Integr. Electron. Photonic Microsystems Collocated with ASME 2015 13th Int. Conf. Nanochannels, Microchannels, Minichannels, American Society of Mechanical Engineers, 2015: p. V001T09A039-V001T09A039.

405) M. Ruiz, C.M. Kunkle, J. Padilla, and V.P. Carey, "Boiling Heat Transfer Performance in a Spiraling Radial Inflow Microchannel Cold Plate," in: ASME 2015 13th Int. Conf. Nanochannels, Microchannels, Minichannels Collocated with ASME 2015 Int. Tech. Conf. Exhib. Packag. Integr. Electron. Photonic Microsystems, American Society of Mechanical Engineers, 2015: p. V001T04A023-V001T04A023.

406) H. Hu, C. Deng, J. Xu, K. Zhang, and M. Sun, "Metastable h -moo 3 and stable α -moo 3 microstructures: controllable synthesis, growth mechanism and their enhanced photocatalytic activity," *J. Exp. Nanosci.*, **10** (*17*) 1336–1346 (2015). doi:10.1080/17458080.2015.1012654.

407) S. Krishnamurthy, and Y. Peles, "Flow boiling heat transfer on micro pin fins entrenched in a microchannel," *J. Heat Transfer*, **132** (*4*) 41007 (2010).

408) A. Recinella, A. Kalani, and S.G. Kandlikar, "Enhanced flow boiling heat transfer using radial microchannels," (2016).

409) M.W. Ashraf, S. Tayyaba, A. Nisar, N. Afzulpurkar, D.W. Bodhale, T. Lomas, A. Poyai, and A.

Tuantranont, “Design, fabrication and analysis of silicon hollow microneedles for transdermal drug delivery system for treatment of hemodynamic dysfunctions,” *Cardiovasc. Eng.*, **10** (*3*) 91–108 (2010).

410) G. Krishnamoorthy, and L. Mulenga, “Impact of radiative losses on flame acceleration and deflagration to detonation transition of lean hydrogen-air mixtures in a macro-channel with obstacles,” *Fluids*, **3** (*4*) 104 (2018).
411) A. Bordbar, A. Taassob, A. Zarnaghsh, and R. Kamali, “Slug flow in microchannels: numerical simulation and applications,” *J. Ind. Eng. Chem.*, **62** 26–39 (2018). doi:10.1016/j.jiec.2018.01.021.
412) Hafidho Ilham Muhammad, A. Rahman, Nining Betawati Prihantini, Deendarlianto, and Nasruddin, “The application of poly-dispersed flow on rectangular airlift photobioreactor mixing performance,” *Evergreen*, **7** (*4*) 571–579 (2020). doi:10.5109/4150508.
413) A. Arjmandfard, D. Toghraie, B. Mehmandoust, M. Hashemian, and A. Karimipour, “Study the time evolution of nanofluid flow in a microchannel with various sizes of fe nanoparticle using molecular dynamics simulation,” *Int. Commun. Heat Mass Transf.*, **118** 104874 (2020). doi:10.1016/j.icheatmasstransfer.2020.104874.
414) A. Nisar, N. Afzulpurkar, B. Mahaisavariya, and A. Tuantranont, “MEMS-based micropumps in drug delivery and biomedical applications,” *Sensors Actuators B Chem.*, **130** (*2*) 917–942 (2008).